

Sensor and Simulation Notes  
Note 219

1 April 1976

Electromagnetic Field Distribution of the TEM Mode  
in a Symmetrical Two-Parallel-Plate Transmission Line

Carl E. Baum, D. V. Giri and Raymond D. González  
Air Force Weapons Laboratory

CLEARED  
FOR PUBLIC RELEASE  
PL/PA 5/12/97

Abstract

Using a special complex variable procedure the electromagnetic field distribution of the TEM mode of a symmetrical two-parallel-plate transmission line is found. The fields as well as the scalar potentials (from the conformal transformation) are analytic functions of the complex coordinates. The formulas obtained are used to produce a parametric set of plots and tables for the appropriately normalized TEM field components and magnitudes, as well as potentials.

PL 96-1234

## Contents

<u>Section</u>		<u>Page</u>
	Title and Abstract	1
	Contents	2
	List of Figures	3
	List of Tables	4
	List of Principal Symbols	5
I.	Introduction	6
II.	The Complex Potential	7
III.	The Complex Field	14
IV.	Numerical Results	17
	A. Contour Plots	21
	B. Plots of Field Components	41
	C. Tabulation of Potentials and Fields along the Symmetry Axes	41
V.	Summary	72
VI.	Acknowledgment	73
VII.	References	74
	Appendix A. Illustration of the Periodicity in the Conformal Transformation	75
	Appendix B. Reduction of the Conformal Transformation for Special Points and Lines in the Complex Coordinate Plane	78

## List of Figures

<u>Figure</u>		<u>Page</u>
2.1	Transverse plane of a symmetrical two-parallel-plate transmission line, which is infinitely long in the longitudinal direction	9
2.2	Complex potential for parallel two-plate transmission line: $Z_c = 100\Omega$	11
4.1	Illustration of the conformal mapping of the z (complex coordinate) plane into w (complex potential) plane	20
4.2 - 4.18	Contour plots of normalized field components ( $E_{x_{rel}}$ , $E_{y_{rel}}$ ), magnitude ( $ E_{rel} $ ) and the differential field magnitude ( $ [E_{rel}(x, y) - E_{rel}(0, 0)]/E_{rel}(0, 0) $ ) in the normalized complex coordinate ( $\xi$ ) plane; 17 figures correspond to the 17 values of b/a listed in Table 4.1	24- 40
4.19 - 4.35	Plots of normalized field components ( $E_{x_{rel}}$ , $E_{y_{rel}}$ or equivalently $H_{y_{rel}}$ , $-H_{x_{rel}}$ ) as a function of normalized x coordinate (x/b) for varying values normalized y coordinate (y/b); 17 figures correspond to the 17 values of b/a listed in Table 4.1	43- 59

## List of Tables

<u>Table</u>		<u>Page</u>
4.1	Parametric description of the seventeen cases considered for numerical computations	22
4.2	Normalized magnetic potential ( $v_{\text{rel}}$ ) and normalized y-component of field ( $E_{y\text{rel}}$ ) along the symmetry axis $y/b = 0$ with $b/a$ as the parameter	62
4.3	Normalized electric potential ( $u_{\text{rel}}$ ) and normalized y-component of field ( $E_{y\text{rel}}$ ) along the symmetry axis $x/b = 0$ with $b/a$ as the parameter	69

List of Principal Symbols

Symbol	Description
$z = x + iy$	Complex coordinates
$w = u + iv$	Complex potential
$Z(p m)$	Jacobi zeta function of argument p given the parameter m
$E(m)$	Complete elliptic integral of the first kind
$K(m)$	Complete elliptic integral of the second kind
$E(\phi m)$ or $E(\phi \alpha)$	Incomplete elliptic integral of the first kind
$F(\phi m)$ or $F(\phi \alpha)$	Incomplete elliptic integral of the second kind
$Z_c$	Impedance of the principal TEM mode
$Z_0$	Characteristic impedance of free space
$\mu_0, \epsilon_0$	Permeability and permitivity of free space respectively
$c$	Velocity of light in free space
$m_1 = (1 - m)$	Complementary parameter
$sn, cn, dn$ $sd, cd, nd$ $sc, dc, nc$ $cs, ds, ns$	The twelve Jacobian elliptic functions
$Sn^2(x m)$	Indefinite integral of $sn^2(x m)$ w.r.t. x
$E_{rel}(x, y)$	Complex electric field

\* With reference to the arguments of incomplete elliptic integrals, Greek and English alphabetical symbols signify different but equivalent representations. See, for instance, equations in Section 17.2 of reference 8.

## I. Introduction

Two previous notes have dealt with the theory and numerical tabulations of some of the properties of the TEM mode (differential) on a symmetrical, two-parallel-plate transmission line.<sup>1, 2</sup> These notes have tabulated the impedance and provided parametric plots for the potential and stream functions for this principal TEM mode. One of these notes<sup>1</sup> has plotted the electromagnetic field variation along a few special paths where the mathematical expressions for the fields simplify somewhat.

This note considers the electromagnetic field distribution of the primary TEM mode, deriving some analytical properties and plotting field magnitudes and components parametrically. As such it is a direct extension of previous work.<sup>1, 2</sup>

A related topic to the TEM mode field distribution is the higher order mode field distribution. Higher order modes include E (or TM) modes, H (or TE) modes, and hybrid (or HE) modes for certain types of waveguides. The principal TEM mode can be considered the lowest order mode in a sequence of modes (including TEM, E, H, and possibly HE modes) and other types of terms for describing the characteristics of a two-dimensional transmission-line (waveguide) structure.<sup>3, 4, 6</sup> The principal TEM mode and its characteristics are then important for comparison to the higher order modes and for understanding how to plot the higher order mode fields.

Subsequent sections of this note then first consider the analytical expressions for the fields of the principal TEM mode (differential). This is followed by the plots and tabulation of the fields.

## II. The Complex Potential

In previous notes the conformal transformation

$$\frac{\bar{z}'}{b} = \frac{2 K(m)}{\pi} Z(w' + i K(m_1) | m) + i \quad (2.1)$$

has been used for the symmetrical two-parallel-plate transmission line.<sup>1, 2, 5, 7</sup>

Here

$$\begin{aligned} z' &= x' + i y' \\ w' &= u' + i v' \end{aligned} \quad (2.2)$$

are the complex coordinate and complex potential (normalized) respectively. A bar over a quantity (as in  $\bar{z}'$ ) indicates the complex conjugate. The Jacobi zeta function is<sup>8</sup>

$$Z(p | m) = E(p | m) - p \frac{E(m)}{K(m)} \quad (2.3)$$

in terms of the common elliptic integrals.

Previous work<sup>1, 5</sup> has established relations for the basic geometrical parameters as

$$\begin{aligned} \frac{a}{b} &= \frac{2}{\pi} \left\{ K(m) E(\phi_0 | m) - E(m) F(\phi_0 | m) \right\} \\ \sin(\phi_0) &= \left[ \frac{1}{m} \left( 1 - \frac{E(m)}{K(m)} \right) \right]^{1/2} \end{aligned} \quad (2.4)$$

where  $m$  is referred to as the parameter of the elliptic functions and  $\phi_0$  is referred to as the amplitude with

$$\phi_0 = \operatorname{am}(p_0) = \operatorname{arc sin}(\operatorname{sn}(p_0)) \quad (2.5)$$

The transmission-line cross section dimensions are illustrated in figure

2.1. The impedance of the principal TEM mode is

$$Z_c = Z_0 f_g$$

$$\begin{aligned} Z_0 &= \text{characteristic impedance of free space} \\ &= \mu_0 c \end{aligned}$$

with

$$\mu_0 = \text{permeability of free space} = 4\pi \times 10^{-7} (\text{H/m})$$

$$c = \text{velocity of light in free space} = 2.997925 \times 10^8 (\text{m/s})$$

$$f_g = K(m_1)/K(m)$$

$$m_1 = \text{complimentary parameter} \equiv (1 - m)$$

The impedance is readily computed for any uniform medium if  $Z_0$  is changed to the wave impedance of that medium. The geometrical impedance factor  $f_g$  has been tabulated as a function of  $b/a$  in a previous note.<sup>2</sup> Note that these results apply to the case of a single plate of width  $2a$  spaced  $b$  from and parallel to an infinitely wide conducting plane by symmetry; the impedance and  $f_g$  are simply halved.

Equation 2.1 has a deficiency in that  $w'$  is not an analytic function of  $z'$  in the complex variable sense. Let us then first modify this equation into a more suitable form.

First use coordinates

$$\begin{aligned} z &\equiv x + iy = -\bar{z}' = -x' + iy' \\ \xi &\equiv \frac{z}{b} \end{aligned} \tag{2.7a}$$

giving

$$\xi = \frac{z}{b} = -\frac{2K(m)}{\pi} Z(w' + iK(m_1)|m) - i \tag{2.7b}$$

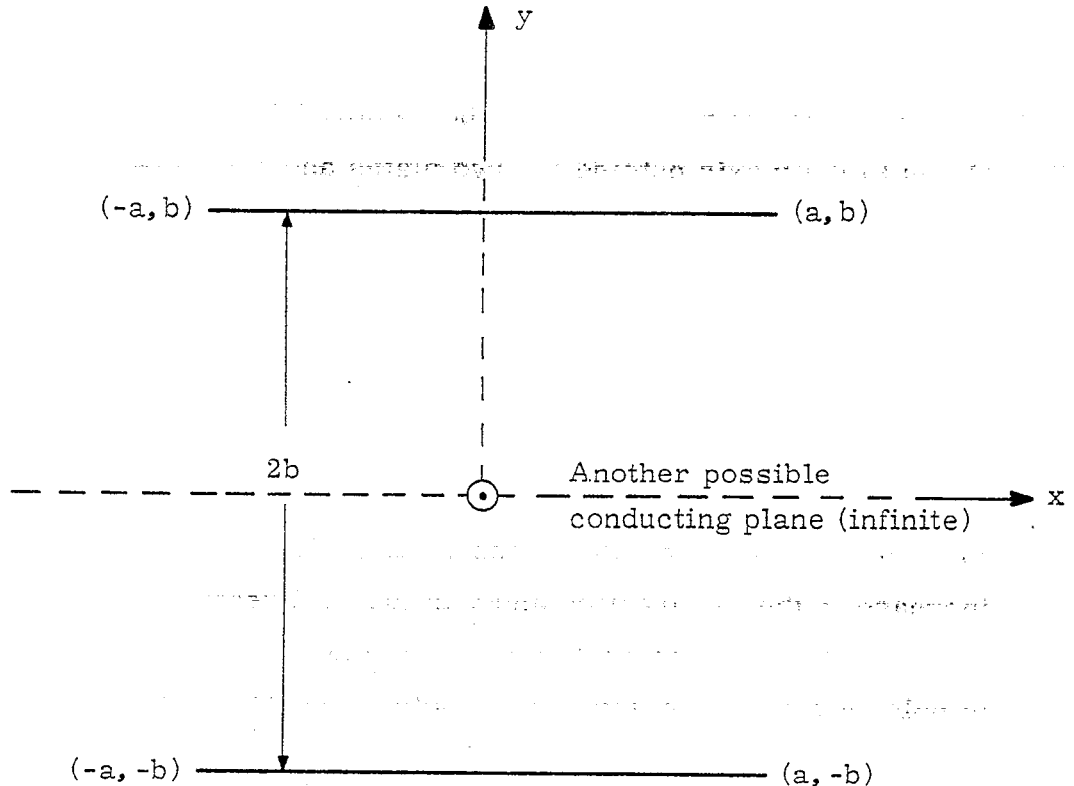


Figure 2.1. Transverse plane of a symmetrical two-parallel-plate transmission line, which is infinitely long in the longitudinal direction

In order to put the transformation in a somewhat standardized form let us make  $u$  the electric potential function and  $v$  the magnetic potential function via

$$\begin{aligned} w &= u + iv \\ &= -iw' + iK(m) \\ &= v' - i[u' - K(m)] \end{aligned} \tag{2.8}$$

In this choice the branch cut can be removed from the  $y$  axis between the plates to the  $y$  axis outside the two plates and preserve the symmetry of the potential function values with respect to the coordinate axes. Only the first quadrant ( $x \geq 0, y \geq 0$ ) will be of interest for the numbers and plots because of the symmetry in the geometry. Note near the origin as in figure 2.2  $u$  is increasing in the  $+y$  direction and  $v$  is increasing in the  $-x$  direction.

An alternate choice would have rotated the coordinate system so as to make the plates parallel to the  $y$  axis. Then near the origin  $u$  would increase in the  $+x$  direction and  $v$  in the  $+y$  direction. The former choice is more convenient in orienting the simulator in a vertical or "y" direction of polarization, corresponding to both previous work and common actual EMP simulators.

The conformal transformation used in this note is then

$$\xi = \frac{z}{b} = -\frac{2K(m)}{\pi} Z(iw + K(m) + iK(m_1)/m) - i \tag{2.9}$$

One can also follow through the full solution for the conformal transformation.<sup>5</sup> Figure 2.2 shows both potential function choices for the same  $x, y$  coordinate system. Also, the periodicity in the conformal transformation is fully illustrated in Appendix A. For numerical purposes, however, it is desirable to rewrite equation 2.9 avoiding the factor  $K(m) + iK(m_1)$  in

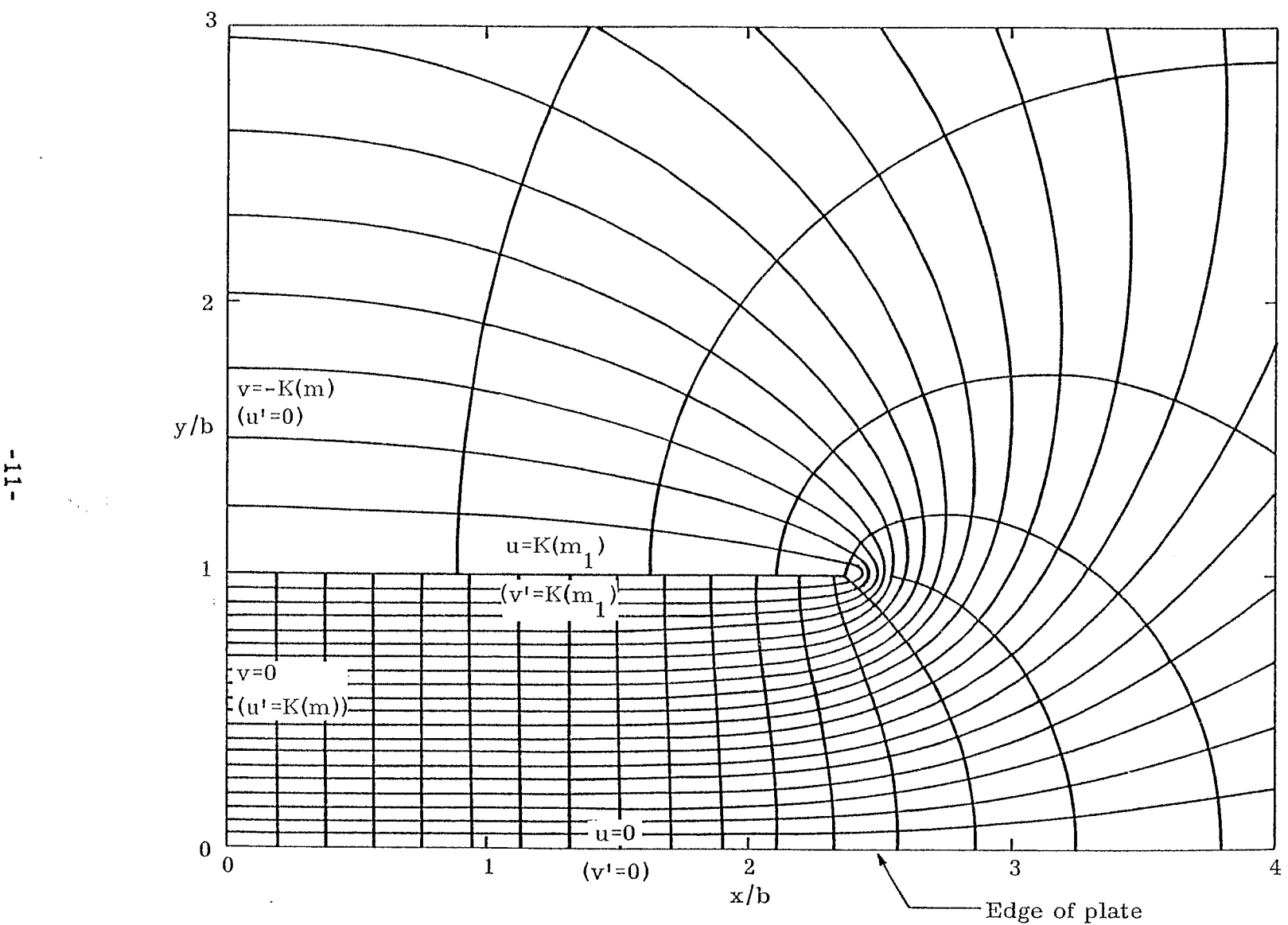


Figure 2.2. Complex potential for parallel, two-plate transmission line:  $Z_c = 100\Omega$

the argument of the Jacobi zeta function. Also, for simplicity, let us denote

$$\begin{aligned} E(m) &\equiv E, & E(m_1) &\equiv E' \\ K(m) &\equiv K, & K(m_1) &\equiv K' \end{aligned} \quad (2.10)$$

and use the addition theorem for zeta functions<sup>8</sup> to get,

$$\frac{z}{b} = -\frac{2K}{\pi} \left[ Z(iw|m) + Z(K+iK'|m) - m \operatorname{sn}(iw|m) \right. \\ \left. \operatorname{sn}(K+iK'|m) \operatorname{sn}(iw+K+iK'|m) \right] - i \quad (2.11)$$

The following identities<sup>8</sup> are useful in simplifying equation 2.11.

$$Z(K+iK'|m) = \pi/(2iK) \quad (2.12a)$$

$$\operatorname{sn}(K+iK'|m) = m^{-1/2} \quad (2.12b)$$

$$\operatorname{sn}(X+K+iK'|m) = m^{-1/2} \operatorname{dc}(X|m) \quad (2.12c)$$

$$\operatorname{sn}(iX|m) = i \operatorname{sc}(X|m_1) \quad (2.12d)$$

$$\operatorname{dc}(iX|m) = \operatorname{dn}(X|m_1) \quad (2.12e)$$

$$E(iX|m) = i[X + \operatorname{dn}(X|m_1) \operatorname{sc}(X|m_1) - E(X|m_1)] \quad (2.12f)$$

$$\int_0^X \operatorname{sn}^2(t|m) dt = \operatorname{Sn}(X|m) \quad (2.12g)$$

and

$$m \operatorname{Sn}(X|m) = -E(X|m) + X \quad (2.12h)$$

Initially, making use of identities (2.12 a, b, c, d, e) in equation 2.11,

$$\frac{z}{b} = -\frac{2K}{\pi} \left[ Z(iw|m) + \frac{\pi}{2iK} - i \operatorname{sc}(w|m_1) \operatorname{dn}(w|m_1) \right] - i \quad (2.13)$$

From the definition of the zeta function given in equation 2.3 and the identity of equation 2.12f,

$$\frac{z}{b} = -\frac{2K}{\pi} \left[ iw - iE(w|m_1) - iw \frac{E}{K} + \frac{\pi}{2iK} \right] - i \quad (2.14)$$

or

$$\frac{z}{b} = \frac{2i}{\pi} \left[ K(m) E(w|m_1) + w(E(m) - K(m)) \right] \quad (2.15)$$

Once again, using the identity of equation 2.12h with m replaced by  $m_1$ , we have

$$\frac{z}{b} = \frac{2}{i\pi} \left[ m_1 K(m) Sn(w|m_1) - w E(m) \right] \quad (2.16)$$

An alternate form, in terms of the Jacobi zeta function through the use of the Legendre relation<sup>8</sup> is

$$\frac{z}{b} = \frac{2i}{\pi} \left[ K(m) Z(w|m_1) + \frac{w\pi}{2K(m_1)} \right] \quad (2.17)$$

Equations 2.9, 2.15, 2.16 and 2.17 are all acceptable forms of describing the conformal transformation used in this note.

### III. The Complex Field

For two-dimensional structures such as parallel-plate transmission lines one can define a complex field as well as a complex potential for the TEM mode.<sup>3</sup> The electric and magnetic fields of the TEM mode are proportional to the two vector distribution functions

$$\begin{aligned}\vec{g}_o(x, y) &= \nabla u(x, y) \\ \vec{h}_o(x, y) &= \nabla v(x, y)\end{aligned}\quad (3.1)$$

which can be combined as

$$\vec{w}(x, y) \equiv \vec{g}_o(x, y) + i\vec{h}_o(x, y) = \nabla w(z) \quad (3.2)$$

Complex electric and magnetic distribution functions for the TEM mode can be defined as

$$\begin{aligned}g_o(z) &= g_{ox}(x, y) - ig_{oy}(x, y) \\ h_o(z) &= h_{ox}(x, y) - ih_{oy}(x, y)\end{aligned}\quad (3.3)$$

where these are related by

$$\begin{aligned}g_{ox}(x, y) &= h_{oy}(x, y), \quad g_{oy}(x, y) = -h_{ox}(x, y) \\ h_o(z) &= -ig_o(z)\end{aligned}\quad (3.4)$$

This gives the important complex derivative result

$$g_o(z) = ih_o(z) = \frac{dw(z)}{dz} \quad (3.5)$$

Thus  $g_o(z)$  is an analytic function of  $z$  and is a direct extension of the conformal transformation  $w(z)$ .

For the problem at hand one can now compute

$$\frac{1}{b} \frac{dz}{dw} = \left( b \frac{dw}{dz} \right)^{-1} = -\frac{2K(m)}{\pi} \frac{dZ(p|m)}{dp} \frac{dp}{dw}$$

$$p \equiv iw + K(m) + iK(m_1) \quad (3.6)$$

$$\frac{dp}{dw} = i$$

Using relations for the Jacobi zeta function<sup>8</sup> gives

$$Z(p|m) = E(p|m) - p \frac{E(m)}{K(m)}$$

$$\frac{d}{dp} E(p|m) = dn^2(p|m) \quad (3.7)$$

Differentiating equation 2.9 w.r.t. w, and making use of equation 3.7 will yield after some rearranging,

$$b \frac{dw}{dz} = \frac{i\pi}{2K(m)} \left\{ dn^2(p|m) - \frac{E(m)}{K(m)} \right\}^{-1}$$

$$= \frac{i\pi}{2} \left\{ K(m) dn^2(iw + K(m) + iK(m_1)|m) - E(m) \right\}^{-1} \quad (3.8)$$

Either by simplifying equation 3.8 or, more easily, by starting from the alternate representations of the conformal transformations given by equations 2.15 and 2.16, we can get

$$b \frac{dw}{dz} = \frac{\pi}{2i} \left\{ K(m) dn^2(w|m_1) + E(m) - K(m) \right\}^{-1} \quad (3.9)$$

or

$$b \frac{dw}{dz} = \frac{i\pi}{2} \left\{ m_1 K(m) sn^2(w|m_1) - E(m) \right\}^{-1} \quad (3.10)$$

Equations 3.8, 3.9 and 3.10 are equivalent forms of representing  $(dw/dz)$  as a function of w. Also from equation 2.15 we implicitly have z as a function of w. Thus from equations 2.15 and 3.10, we can determine the TEM fields and potentials as a function of the coordinates z.

For graphing and tabulating the numerical results an appropriate normalization for the fields is needed. Since the change in the electric potential ( $\Delta u$ ) is just  $2K(m_1)$  with a plate spacing of  $2b$ , we then define a normalized complex electric field as

$$\begin{aligned}
 E_{\text{rel}}(z) &= E_{x_{\text{rel}}}(x, y) - iE_{y_{\text{rel}}}(x, y) \\
 &= \frac{b}{K(m_1)} g_0(z) \\
 &= \frac{1}{K(m_1)} b \frac{dw}{dz}
 \end{aligned} \tag{3.11}$$

With this choice of normalization  $E_{y_{\text{rel}}}$  between the plates tends to 1 as the plate width  $a \rightarrow \infty$ , the case of a uniform field. These normalized quantities  $E_{y_{\text{rel}}}$  and  $E_{x_{\text{rel}}}$ , also apply to the magnetic field with an appropriate coordinate interchange and sign interchange.

Some special cases of the normalized electric field have been previously considered.<sup>1</sup> The present results are consistent with the former and generalize them to the entire cross section of the transmission line.

#### IV. Numerical Results

We begin this section by writing down the relevant equations for computing the potentials and the field components in the parallel plate region, i.e.,

$$\frac{z}{b} \equiv \xi = \frac{2i}{\pi} \left[ K(m) E(w|m_1) + w(E(m) - K(m)) \right] \quad (4.1)$$

$$b \frac{dw}{dz} = \frac{i\pi}{2} \left[ m_1 K(m) \operatorname{sn}^2(w|m_1) - E(m) \right]^{-1} \quad (4.2)$$

Other equivalent forms of the above equations are available in earlier sections, but these are preferable by virtue of their simplicity. In equations 4.1 and 4.2,

$$z = (x + iy) = \text{complex coordinate} \quad (4.3)$$

$$w = (u + iv) = \text{complex potential} \quad (4.4)$$

$$\frac{dw}{dz} = E_x(x, y) - iE_y(x, y) = \text{complex field} \quad (4.5)$$

As was mentioned earlier, for purposes of plotting and tabulation, the following normalization is employed.

$$(z/b) \equiv \xi = (x + iy)/b = \text{normalized complex coordinate} \quad (4.6)$$

$$u_{\text{rel}} \equiv \left[ u/K(m_1) \right] = \text{normalized electric potential} \quad (4.7)$$

$$v_{\text{rel}} \equiv \left[ -v/K(m) \right] = \text{normalized magnetic potential} \quad (4.8)$$

$$E_{\text{rel}}(x, y) \equiv \frac{b}{K(m_1)} \frac{dw}{dz} \quad (4.9)$$

and therefore

$$E_{x_{\text{rel}}}(x, y) = \frac{b}{K(m_1)} \operatorname{Re} \left[ \frac{dw}{dz} \right] = H_{y_{\text{rel}}}(x, y) \quad (4.10)$$

$$E_{y_{\text{rel}}}(x, y) = -\frac{b}{K(m_1)} \operatorname{Im} \left[ \frac{dw}{dz} \right] = -H_{x_{\text{rel}}}(x, y) \quad (4.11)$$

Returning to equations 4.1 and 4.2, the procedure to obtain the complex potential ( $w$ ) and field ( $dw/dz$ ) is conceptually straightforward and may be summarized by the following three steps.

- Step 1. Given a normalized complex coordinate  $\xi$ , we find the complex potential  $w$  by solving the transcendental equation 4.1.
- Step 2. Use the  $w$  (determined in Step 1) in equation 4.2 to determine the complex field.
- Step 3. Obtain normalized potentials and field components using equations 4.7 through 4.11.

In order to accomplish Step 1, equation 4.1 is rewritten as

$$F(w) = \frac{2i}{\pi} \left[ K(m) E(w|m_1) + w(E(m) - K(m)) \right] - \xi = 0 \quad (4.12)$$

so that Step 1 becomes that of finding the zero of a complex function  $F(w)$  of a complex variable  $w$  ( $= u + iv$ ), for a given value of  $\xi$ . This is accomplished by the subroutines CONTOUR and SEEK<sup>9</sup> which find the zero, say

$w_o$ ,

$$F(w_o) = 0 \quad (4.13)$$

by using

$$w_o = \frac{1}{2\pi i} \oint_C w' \frac{1}{F(w')} \frac{dF(w')}{dw'} dw' \quad (4.14)$$

where  $C$  is an appropriately chosen rectangular contour in the complex  $w$  plane. Equation 4.14 is valid only when a single simple zero is enclosed by  $C$ . For a more general and detailed discussion of finding the zeros of a complex function by this contour integration method (henceforth called the SGB technique), the interested reader is referred to Singaraju, Giri, Baum.<sup>9</sup> Once the complex potential  $w$  is determined for a given  $\xi$ , by the

use of SGB technique, the remainder of steps (2 and 3) is easily accomplished. Figure 4.1 shows the mapping between z and w planes. It is noted that the incomplete elliptic integral of second kind  $E(w|m_1)$  is computed via,<sup>12,8</sup>

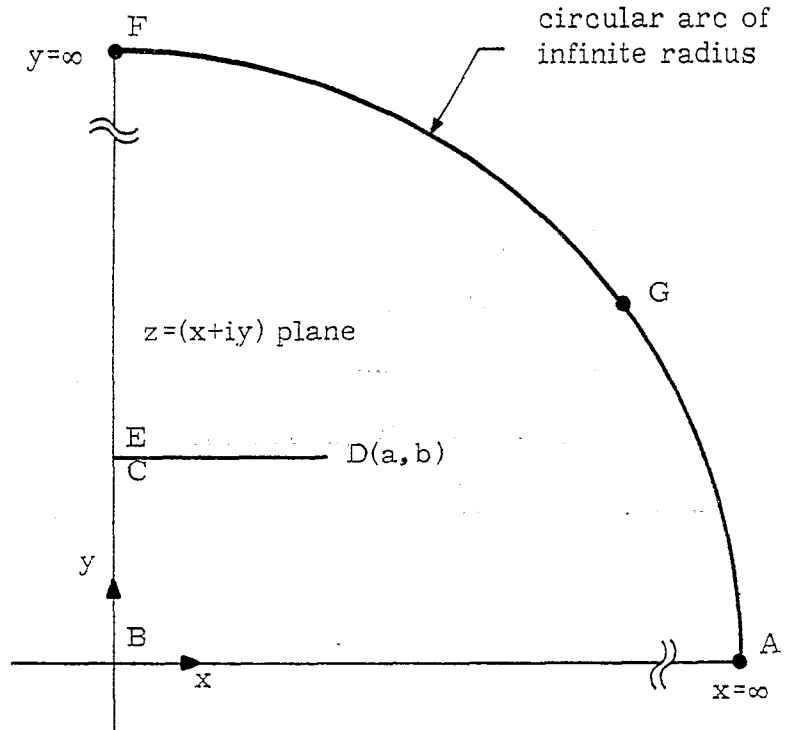
$$\begin{aligned}
 E(w|m_1) &= E(u + iv|m_1) \\
 &= E(u|m_1) + E(iv|m_1) - m_1 \operatorname{sn}(u|m_1) \operatorname{sn}(iv|m_1) \operatorname{sn}(u + iv|m_1) \\
 &= E(u|m_1) + i[v + \operatorname{dn}(v|m) \operatorname{sc}(v|m) - E(v|m)] \\
 &\quad - im_1 \operatorname{sn}(u|m_1) \operatorname{sc}(v|m) \operatorname{sn}(u + iv|m_1) \\
 &= E(\phi_u|\alpha_1) + i[v + \operatorname{dn}(v|m) \operatorname{sc}(v|m) - E(\phi_v|\alpha)] \\
 &\quad - im_1 \operatorname{sn}(u|m_1) \operatorname{sc}(v|m) \operatorname{sn}(u + iv|m_1) \tag{4.15}
 \end{aligned}$$

where

$$\begin{aligned}
 m + m_1 &= 1 \\
 m &= \sin^2 \alpha \\
 m_1 &= \cos^2 \alpha = \sin^2 \alpha_1 \\
 \alpha_1 &= (\pi/2) - \alpha \\
 \phi_u &= \operatorname{arc sin} [\operatorname{sn}(u|m_1)] \\
 \phi_v &= \operatorname{arc sin} [\operatorname{sn}(v|m)] \\
 E(\phi|\alpha) &= \int_0^\phi \left[ 1 - \sin^2 \alpha \sin^2 \theta \right]^{1/2} d\theta \tag{4.16}
 \end{aligned}$$

Although simpler looking formulas<sup>8,10</sup> exist for computing  $E(w|m_1)$ , equation 4.15 turned out to be numerically most efficient. The integral in equation 4.16 was easily performed by a 12-point Gaussian quadrature routine.

Seventeen values of  $(b/a)$  corresponding to varying geometries of the two-parallel plates are considered in this note. They also include



Note: The conformal transformation is nonanalytic on the infinite circle and also at the point D.

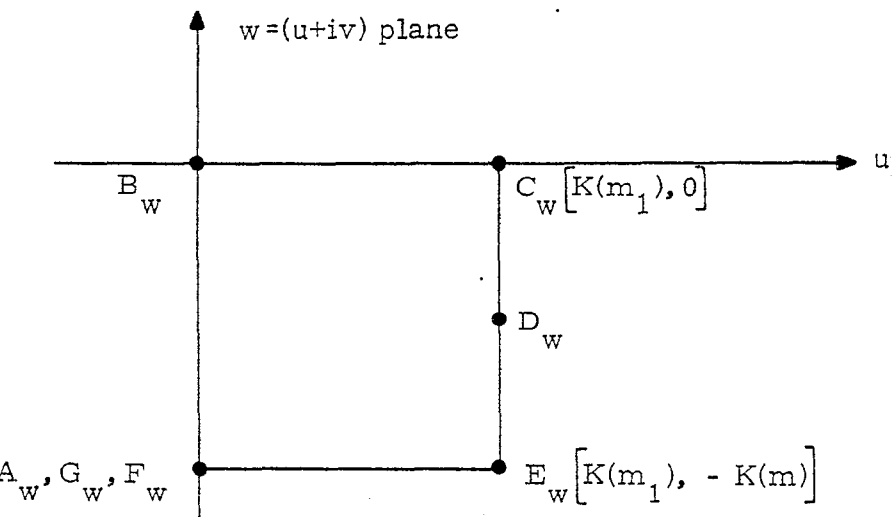


Figure 4.1. Illustration of the conformal mapping of the  $z$  (complex coordinate) plane into  $w$  (complex potential) plane

four special values of  $(b/a)$  which correspond to the impedance values of very nearly 50, 100, 200 and 400 ohms. In actual computations, the impedance values are 50.240, 99.96, 199.896, 399.722 ohms. They differ from the nominal values only slightly because of certain interpolation problems in determining the parameter  $m$ . Table 4.1 summarizes the seventeen cases considered here and serves as a quick reference to identify any particular case. The arrangement is in the increasing order of  $b/a$ ,  $f_g$  and  $Z_c$ , or decreasing order of the parameter  $m$ .  $Z_c$  in Table 4.1 is computed by using equation 2.6 with

$$\mu_0 = \text{permeability of free space} = 4\pi \times 10^{-7} \text{ henries/meter}$$

$$c = \text{velocity of light in free space} = 2.997925 \times 10^8 \text{ meters/sec}$$

In what follows, the results of numerical computations will be presented as three different subsections.

#### A. Contour plots

Contour plots (figures 4.2 through 4.18) for the seventeen configurations described in table 4.1, were generated on the Calcomp plotter of the

CDC-7600 computer system for the quantities  $E_{x_{rel}}(x, y)$ ,  $E_{y_{rel}}(x, y)$ ,  $|E_{rel}(x, y)|$  and  $\left| \frac{[E_{rel}(x, y) - E_{rel}(0, 0)]}{E_{rel}(0, 0)} \right|$ . These contour plots are helpful in a physical understanding of the distribution of electric (or magnetic) field components and magnitudes in the parallel plate region.

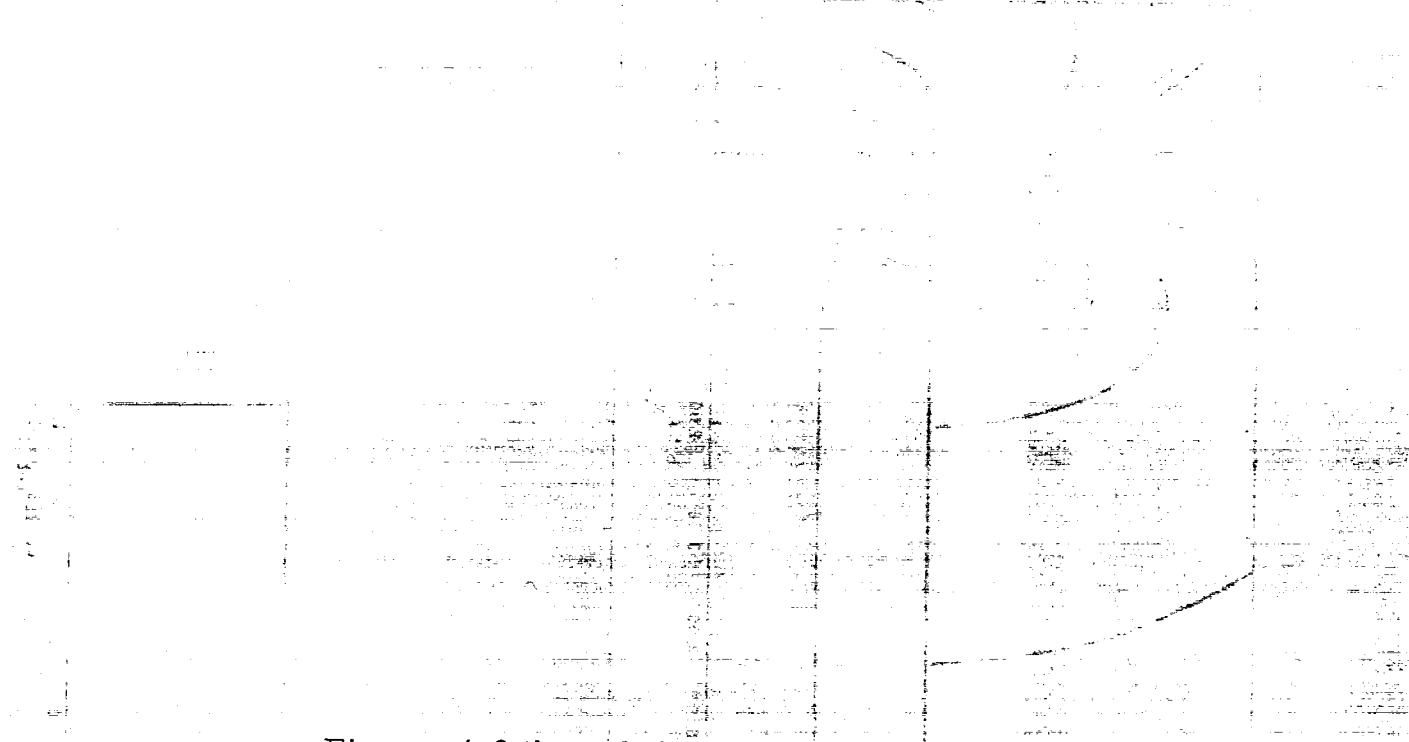
The area described by the contour plots is a rectangle whose sides are nearly  $[(a/b) + 2.]$  along the  $+x$  axis and  $(3b/b)$  along the  $+y$  axis. The

plots are made only in the first quadrant because of inherent symmetry in the problem (see figure 2.1). The contours of constant  $\left| \frac{E_{rel}(x, y) - E_{rel}(0, 0)}{E_{rel}(0, 0)} \right|$  which is a measure of nonuniformity in the absolute value of the complex field at any point in the parallel plate region with respect to the field at the origin, should prove to be useful information in design and measurement situations involving this type of structures.

Case No.	b/a	Parameter m from Ref. 2	Geometrical Impedance Factor f <sub>g</sub> from Ref. 2	Principal TEM Mode Impedance Z <sub>c</sub> (ohms)
1*	0.16670	.99999999906	0.13336	50.240
2*	0.40679	.99988464130	0.26534	99.961
3	0.5	.99943584596	0.30642	115.439
4	0.6	.99817229136	0.34613	130.397
5	0.7	.99571526791	0.38204	143.927
6	0.8	.99181434812	0.41479	156.266
7	0.9	.98637895070	0.44487	167.595
8	1.0	.97944581910	0.47264	178.058
9	1.2	.96161387120	0.52245	196.824
10*	1.23526	.95797700060	0.53061	199.896
11	1.4	.93967447110	0.56609	213.262
12	1.6	.91504156590	0.60483	227.859
13	1.8	.88889423440	0.63962	240.966
14	2.0	.86212031080	0.67116	252.848
15	2.5	.79609313350	0.73901	278.407
16	3.0	.73485375600	0.79525	299.593
17*	6.9900	.43546844510	1.06103	399.722

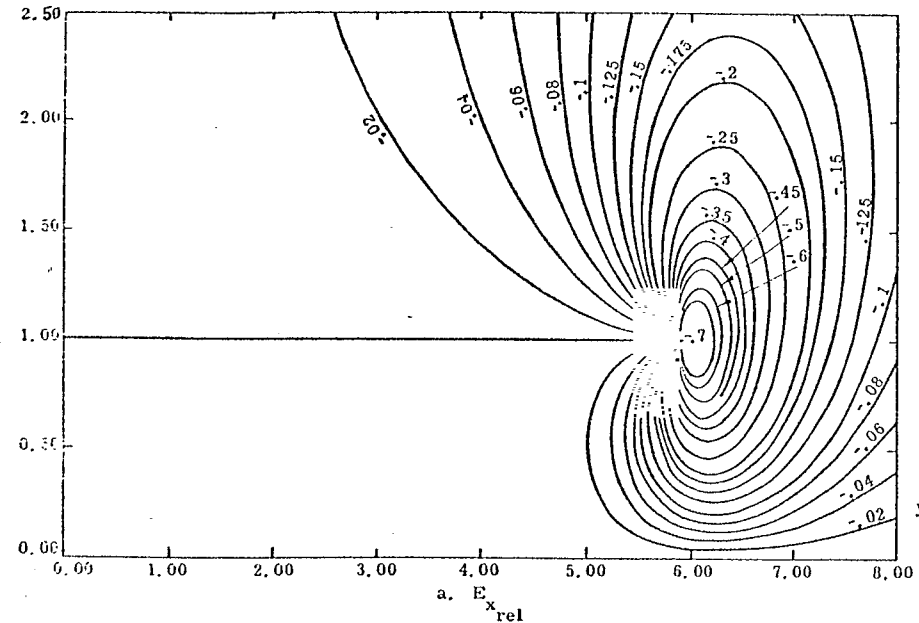
\*Four special cases corresponding to Z<sub>c</sub> values of nearly 50, 100, 200 and 400 ohms.

Table 4.1. Parametric description of the seventeen cases considered for numerical computations

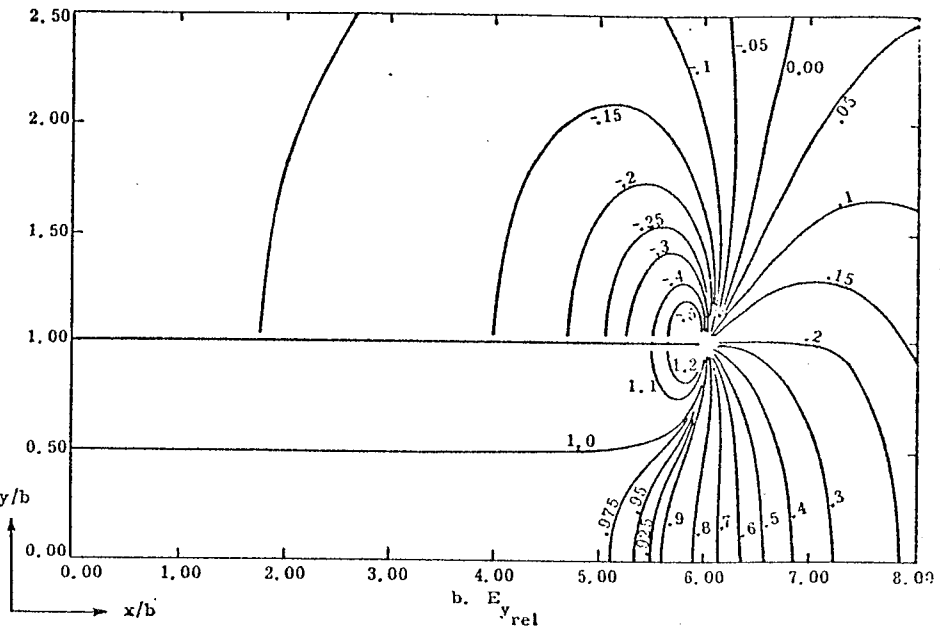


Figures 4.2 through 4.18

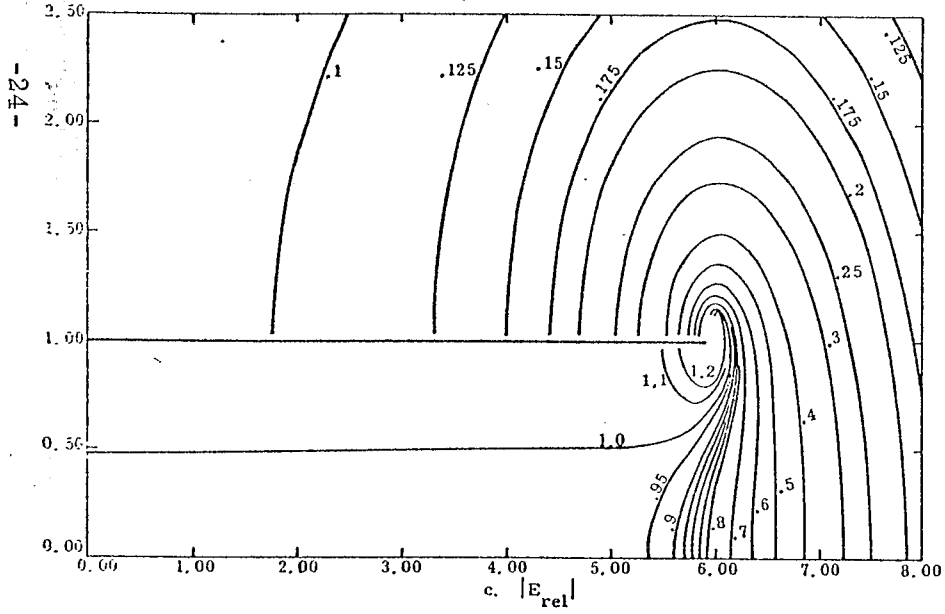
Contour plots of normalized field components ( $E_{x\text{rel}}$ ,  $E_{y\text{rel}}$ ), magnitude ( $|E_{\text{rel}}|$ ) and the differential field magnitude  $\left|\left[\frac{(E_{\text{rel}}(x,y) - E_{\text{rel}}(0,0))}{E_{\text{rel}}(0,0)}\right]\right|$  in the normalized complex coordinate ( $\zeta$ ) plane; seventeen figures correspond to the seventeen values of  $b/a$  listed in table 4.1.



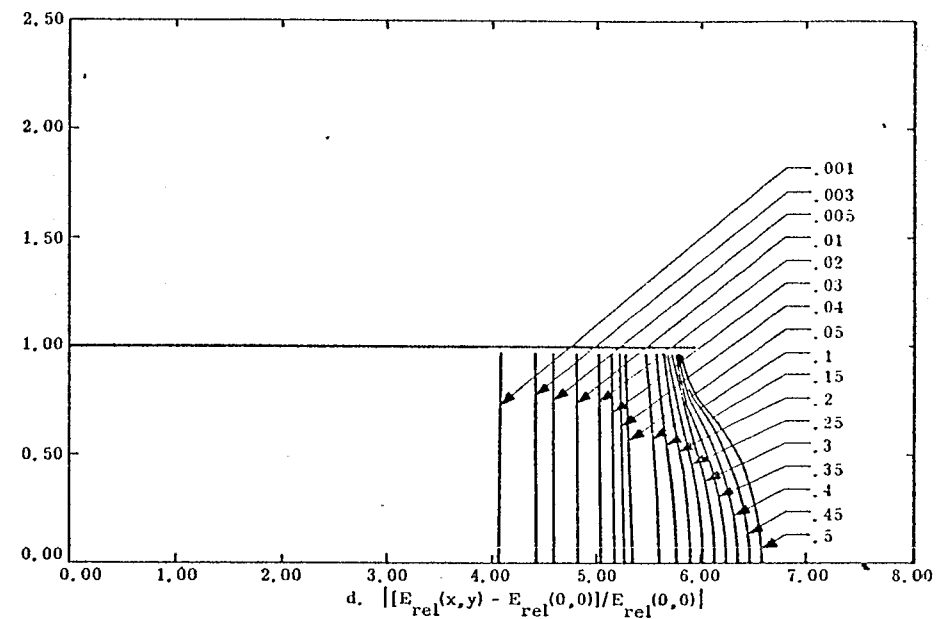
a.  $E_{x\text{ rel}}$



b.  $E_{y\text{ rel}}$



c.  $|E_{\text{rel}}|$



d.  $\frac{|[E_{\text{rel}}(x,y) - E_{\text{rel}}(0,0)|}{E_{\text{rel}}(0,0)}$

Figure 4.2.  $b/a = 0.16670$

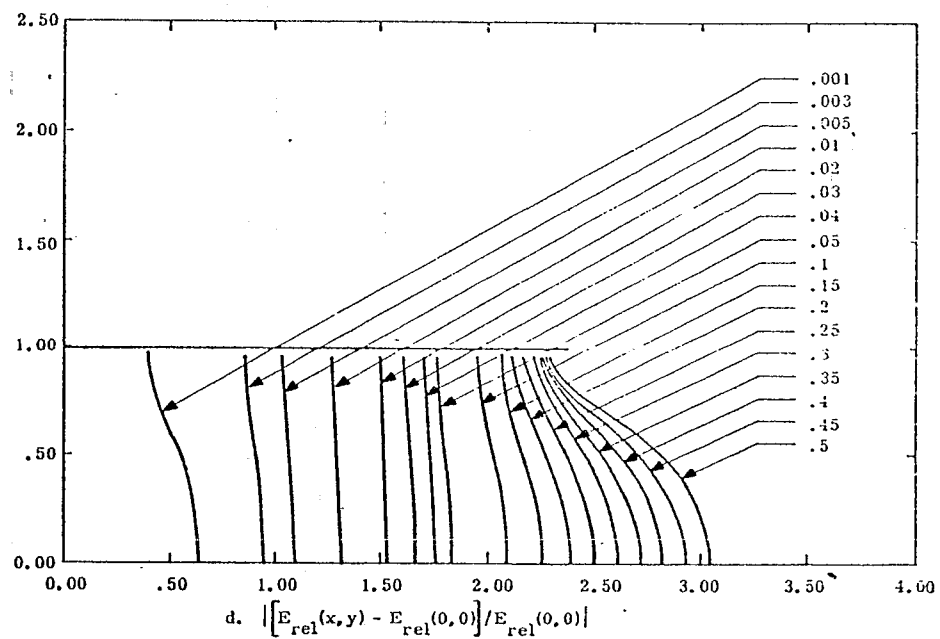
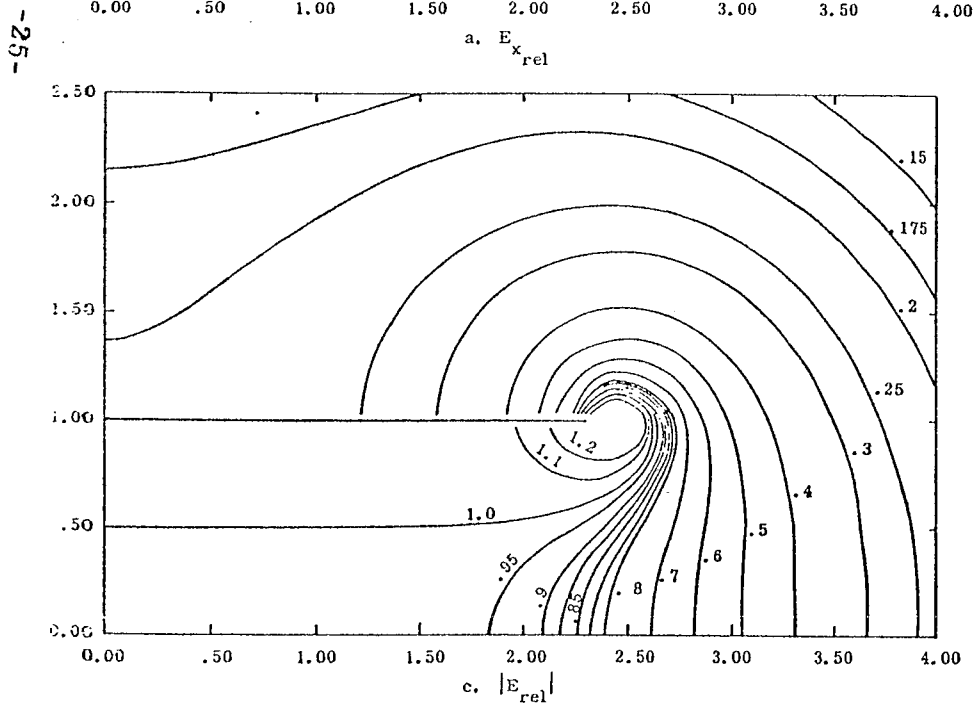
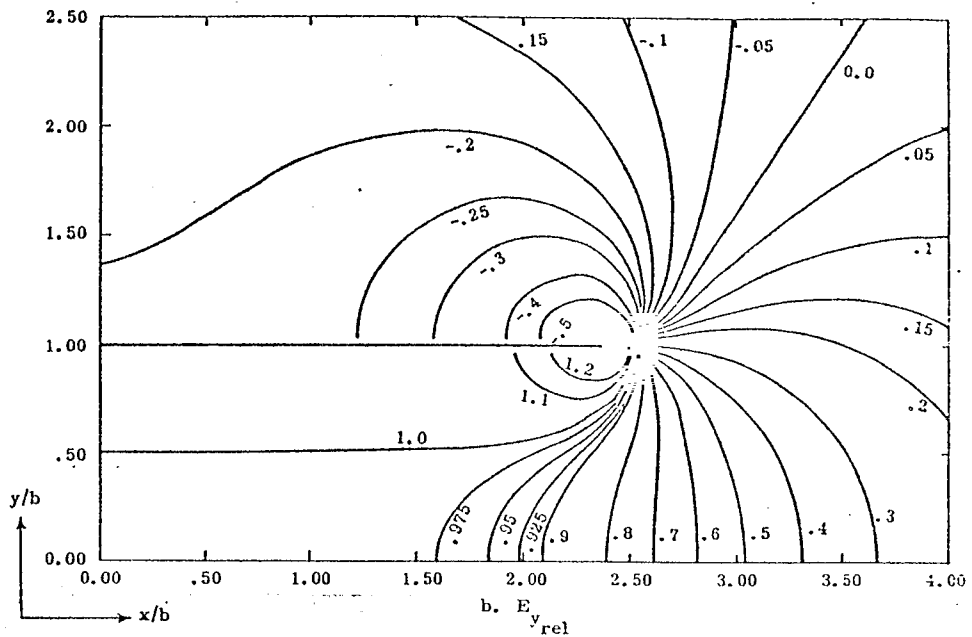
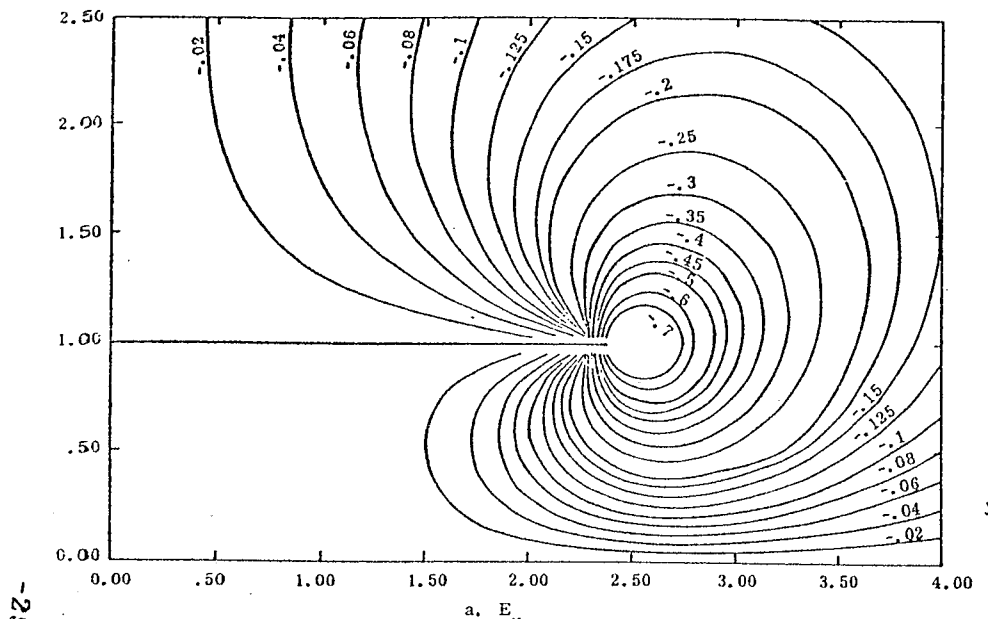
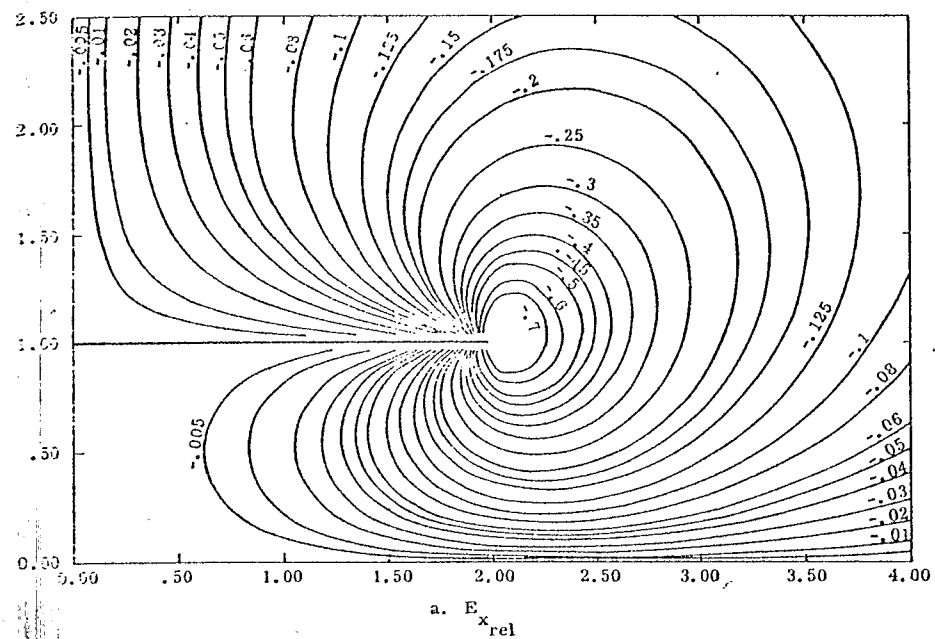
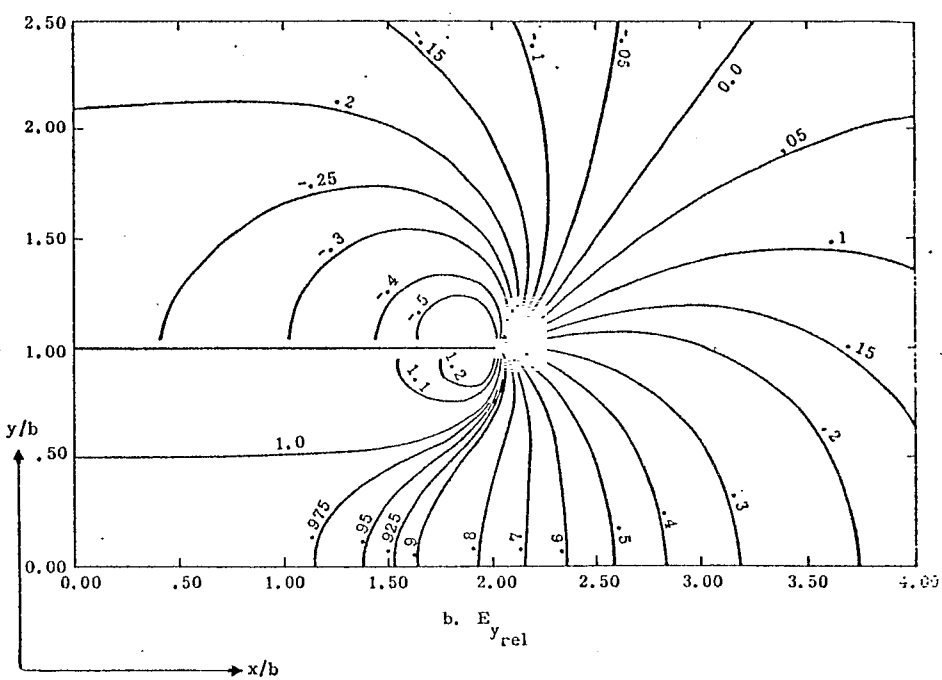


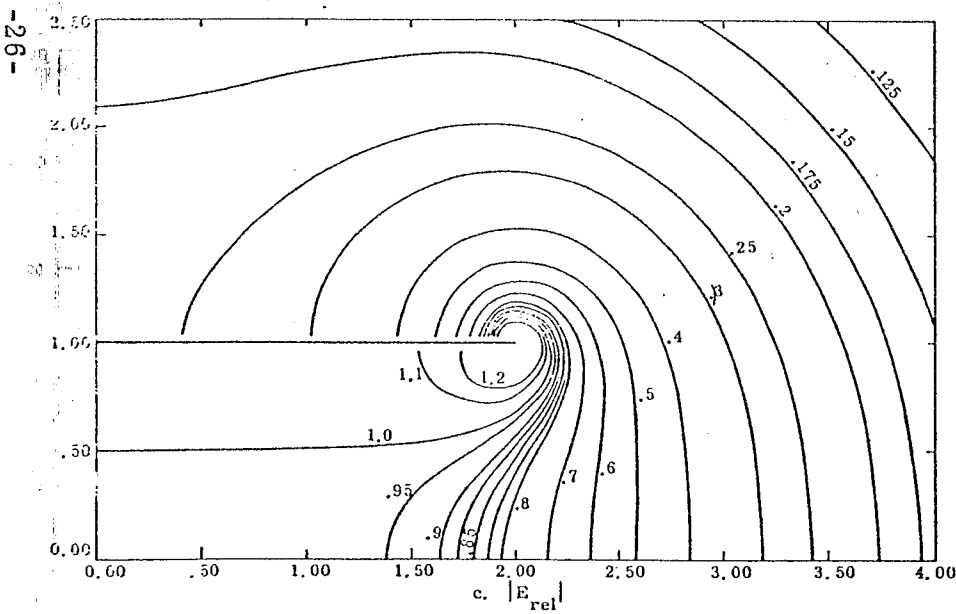
Figure 4.3.  $b/a = 0.40679$



a.  $E_x$ <sub>rel</sub>



b.  $E_{y_{\text{rel}}}$



c.  $E_r$

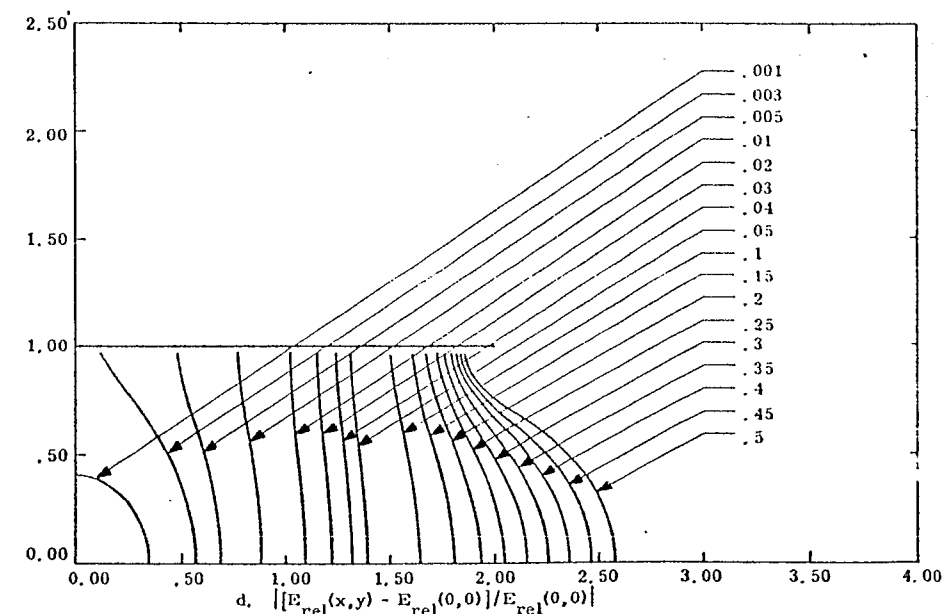
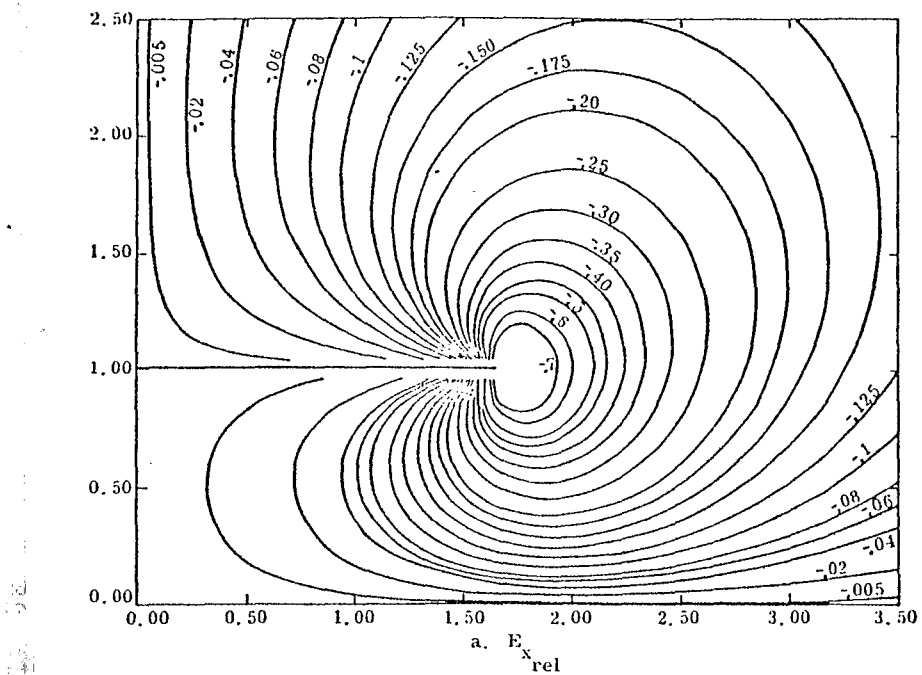
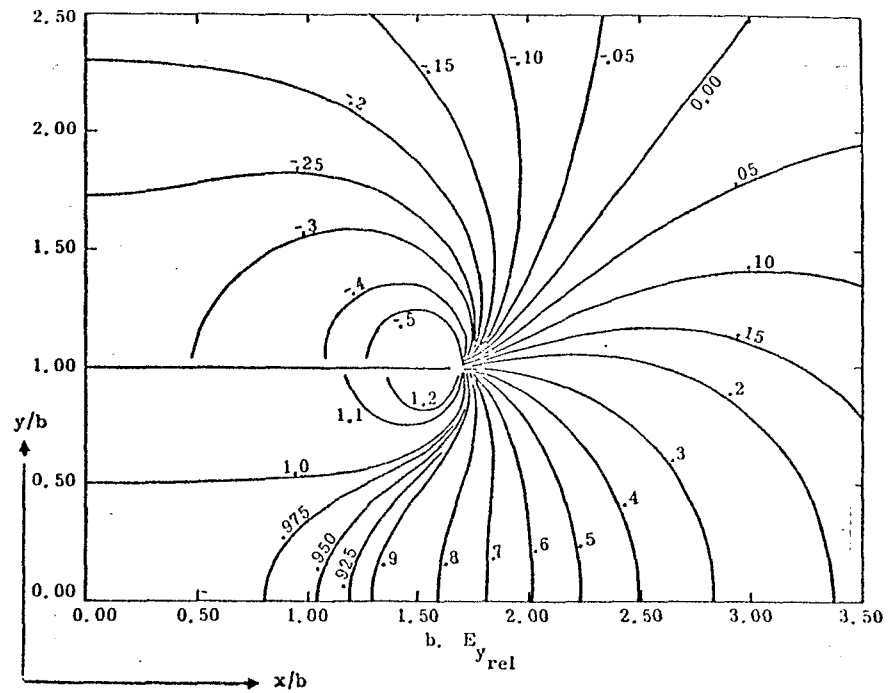


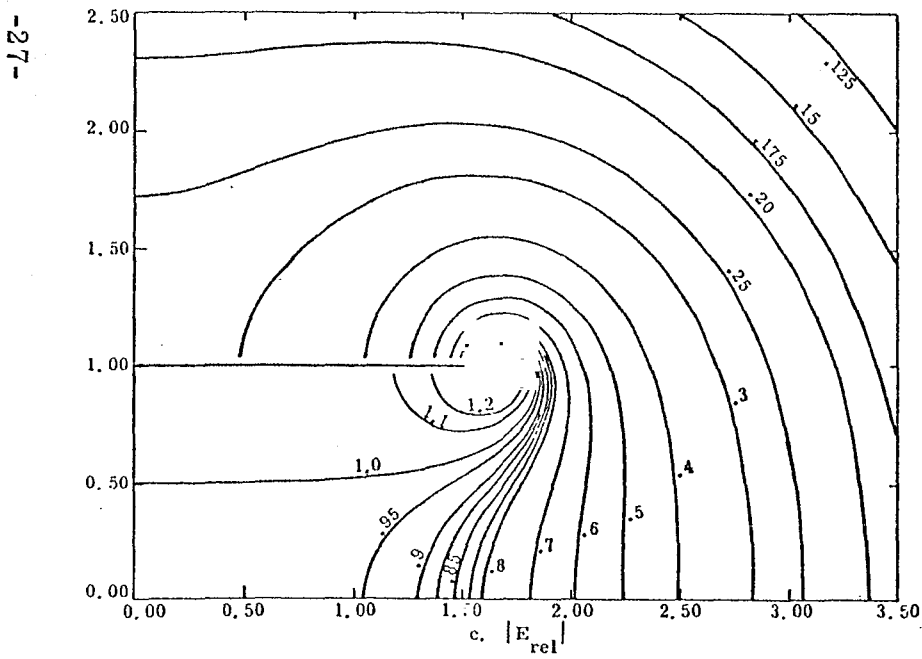
Figure 4.4.  $b/a = 0.5$



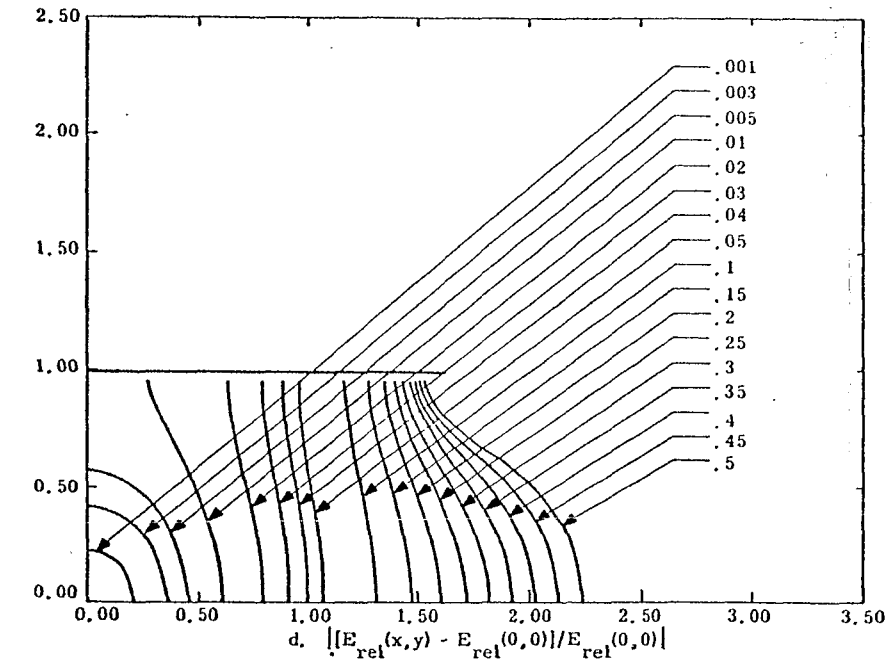
a.  $E_{x\text{ rel}}$



b.  $E_{y\text{ rel}}$



c.  $|E_{\text{rel}}|$



d.  $\frac{|E_{\text{rel}}(x,y)| - |E_{\text{rel}}(0,0)|}{|E_{\text{rel}}(0,0)|}$

Figure 4.5.  $b/a = 0.6$

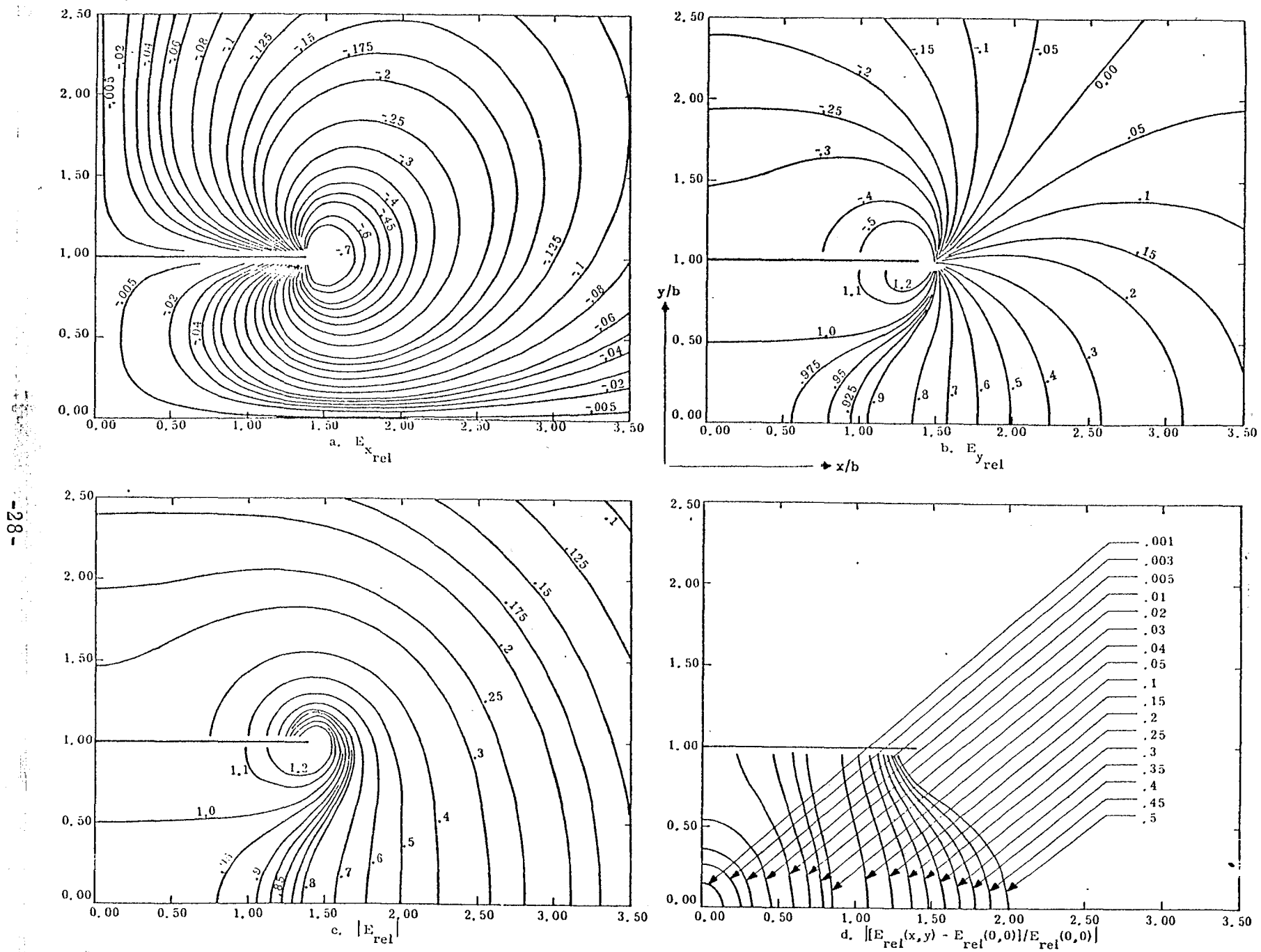


Figure 4.6.  $b/ \quad 0.7$

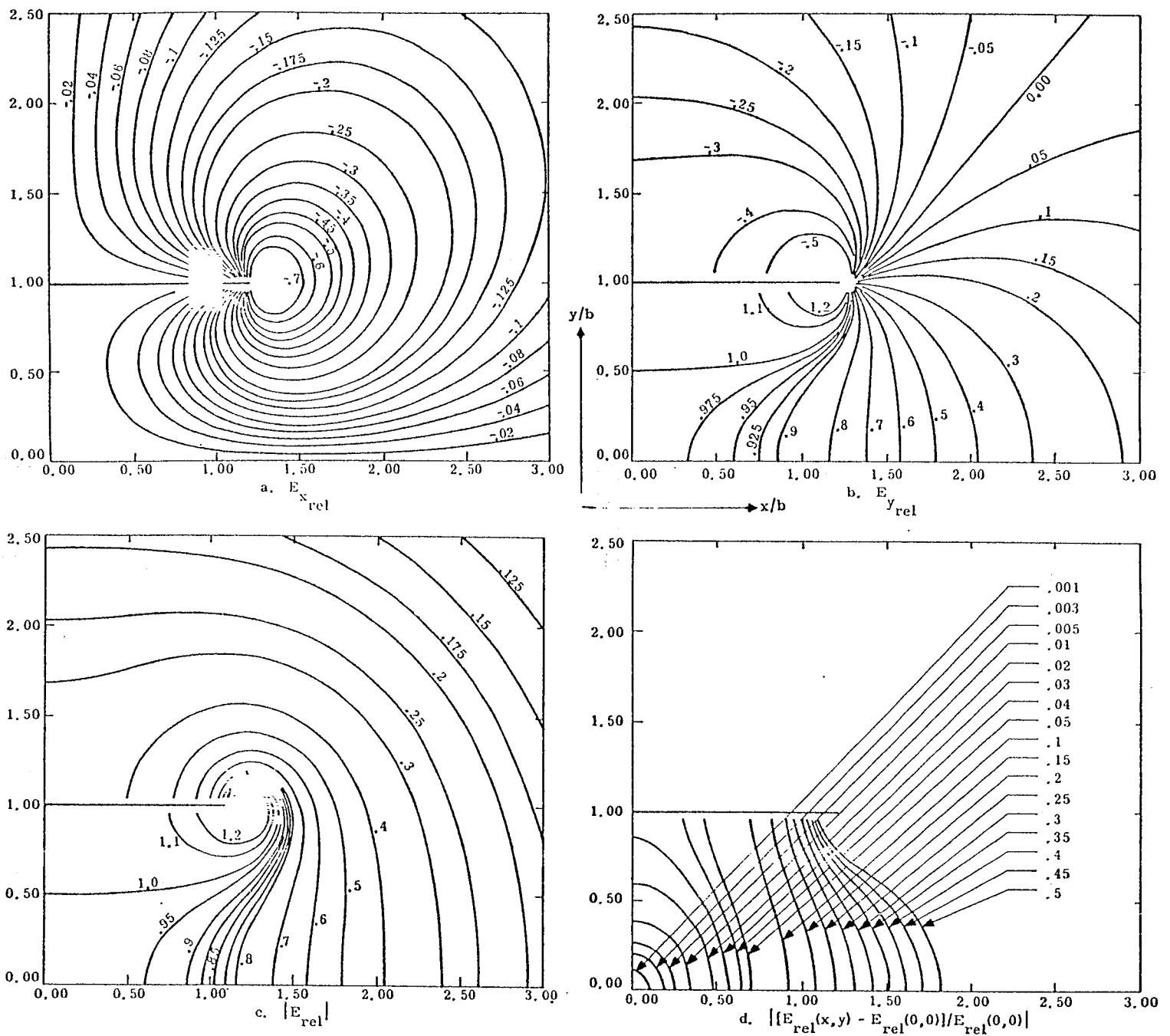
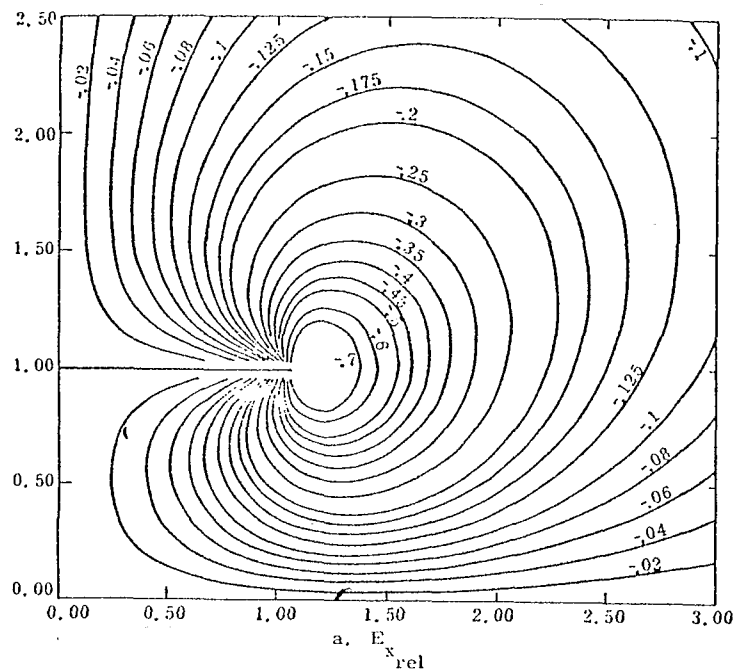
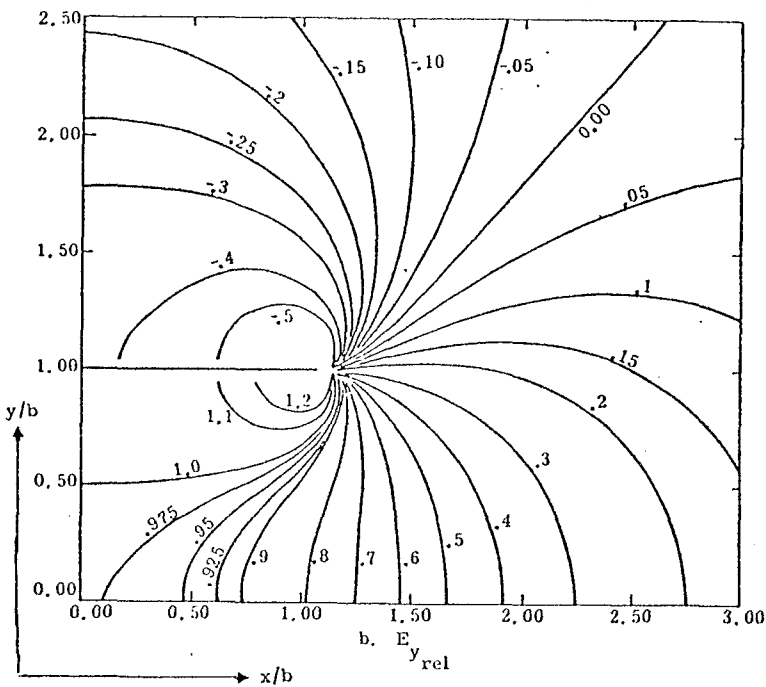


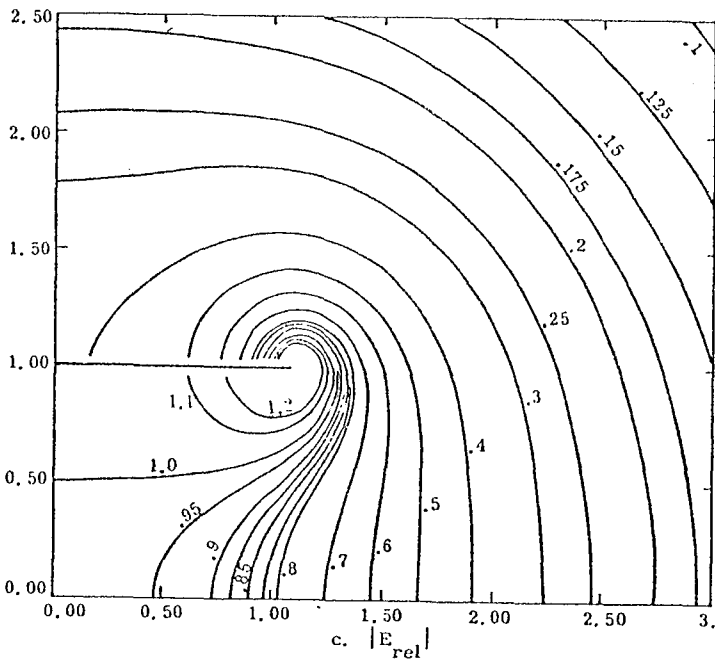
Figure 4.7.  $b/a = 0.8$



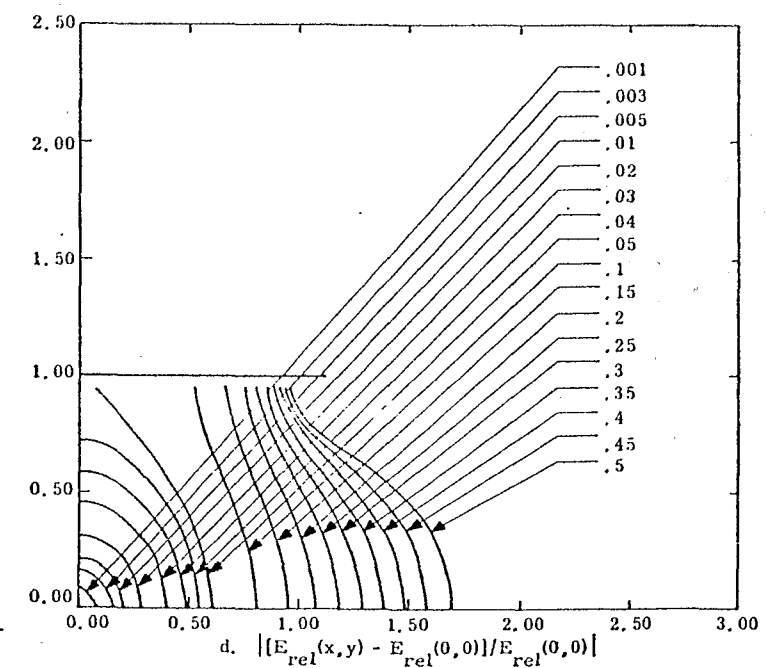
a.  $E_{x\text{rel}}$



b.  $E_{y\text{rel}}$



c.  $|E_{\text{rel}}|$



d.  $\left| \frac{[E_{\text{rel}}(x, y) - E_{\text{rel}}(0, 0)]}{E_{\text{rel}}(0, 0)} \right|$

Figure 4.8. b/ = 0.9

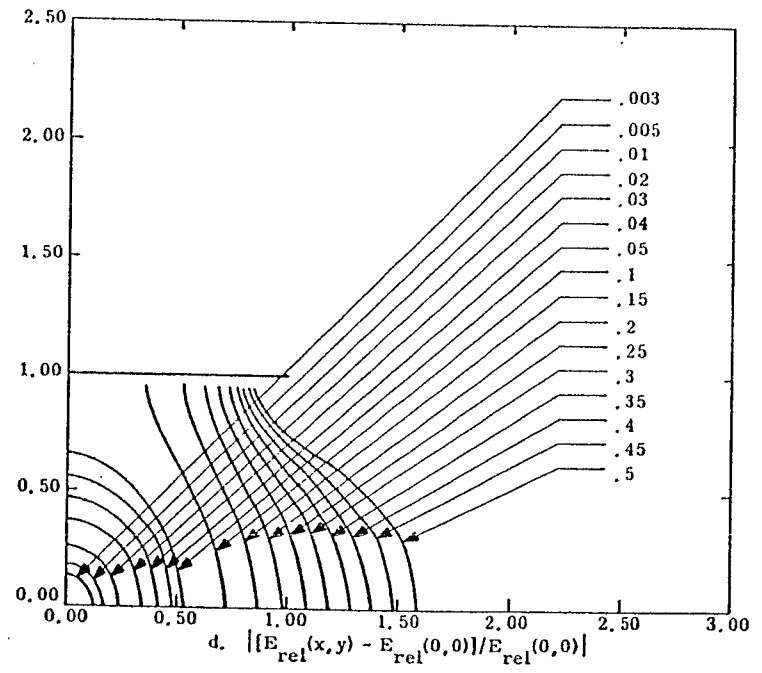
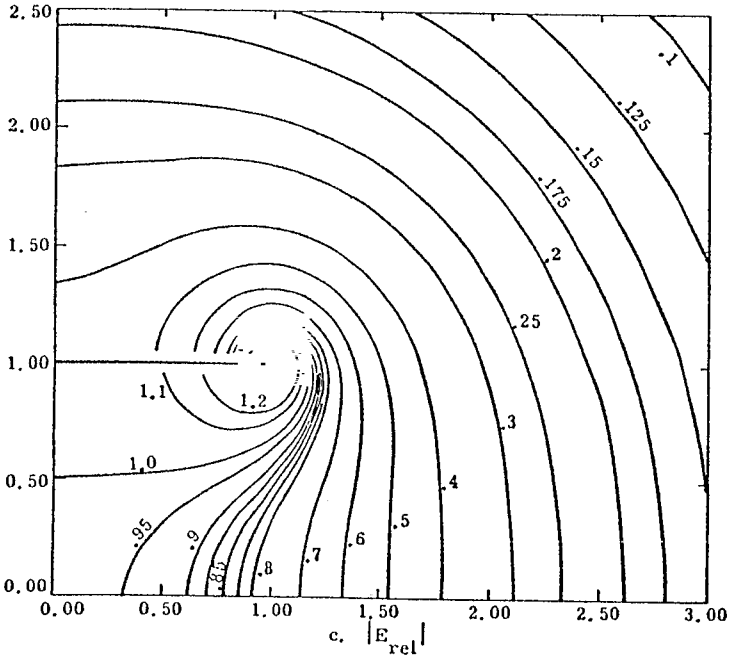
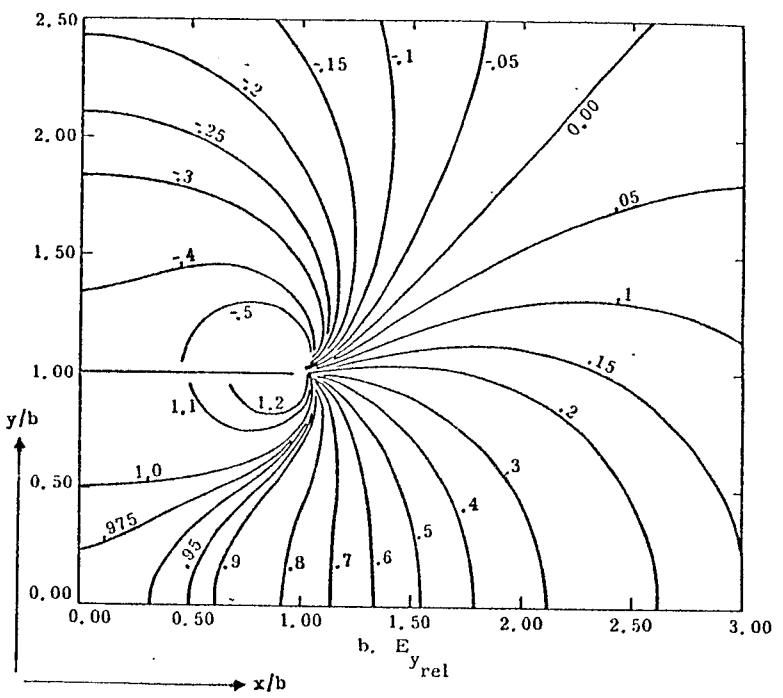
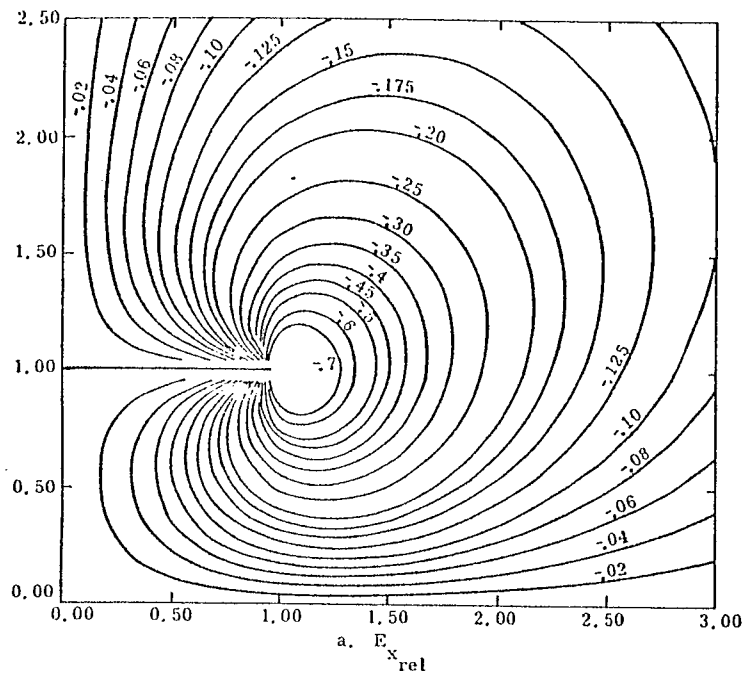


Figure 4.9.  $b/a = 1.0$

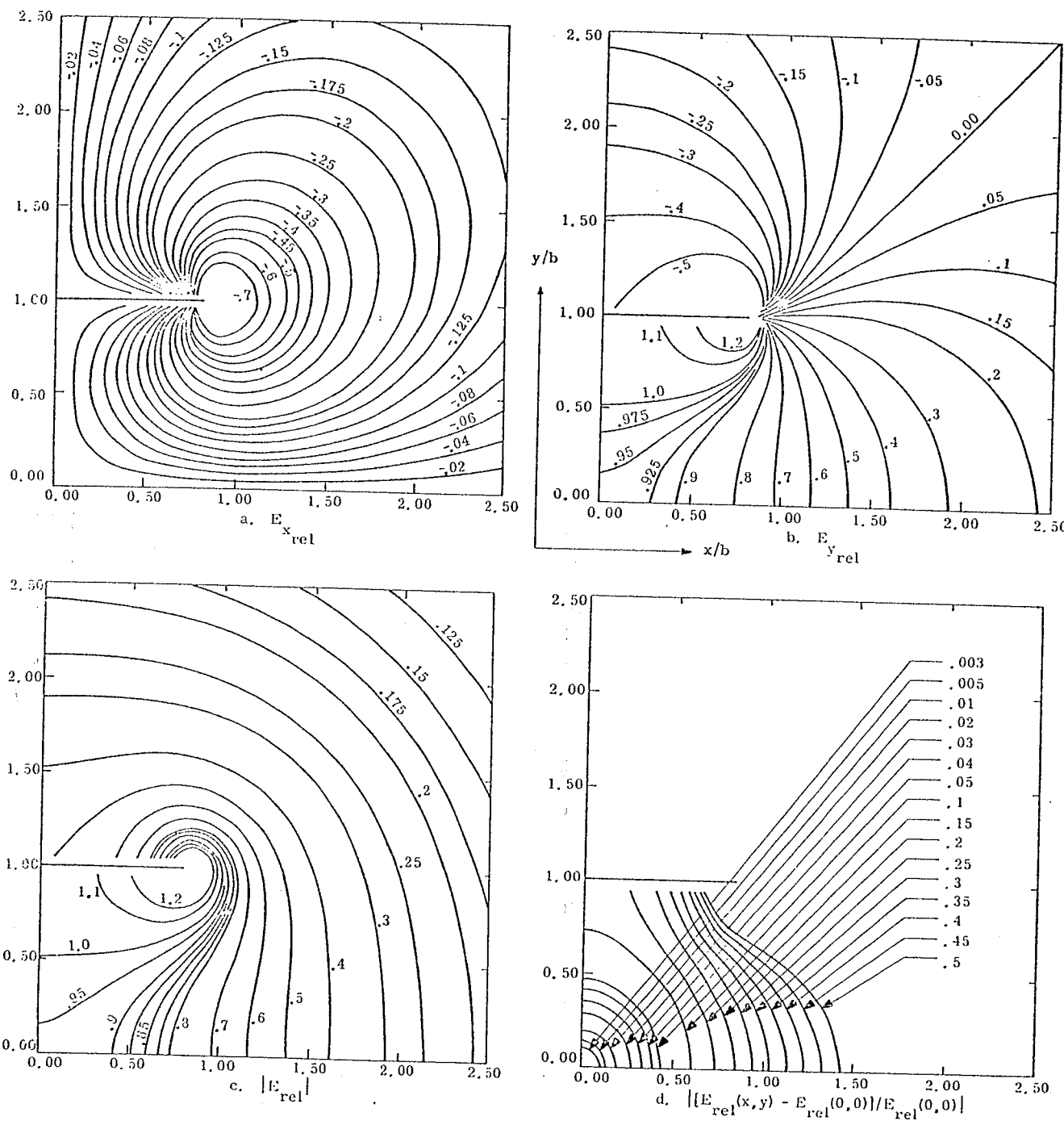
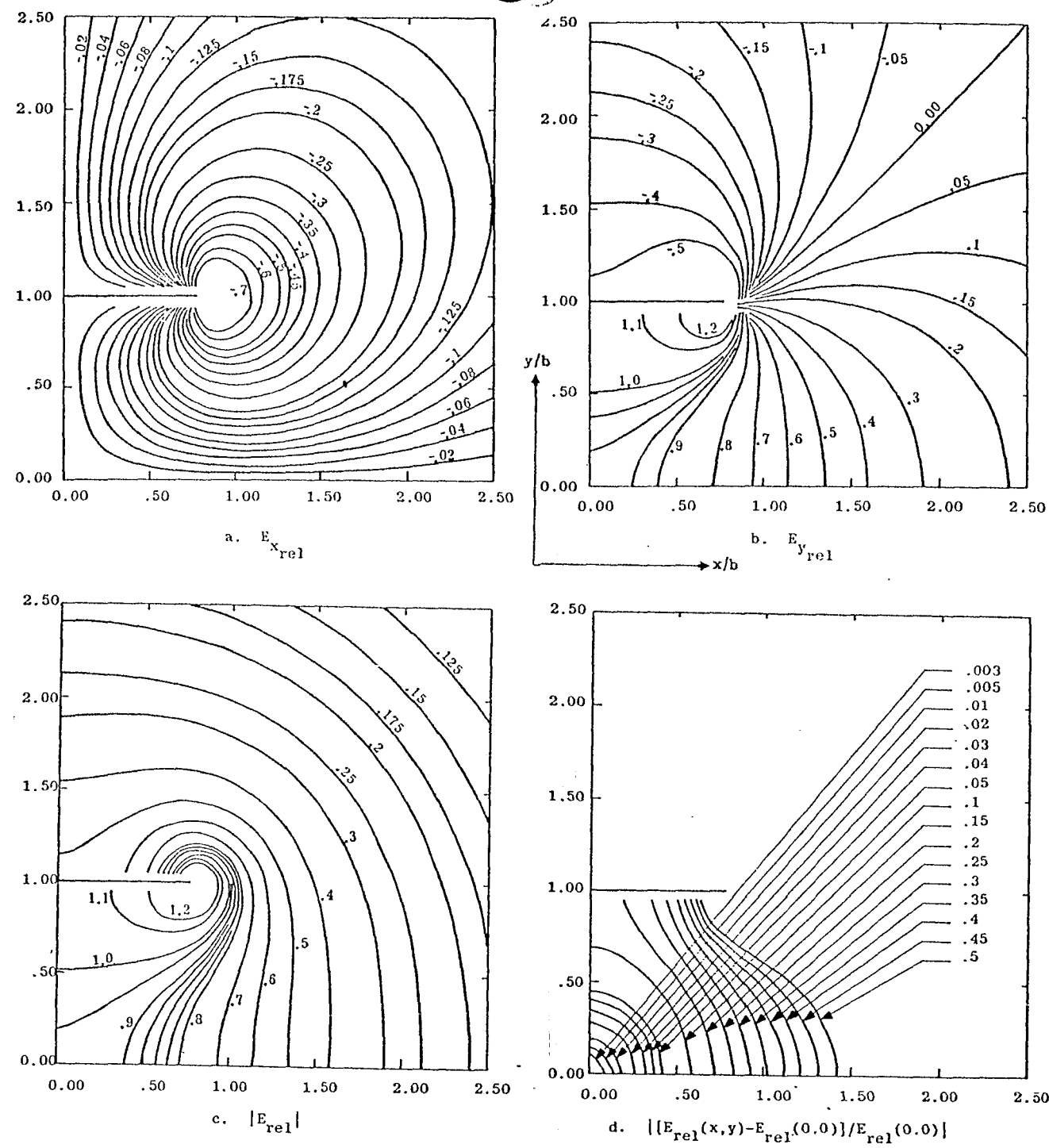
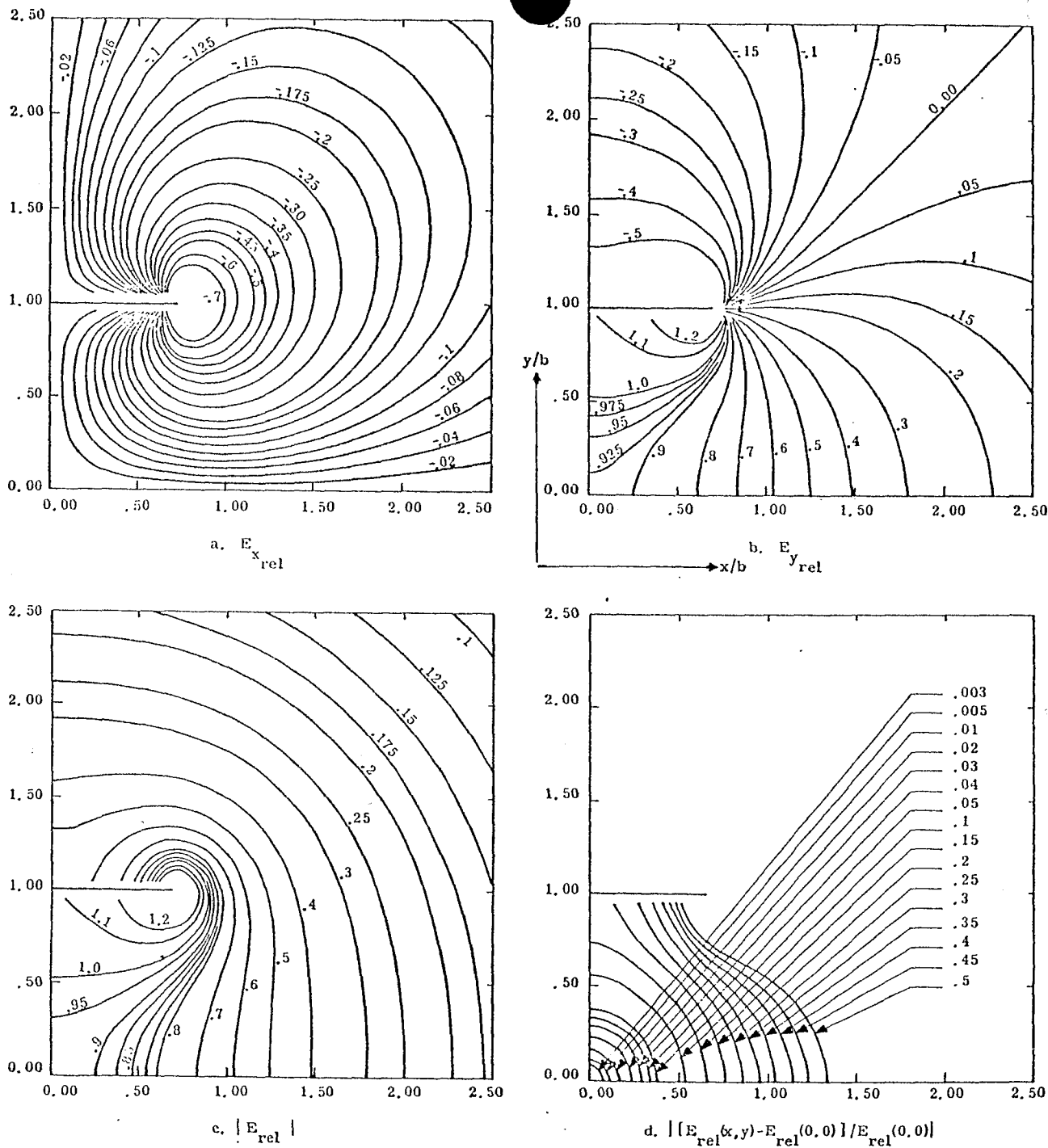
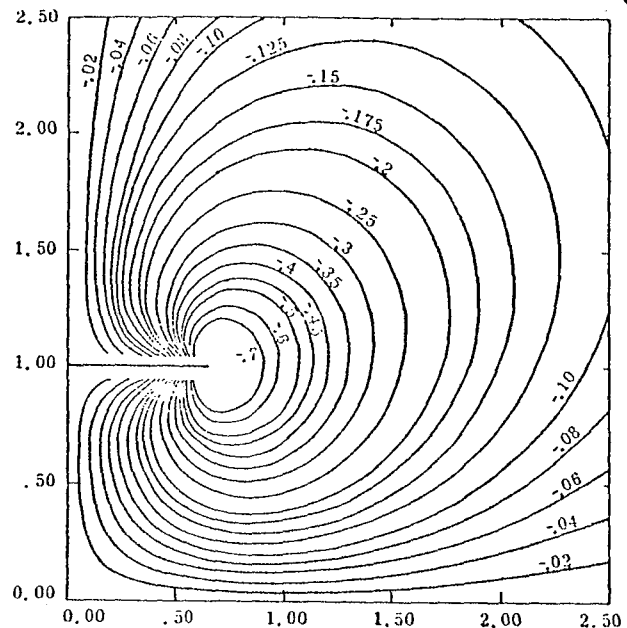


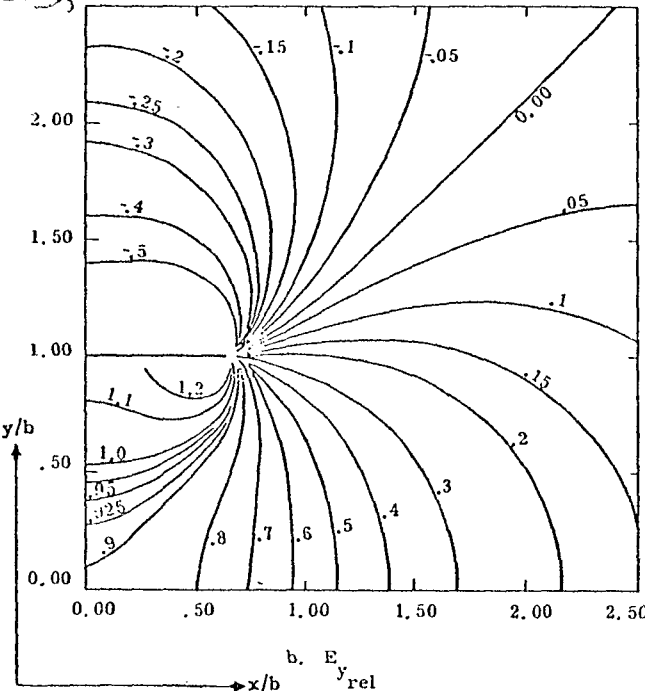
Figure 4.10. b/a 1.2

Figure 4.11.  $b/a = 1.23526$

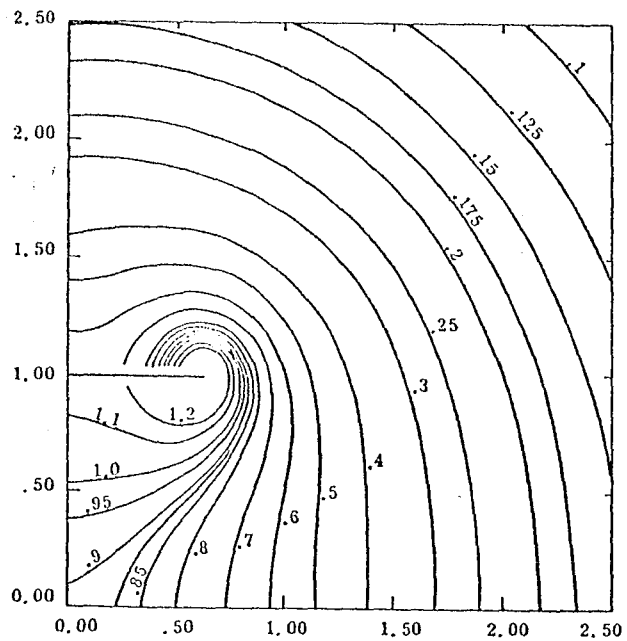
Figure 4.12.  $k = 1.4$



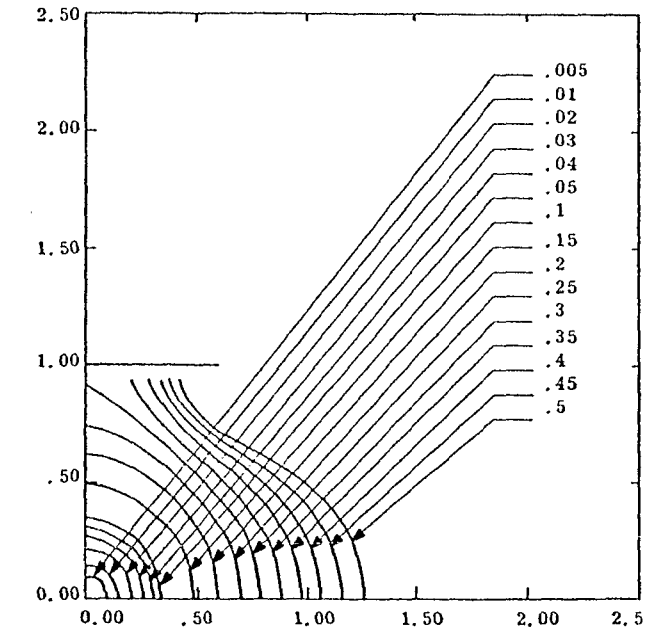
a.  $E_x^{\text{rel}}$



b.  $E_y^{\text{rel}}$

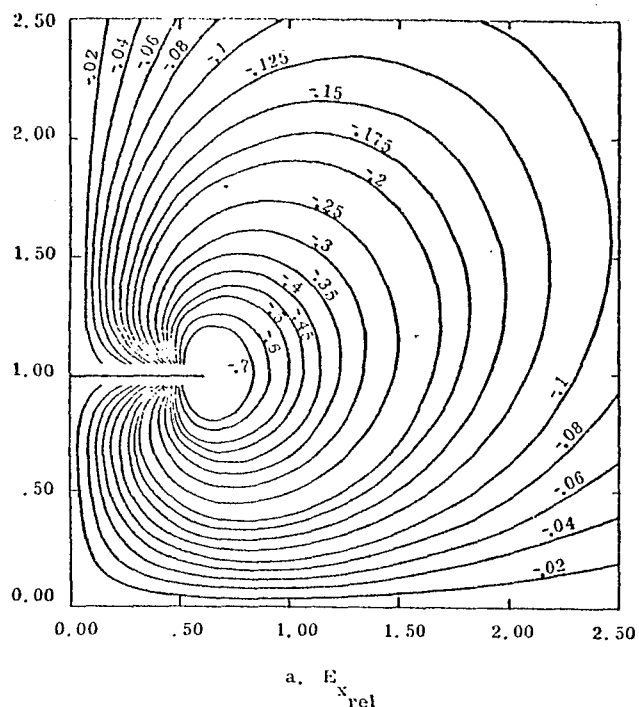


c.  $|E_{\text{rel}}|$

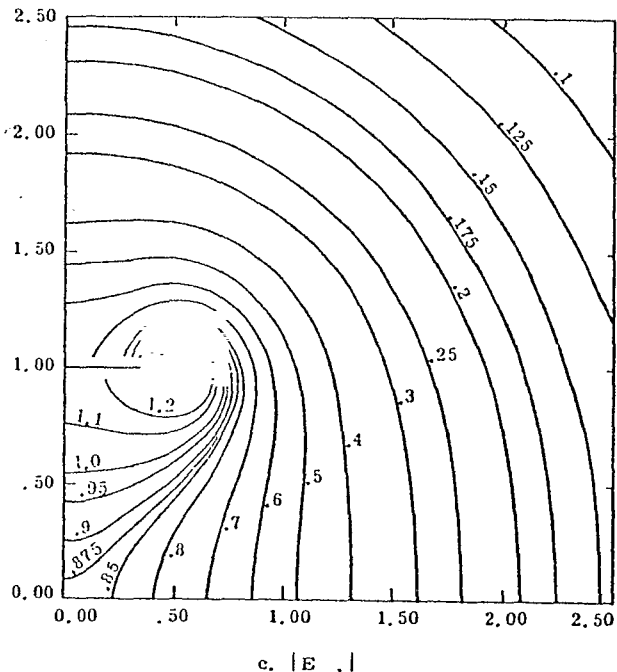
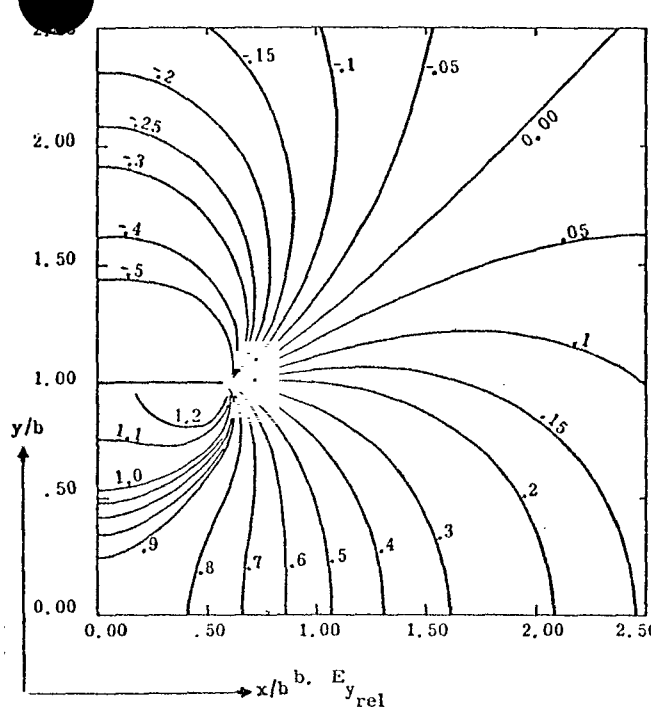


d.  $|(E_{\text{rel}}(x,y) - E_{\text{rel}}(0,0)) / E_{\text{rel}}(0,0)|$

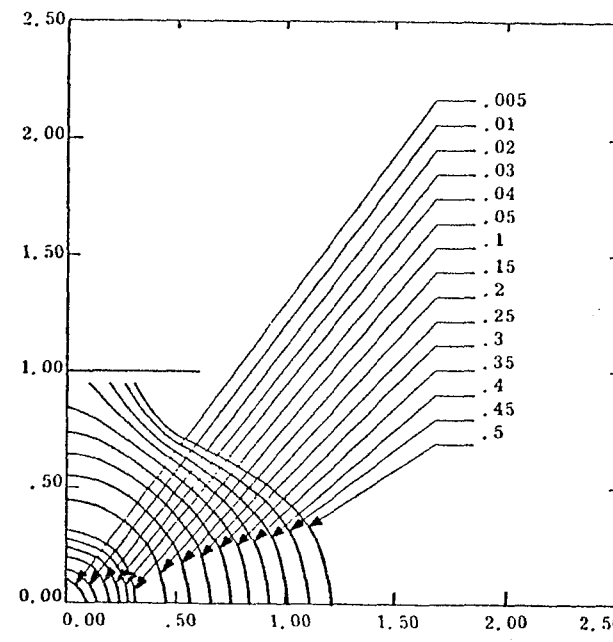
Figure 4.13.  $b/a = 1.6$



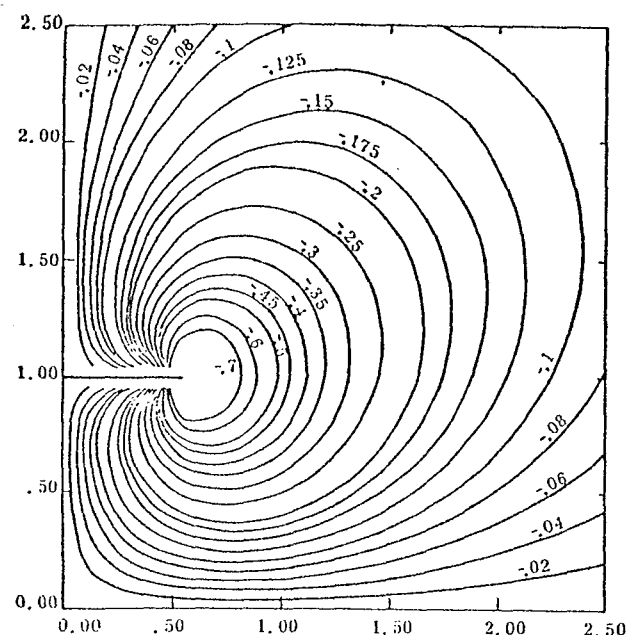
a.  $E_x$ <sub>rel</sub>



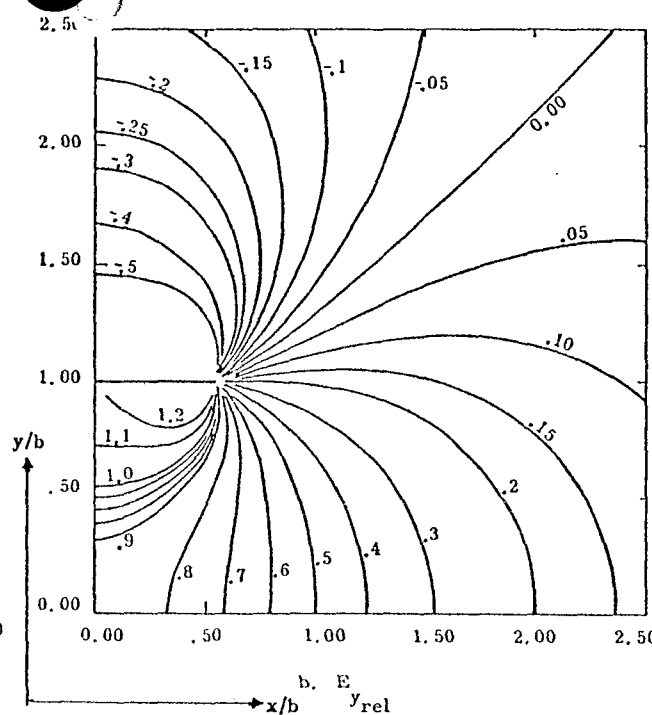
c.  $|E_{rel}|$



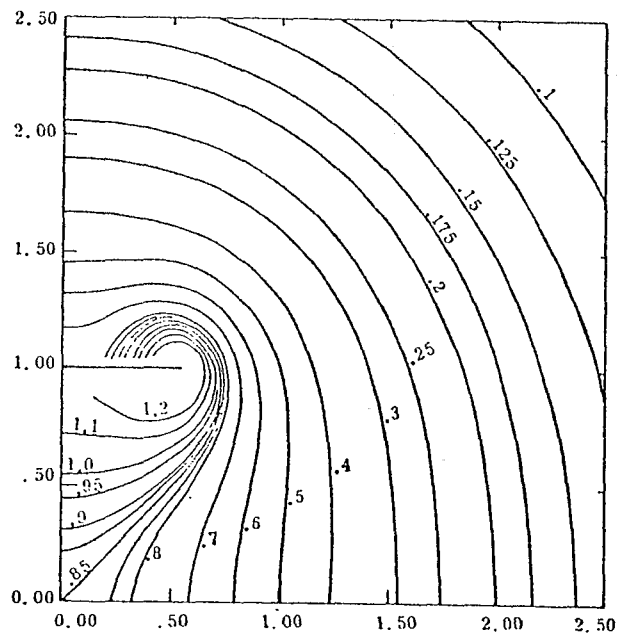
$$d. \left[ (E_{rel}(x,y) - E_{rel}(0,0)) / E_{rel}(0,0) \right]$$



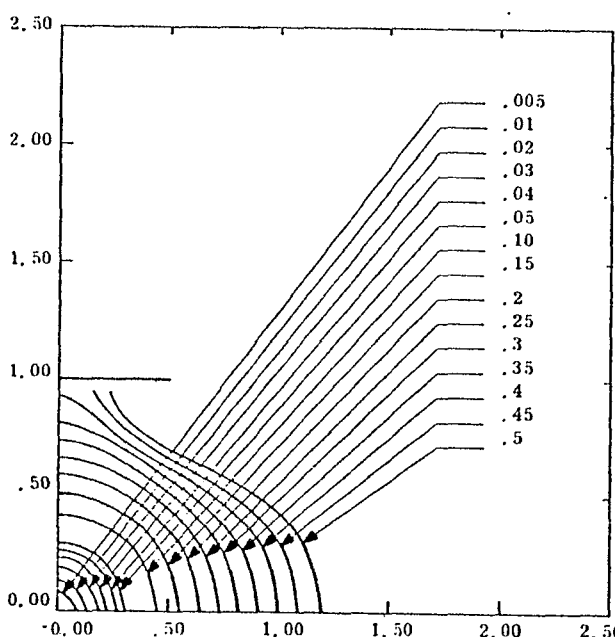
a.  $E_{x\text{ rel}}$



b.  $E_{y\text{ rel}}$

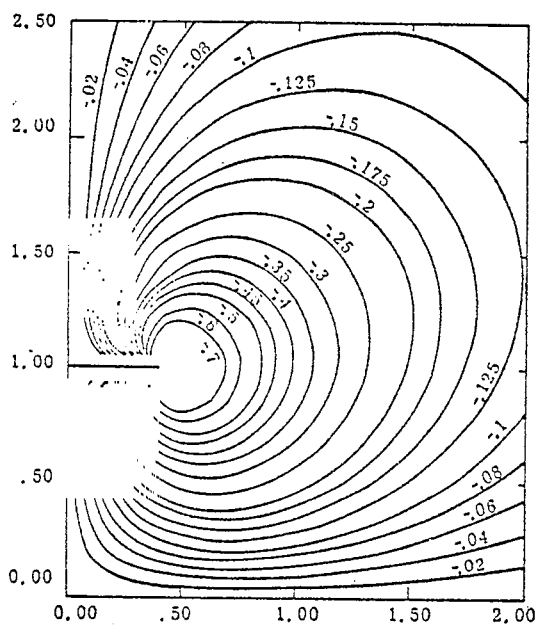


c.  $|E_{\text{rel}}|$

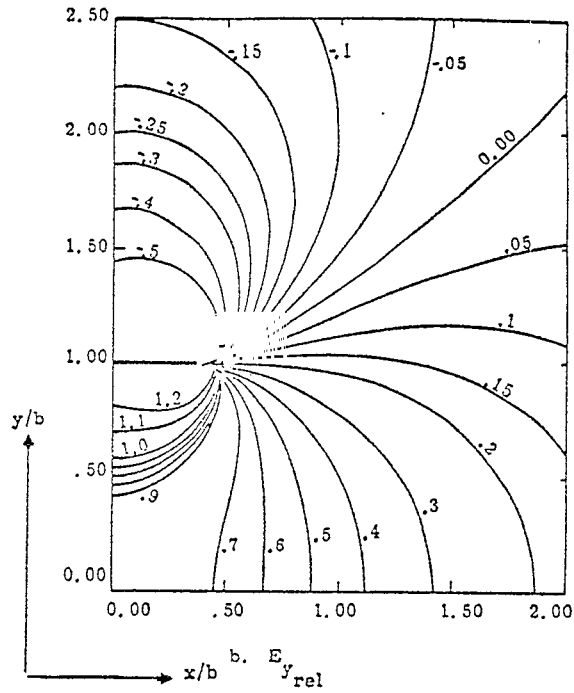


d.  $\left| \frac{[E_{\text{rel}}(x,y) - E_{\text{rel}}(0,0)]}{E_{\text{rel}}(0,0)} \right|$

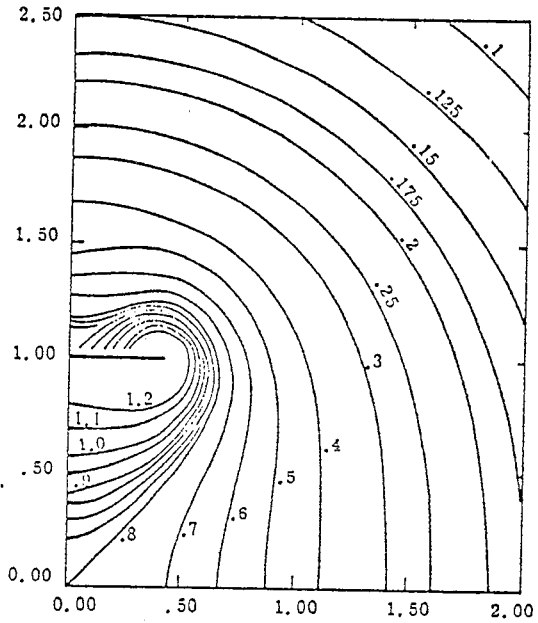
Figure 4.15.  $b/ = 0$



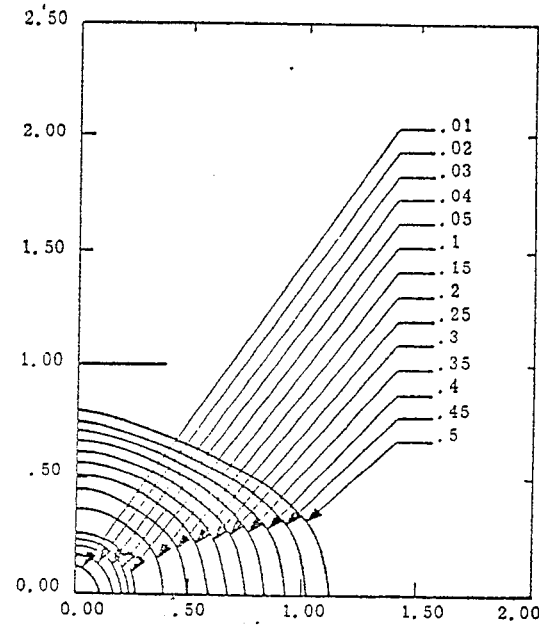
a.  $E_{x\text{ rel}}$



b.  $E_{y\text{ rel}}$

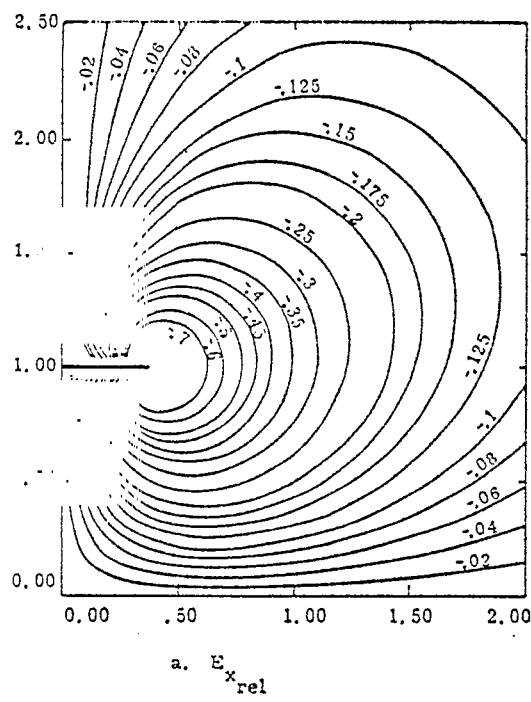


c.  $|E_{\text{rel}}|$

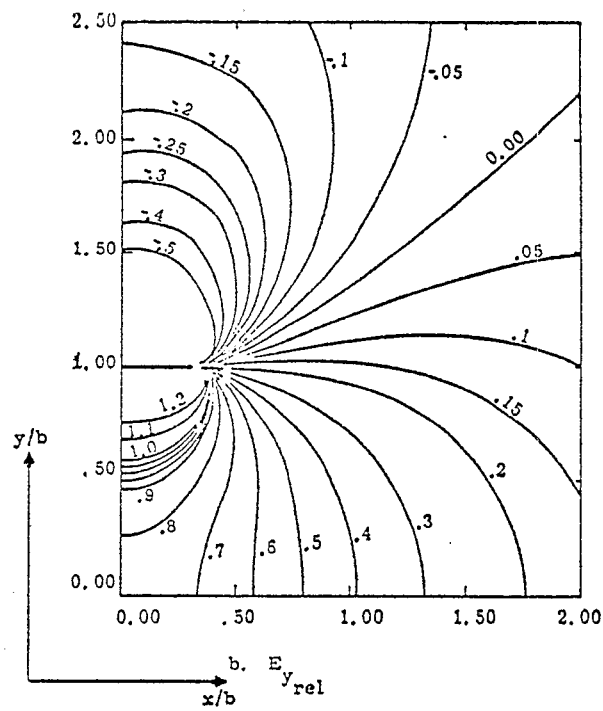


d.  $|[E_{\text{rel}}(x,y) - E_{\text{rel}}(0,0)] / E_{\text{rel}}(0,0)|$

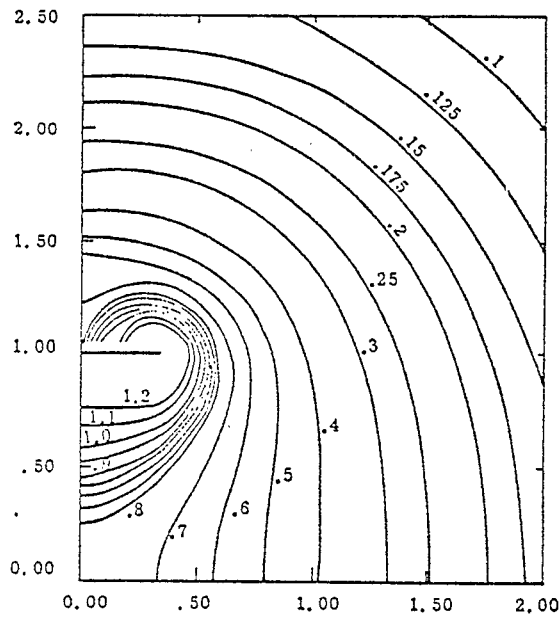
Figure 4.16.  $b/a = 2.5$



a.  $E_{x\text{rel}}$



b.  $E_{y\text{rel}}$



c.  $|E_{\text{rel}}|$

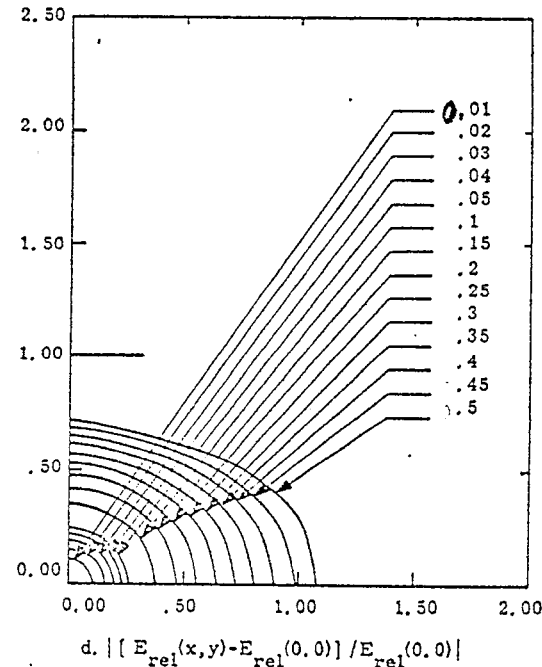


Figure 4.17.  $b/a = 3.0$

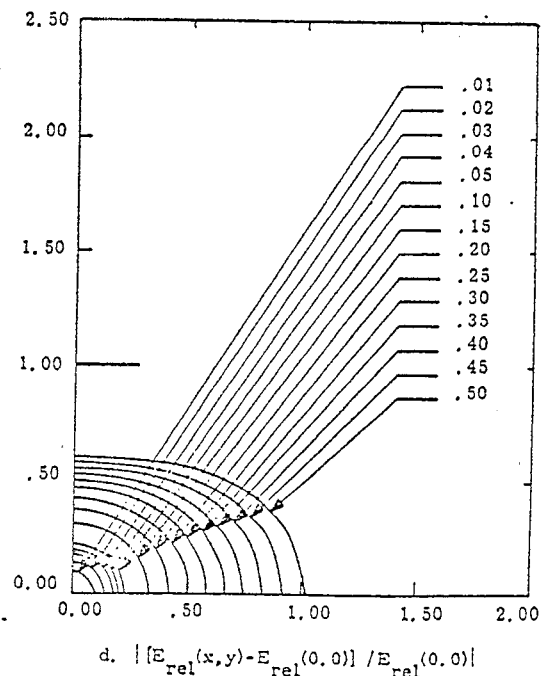
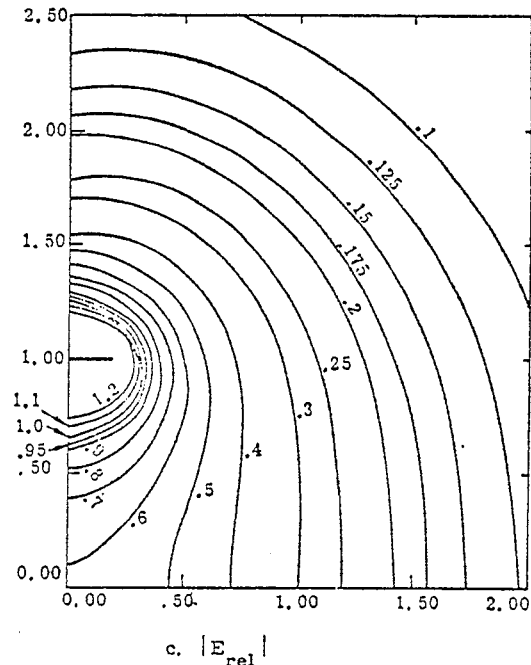
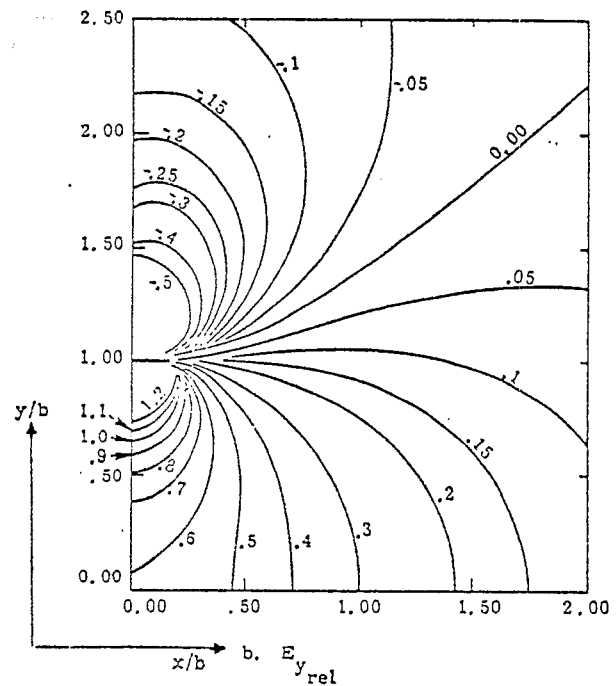
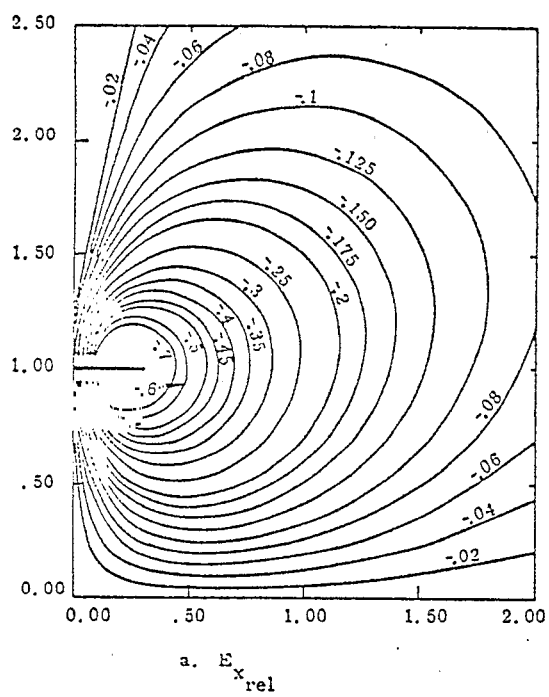


Figure 4.18.  $b/a = 6.99$

The contour plots were generated by making use of a family of computer programs titled BRUT in reference 11.

### B. Plots of field components

In this subsection we compute, using equations 4.2, 4.10 and 4.11, the x and y components of relative electric (equivalently, magnetic also) field. The unnormalized complex field ( $dw/dz$ ) in equations 4.10 and 4.11 is determined from equation 4.2 by using the value of w obtained by the SGB technique as a solution of equation 4.12.

$E_{x\text{rel}}(x, y)$  and  $E_{y\text{rel}}(x, y)$  (or  $H_{y\text{rel}}(x, y)$  and  $-H_{x\text{rel}}(x, y)$ ) are once again computed for the 17 configurations of the parallel-plate geometries described in table 4.1. The field components are computed as a function of  $(x/b)$  for fixed values of  $y/b$  at 0.0, 0.2, 0.4, 0.6, 0.8 and 0.9. These are shown plotted in figures 4.19 through 4.35. In all these plots, the value of the normalized x coordinate (i.e.,  $x/b$ ) ranges from 0 to nearly  $(a/b) + 2$ . The special cases of  $(y/b) = 1.0^-$  and  $1.0^+$  which correspond to the lines just below and above the plate are not considered numerically. For these special lines, however, the conformal transformation simplifies considerably and this and other special cases are analytically illustrated in Appendix B.

As may be expected, the plots of  $E_{x\text{rel}}(x, y)$  and  $E_{y\text{rel}}(x, y)$  respectively display "valleys" and "peaks" under the plate edge. These valleys and peaks grow as  $(y/b)$  is increased from 0 to 1. In all of these plots (figures 4.19 through 4.35) the numerically computed points on each curve are shown marked. These plots should provide useful guidelines for the design and construction of two-parallel plate transmission line structures.

### C. Tabulation of potentials and fields along the symmetry axes

In this subsection, we tabulate the normalized potentials  $u_{\text{rel}}$ ,  $v_{\text{rel}}$  and the relative normal component  $[E_{y\text{rel}}(x, y)]$  of the electric field along

4.19. FIELD PLOTS FOR B/A = 0.1

The following figures show field plots for  $b/a = 0.1$ . The field components are plotted as a function of normalized  $x$  coordinate ( $x/b$ ) for varying values of normalized  $y$  coordinate ( $y/b$ ). The field components are normalized by their respective values at the center of the cell. The plots are arranged in a grid of 4 rows and 5 columns. The first column contains plots for  $y/b = 0.0$ , the second column for  $y/b = 0.1$ , the third column for  $y/b = 0.2$ , the fourth column for  $y/b = 0.3$ , and the fifth column for  $y/b = 0.4$ . The plots show the variation of normalized field components with normalized  $x$  coordinate for different normalized  $y$  coordinates.

Figures 4.19 through 4.35

Plots of normalized field components ( $E_{x_{\text{rel}}}$ ,  $E_{y_{\text{rel}}}$  or equivalently  $H_{y_{\text{rel}}}$ ,  $-H_{x_{\text{rel}}}$ ) as a function of normalized  $x$  coordinate ( $x/b$ ) for varying values of normalized  $y$  coordinate ( $y/b$ ); seventeen figures correspond to the seventeen values of  $b/a$  listed in table 4.1.

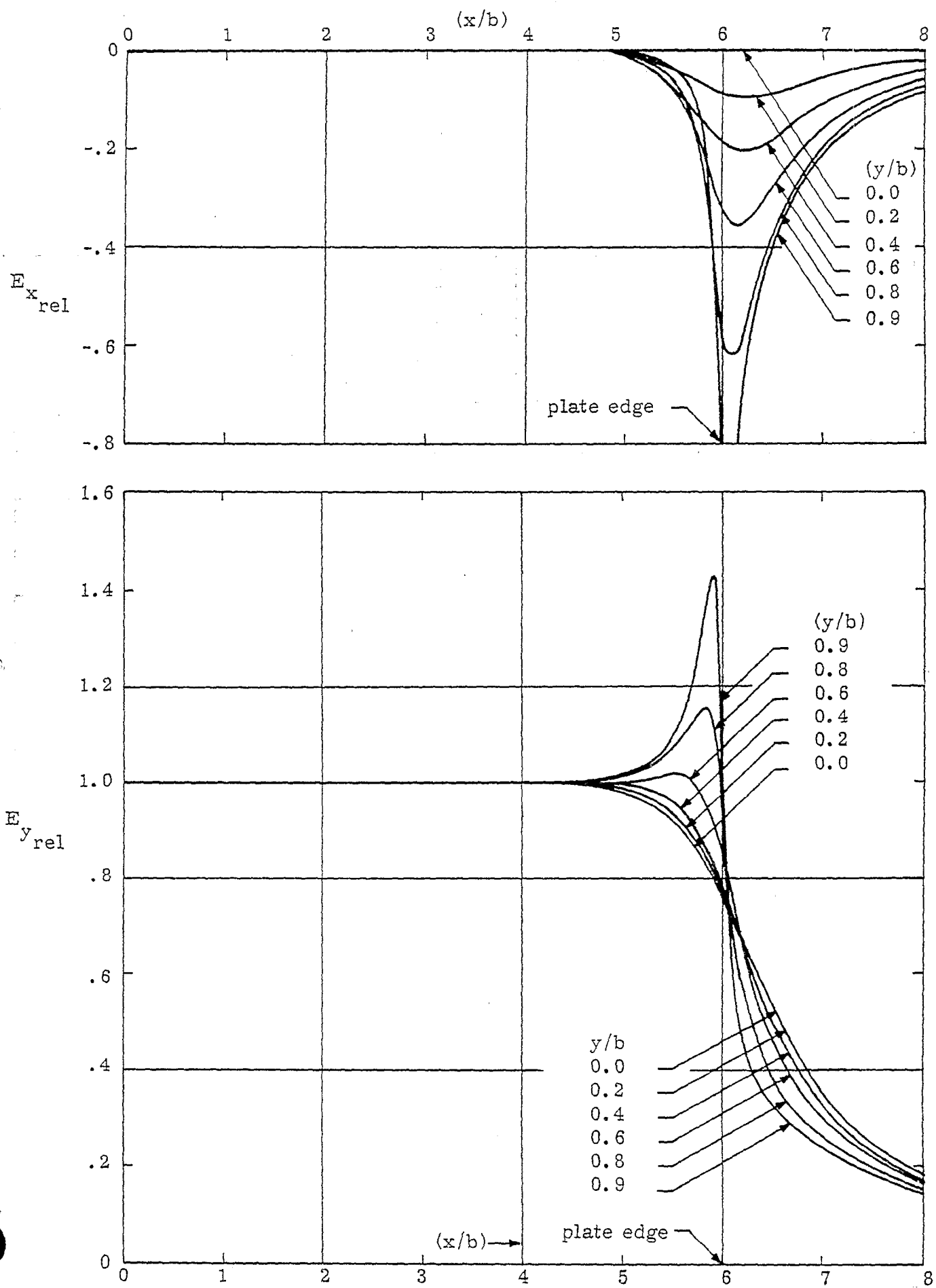


Figure 4.19.  $b/a = 0.1667$

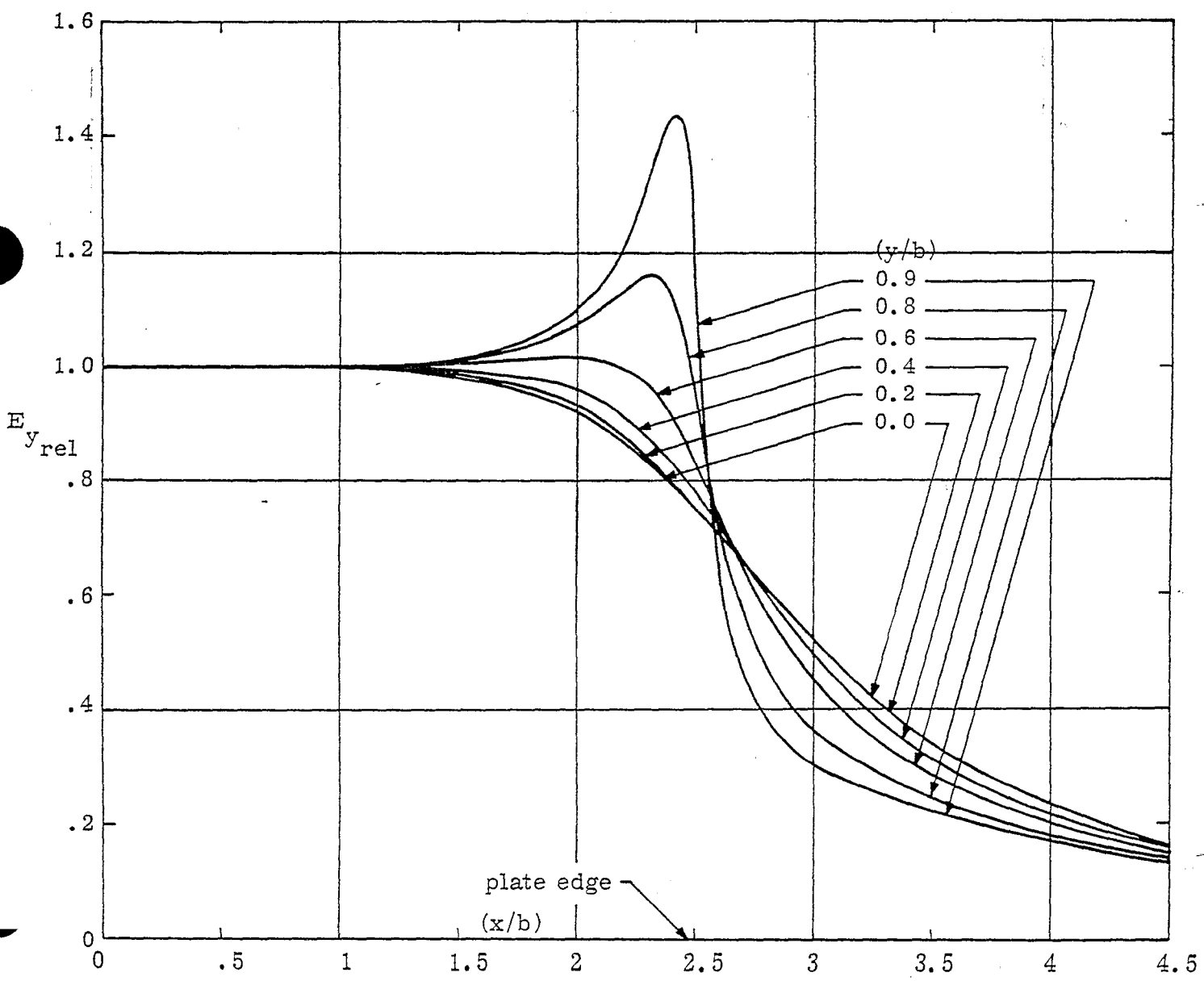
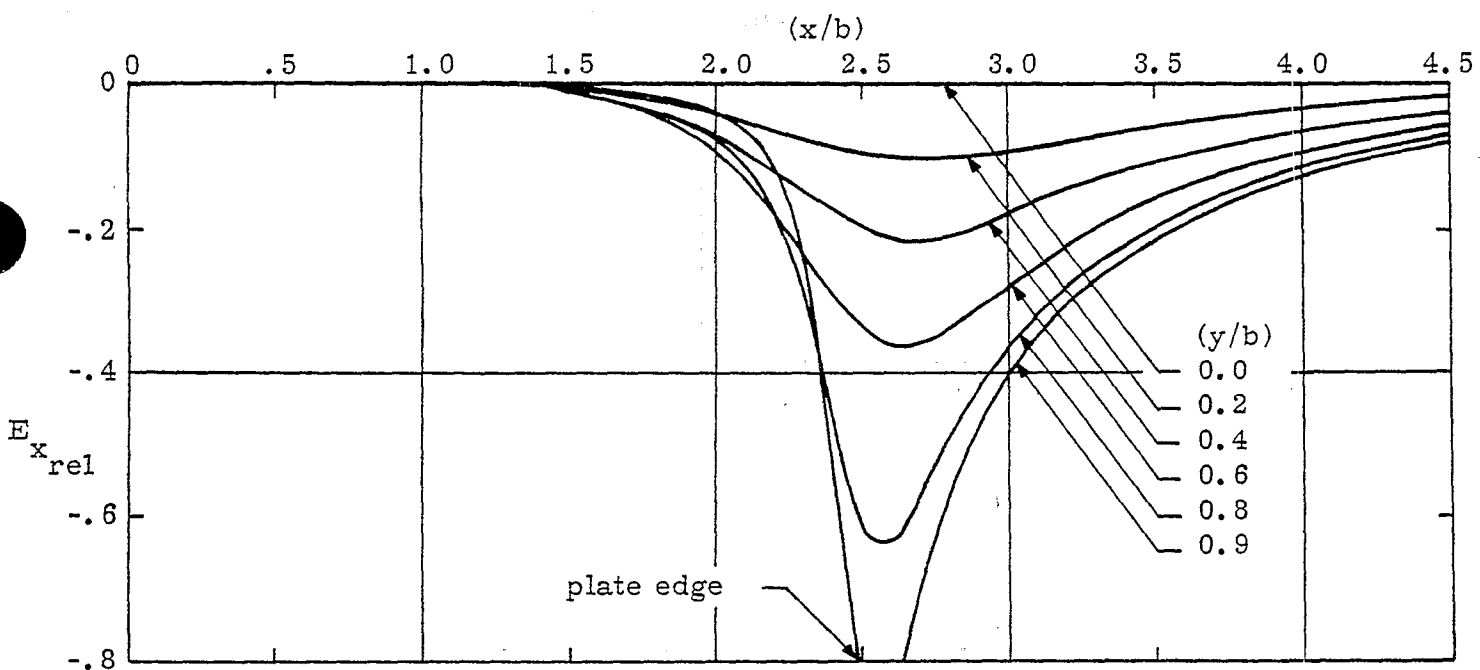


Figure 4.20.  $(b/a) = .40679$

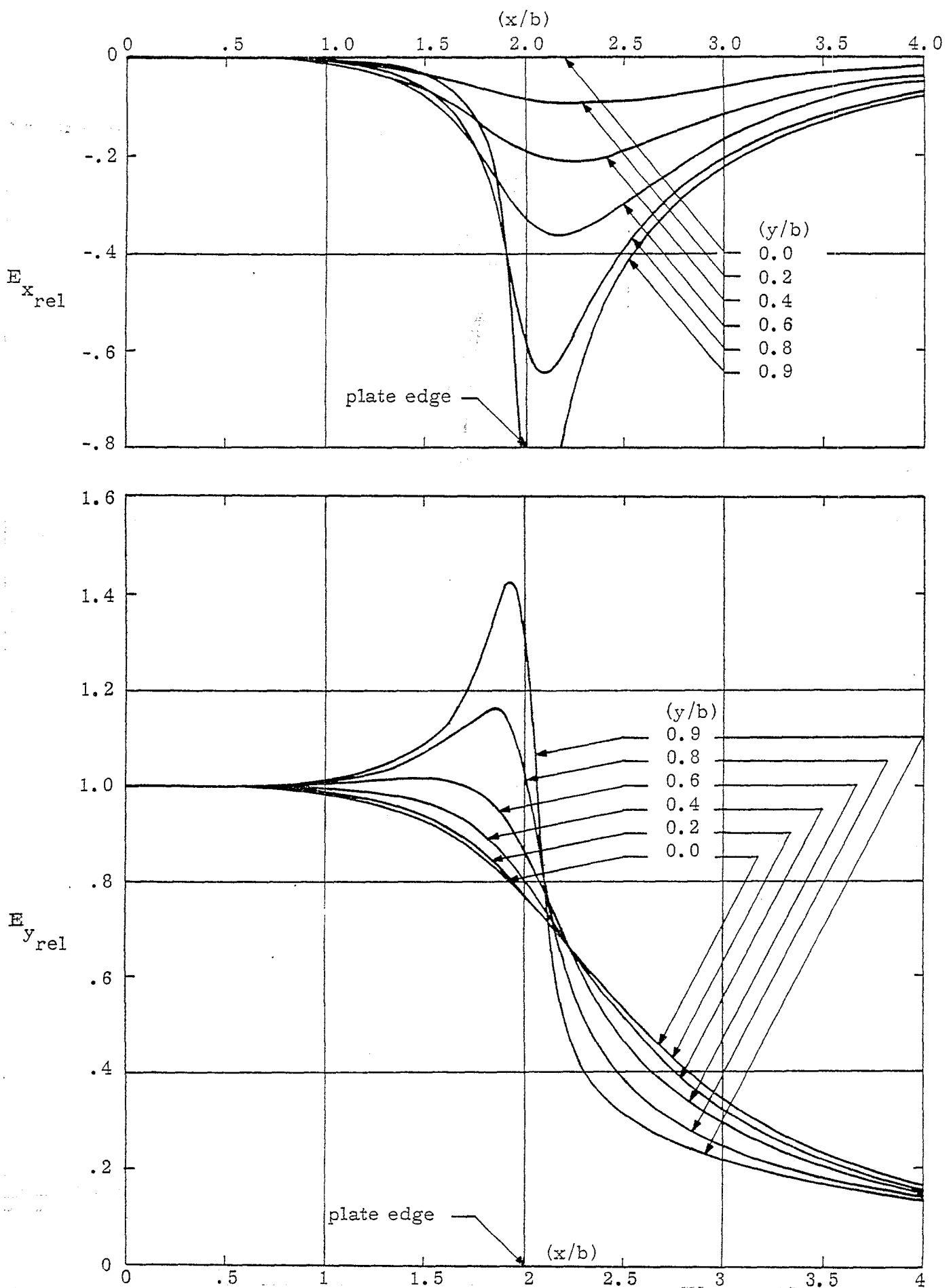


Figure 4.21.  $(b/a) = .5$

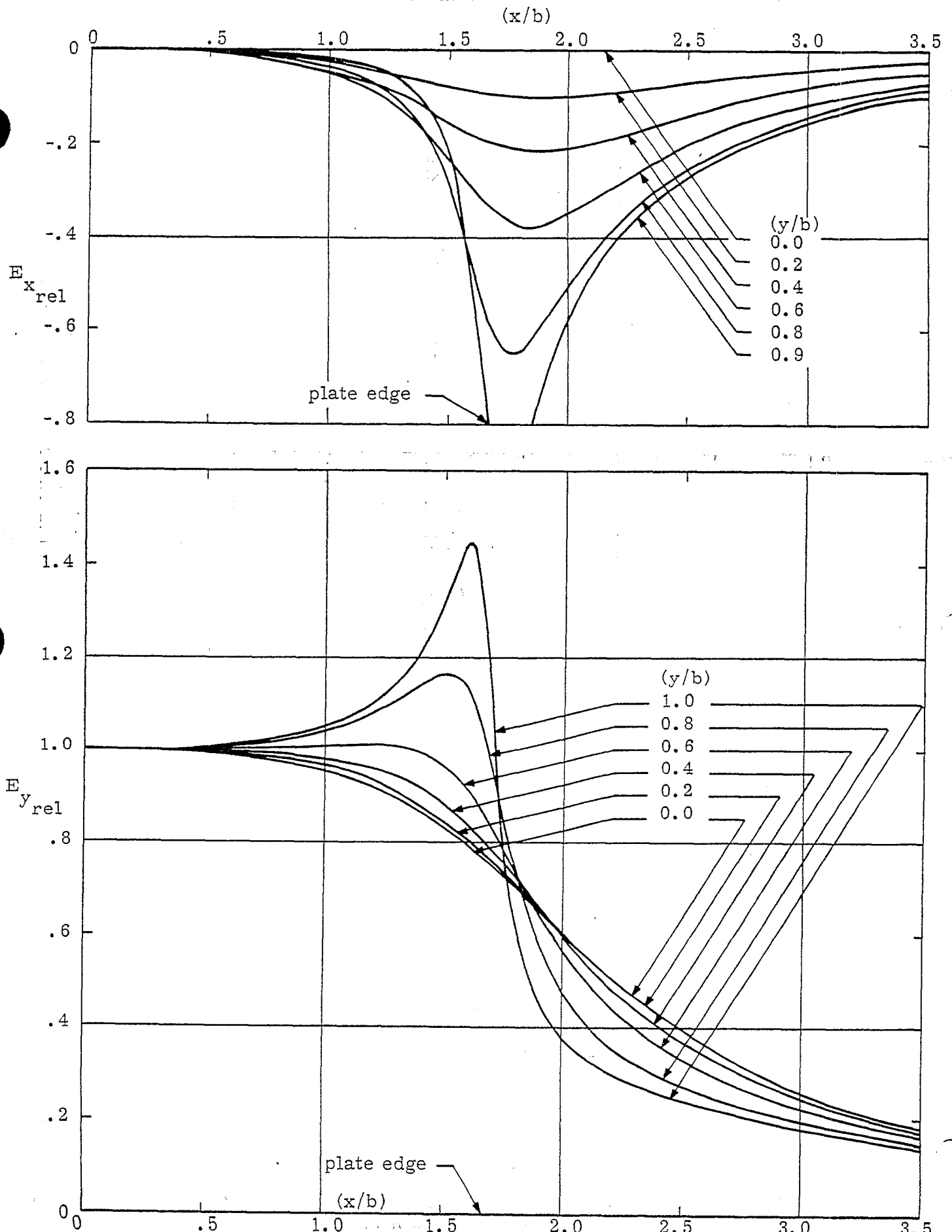


Figure 4.22.  $(b/a) = .60$

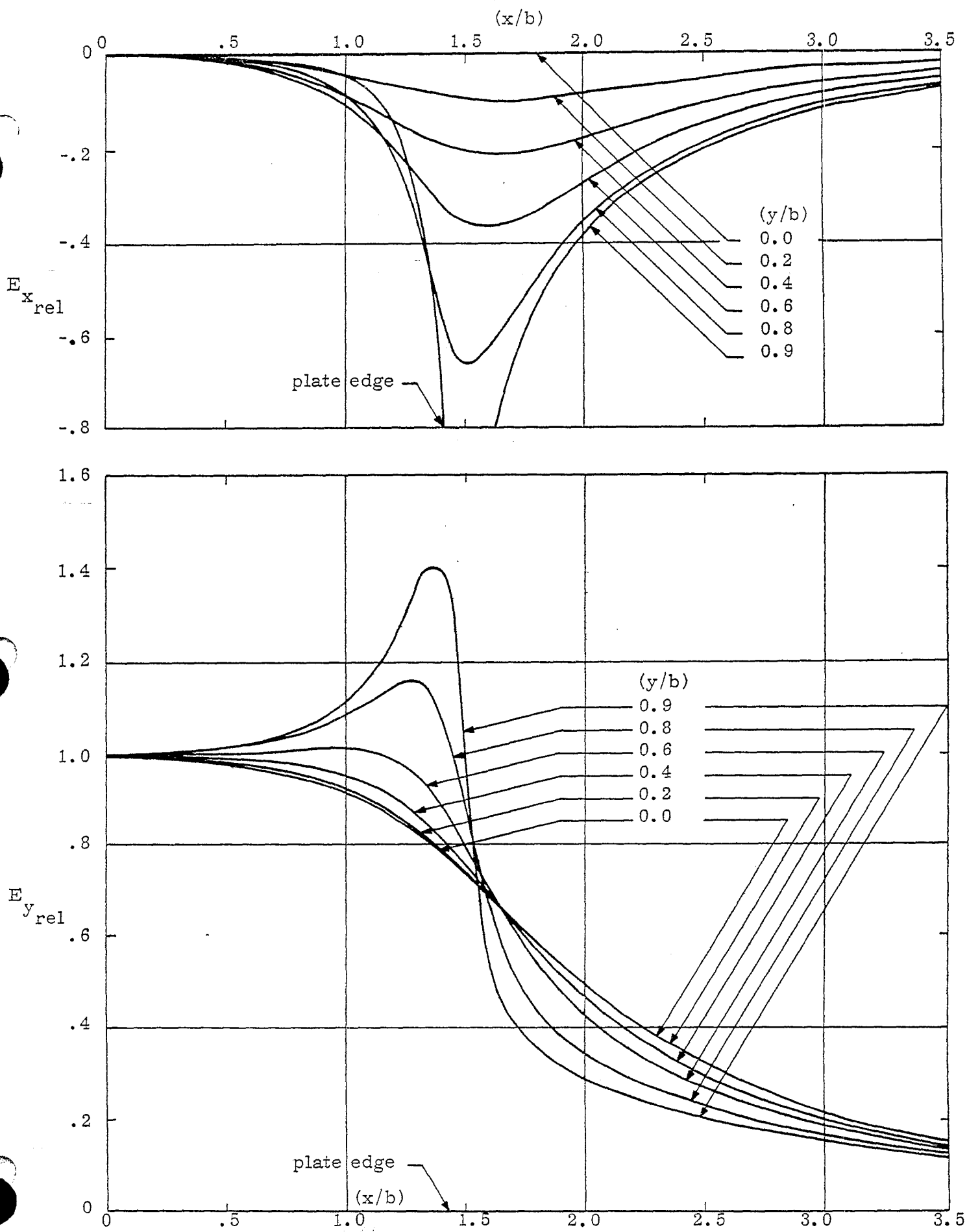


Figure 4.23.  $(b/a) = .70$

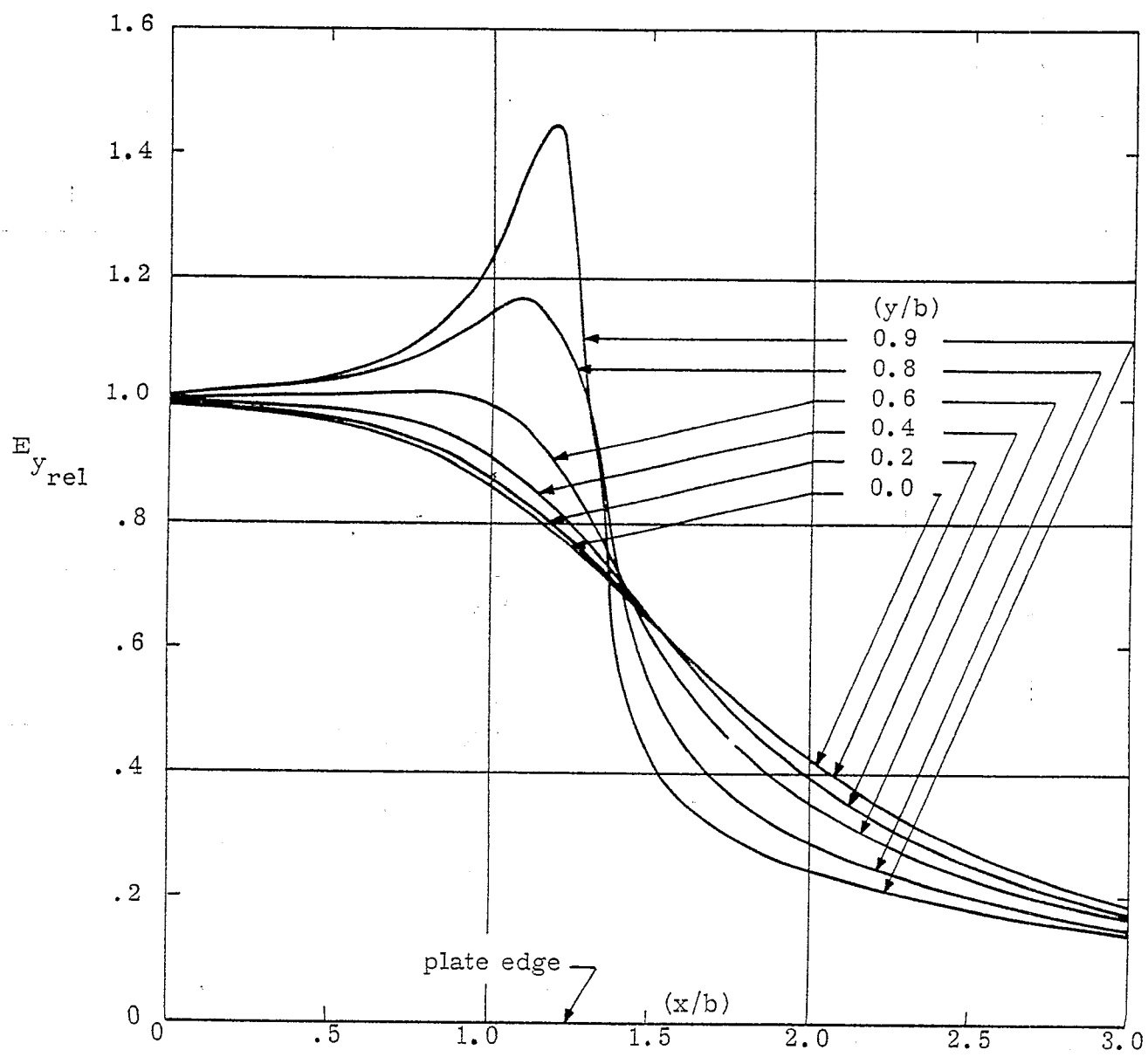
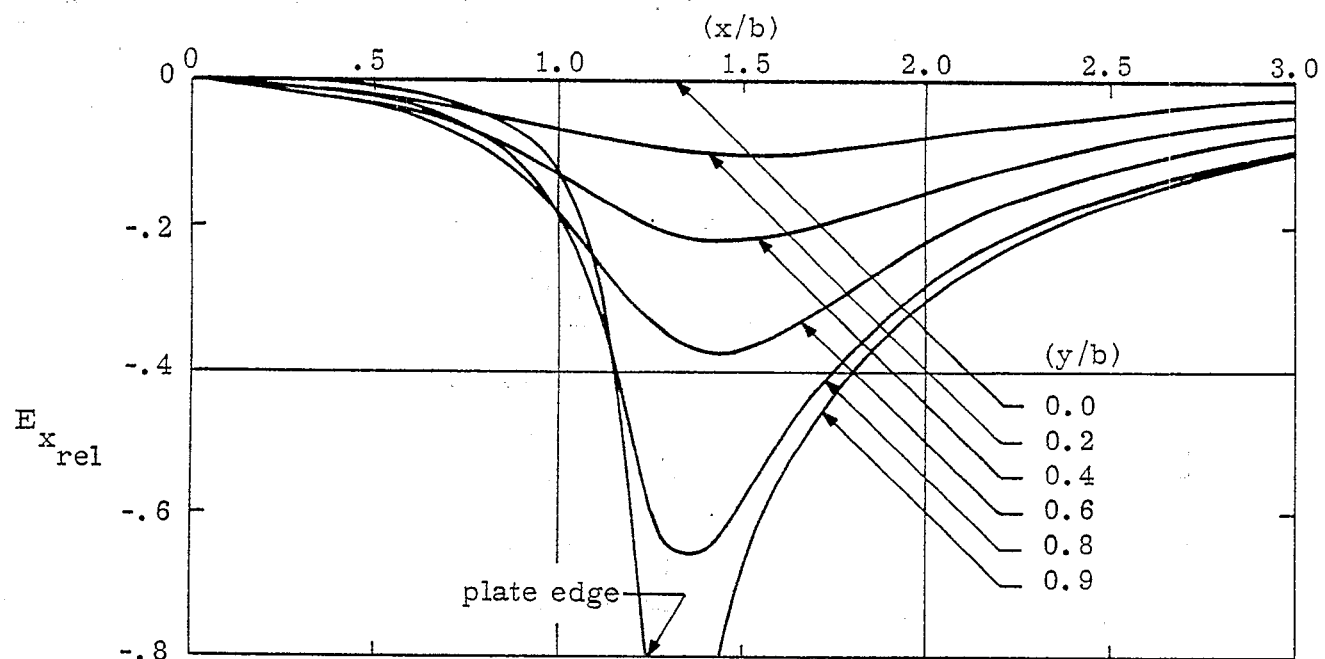


Figure 4.24.  $(b/a) = .80$

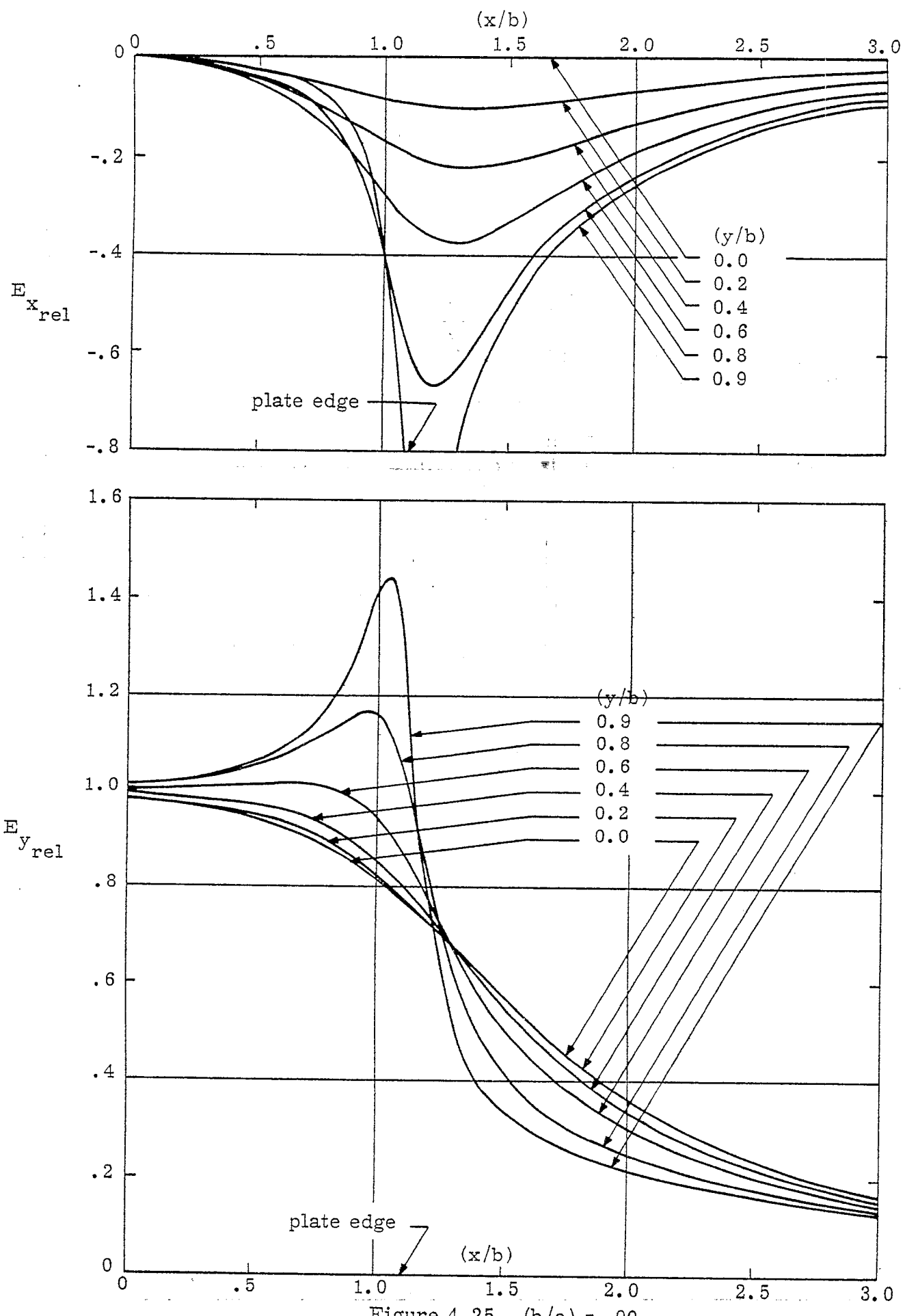


Figure 4.25.  $(b/a) = .90$

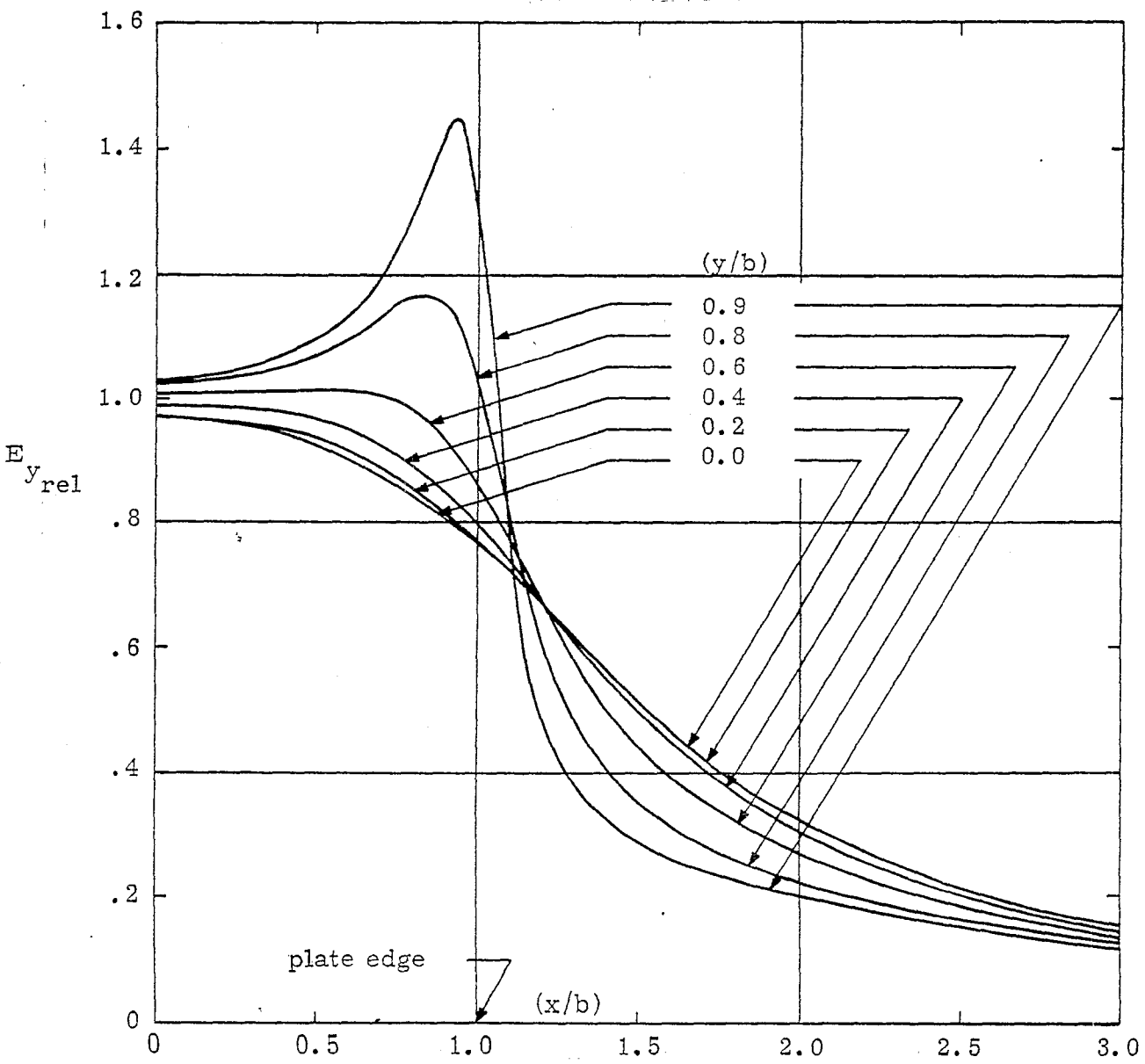
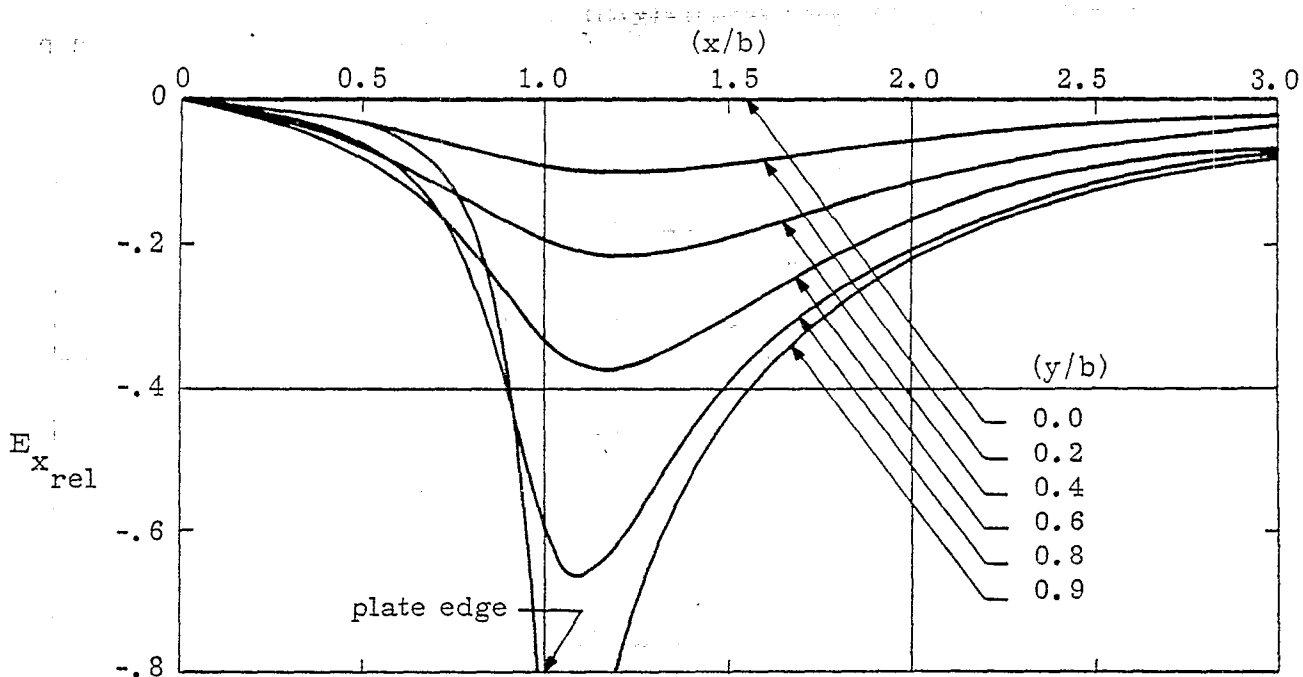


Figure 4.26.  $(b/a) = 1.00$

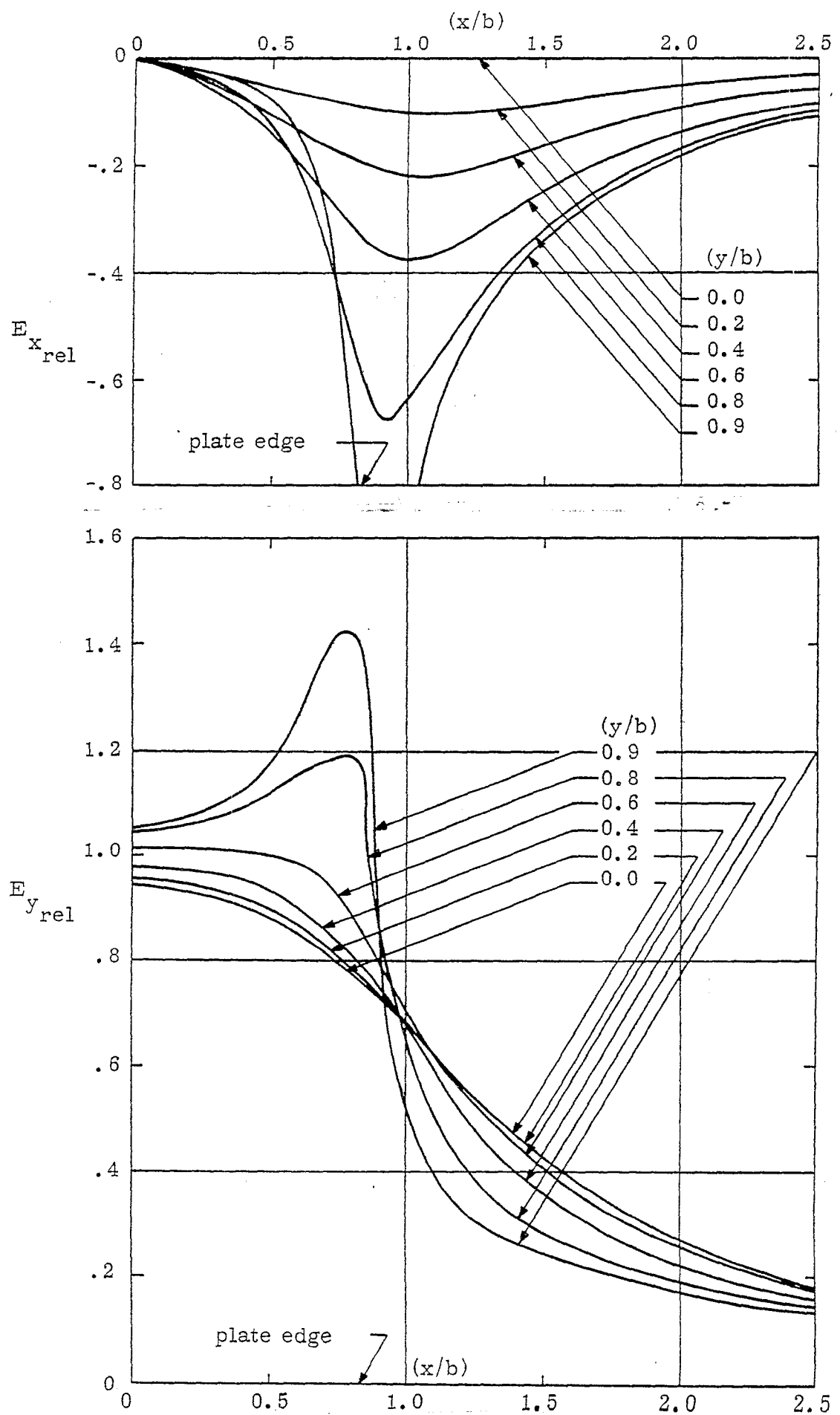


Figure 4.27.  $(b/a) = 1.20$

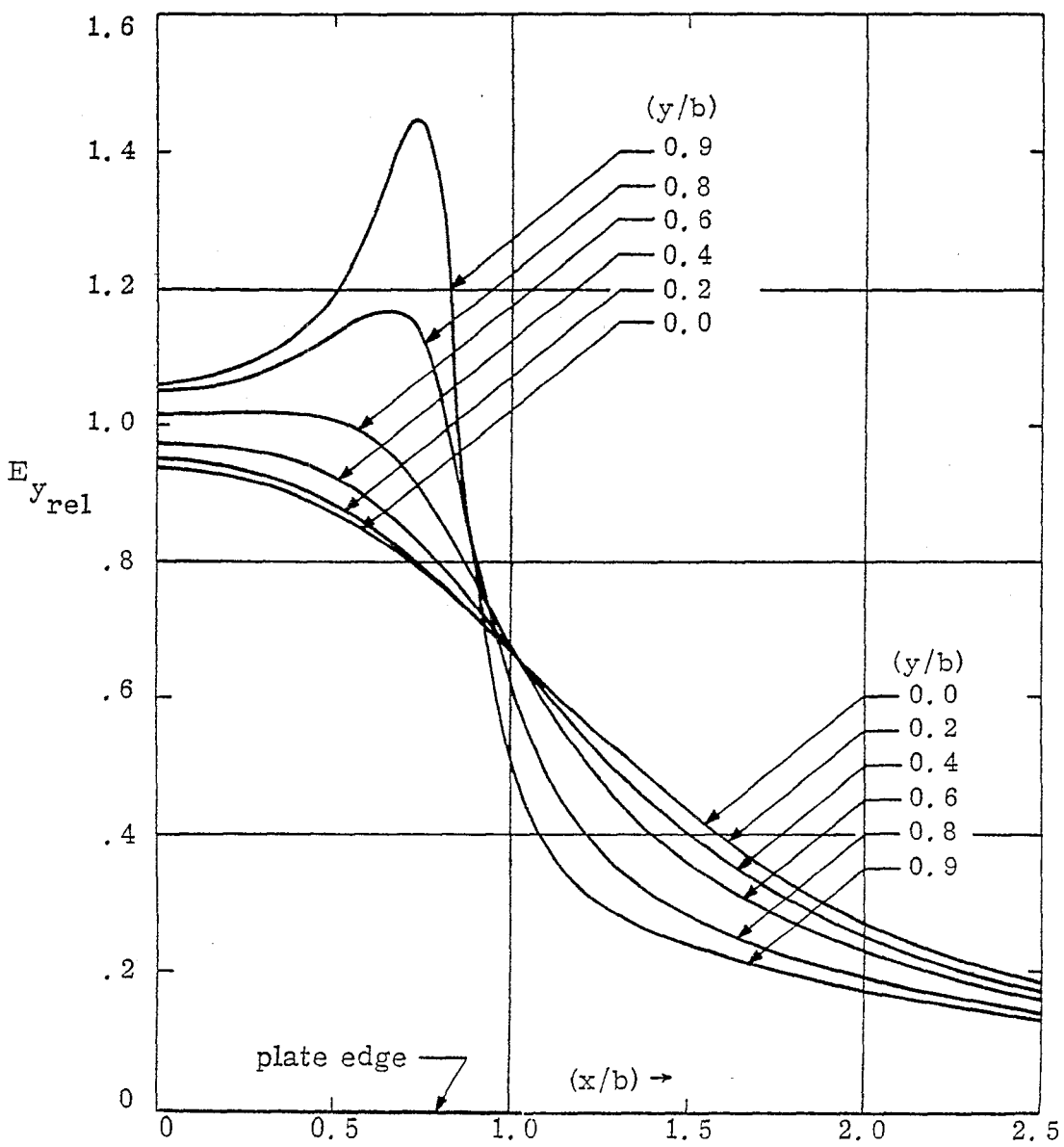
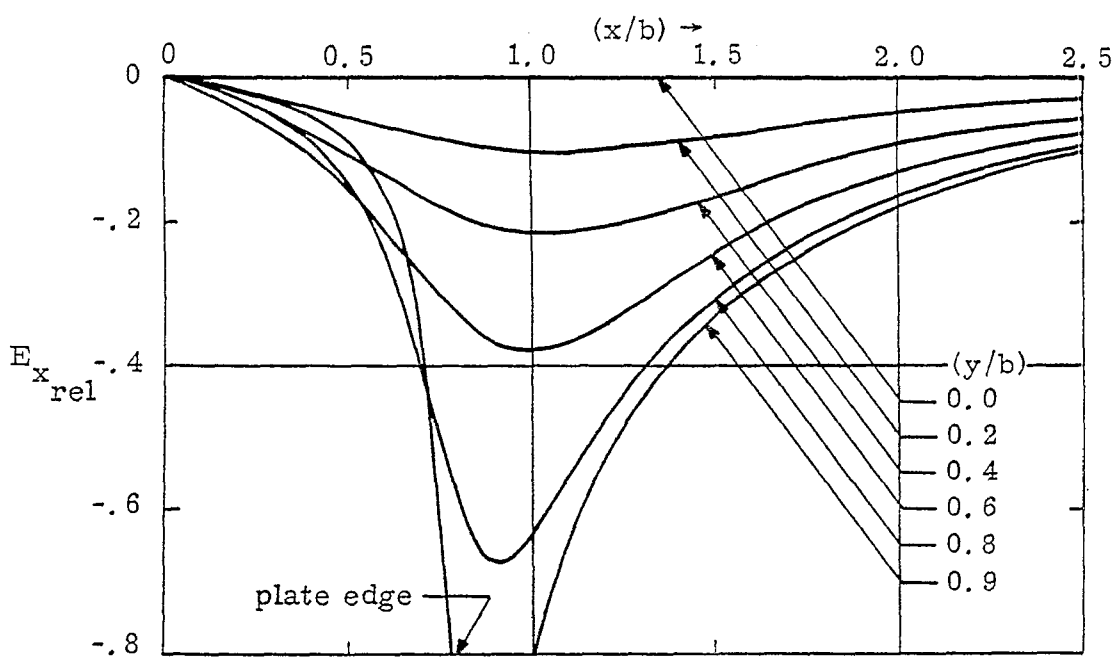


Figure 4.28.  $(b/a) = 1.23526$

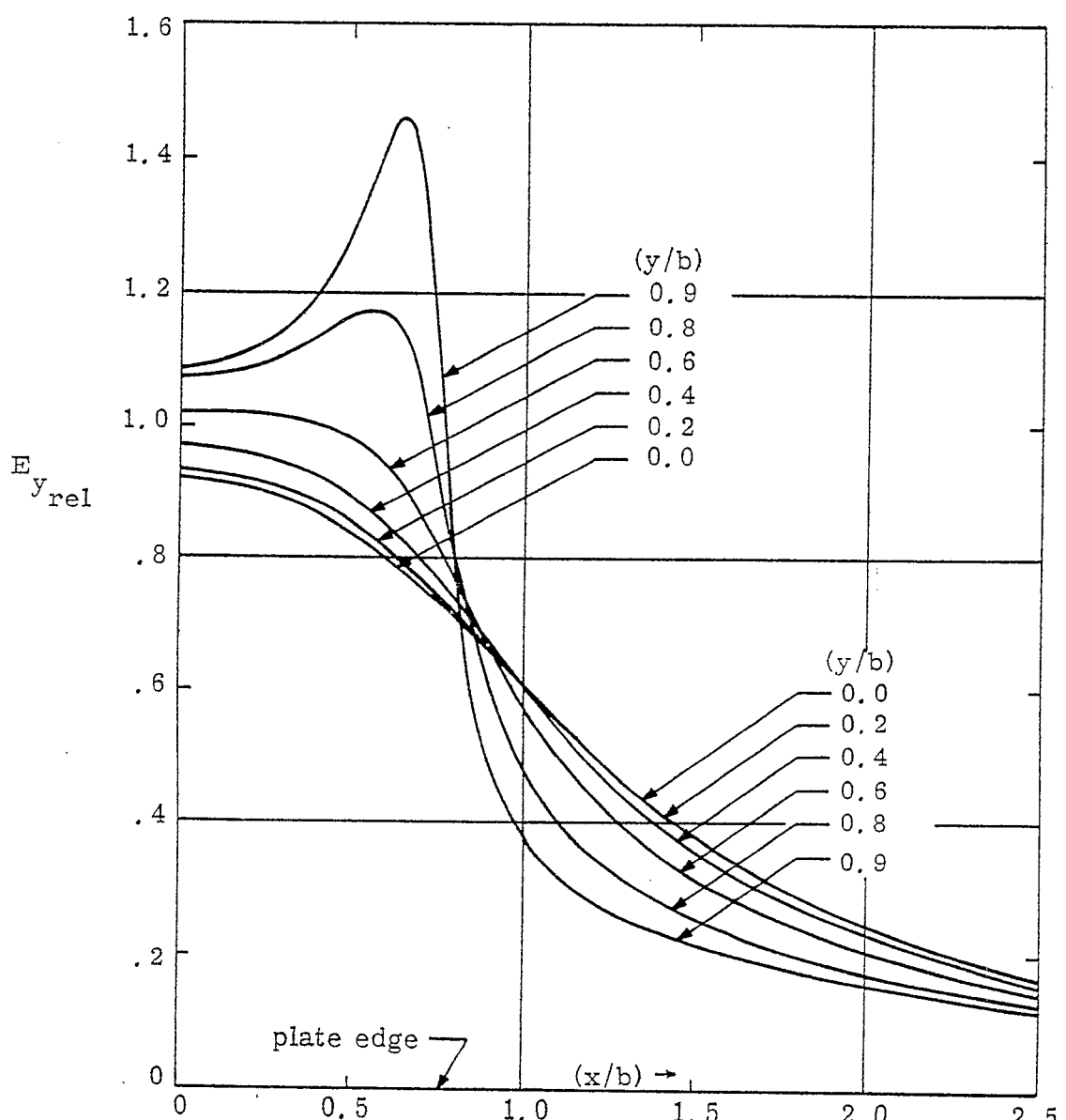
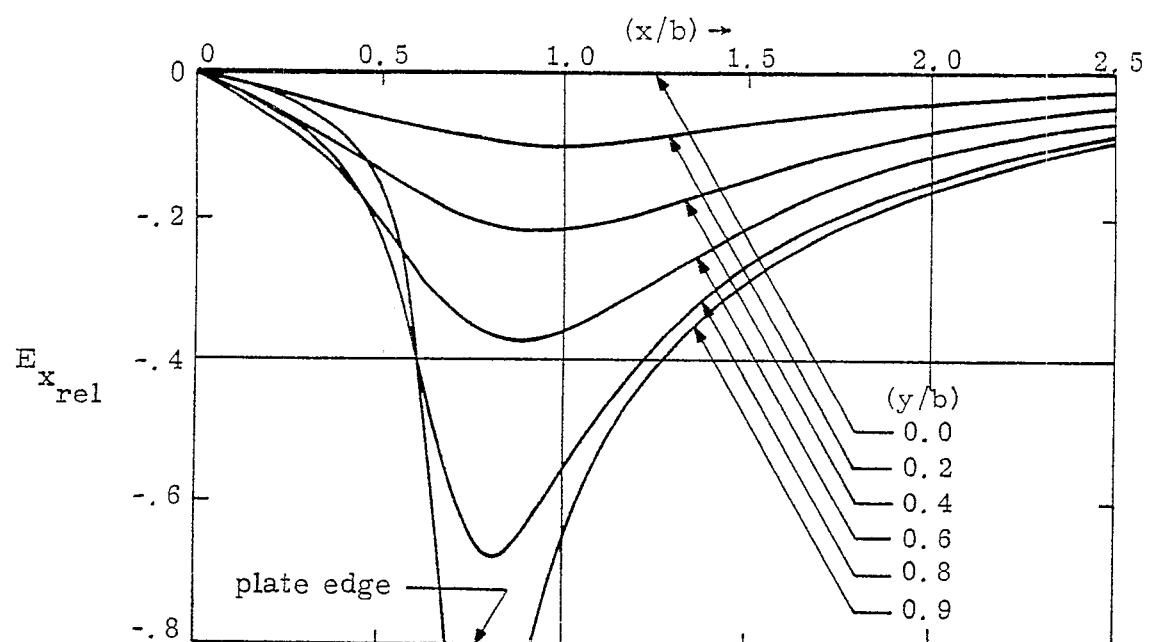


Figure 4.29.  $(b/a) = 1.4$

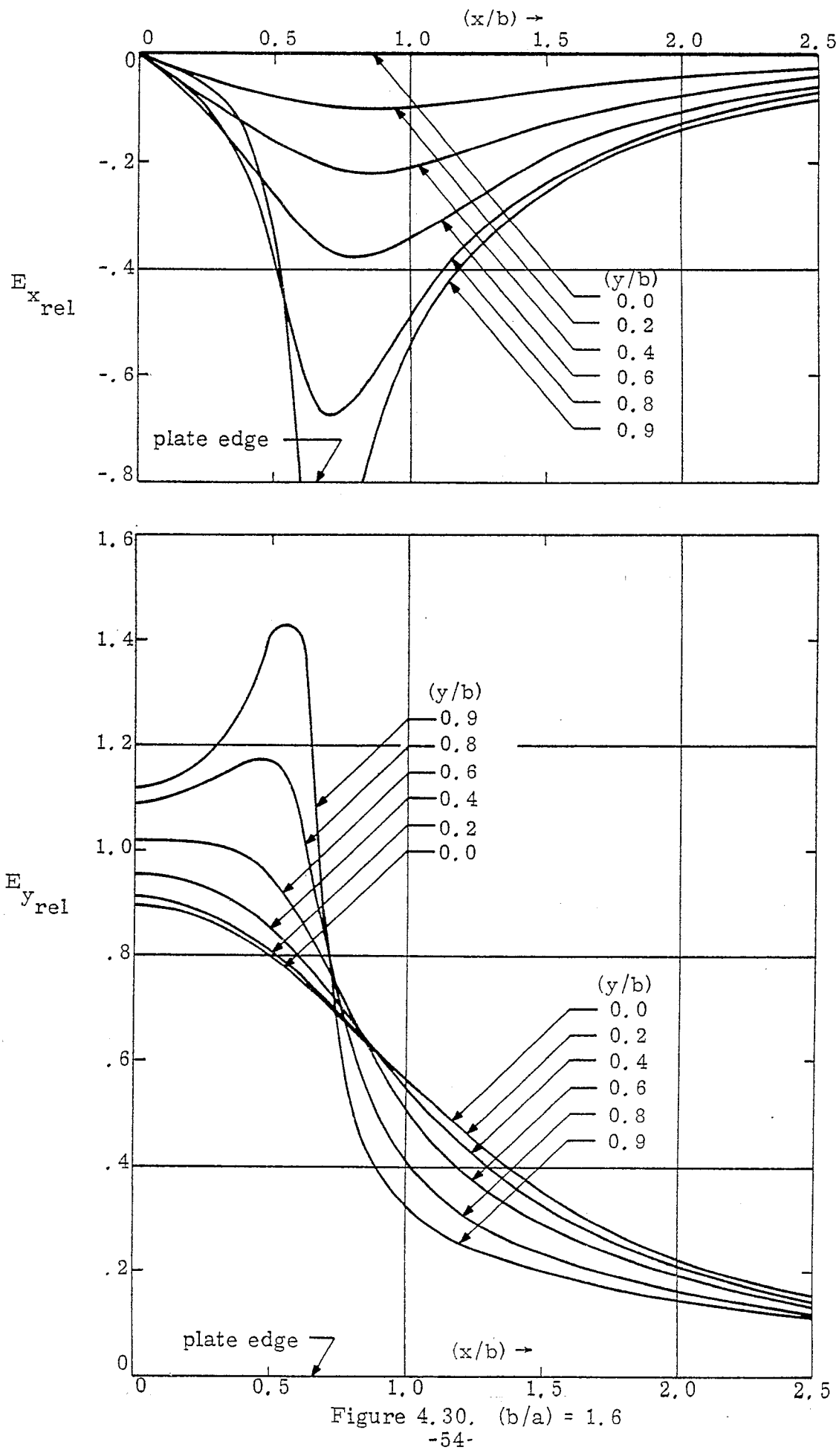


Figure 4.30.  $(b/a) = 1.6$

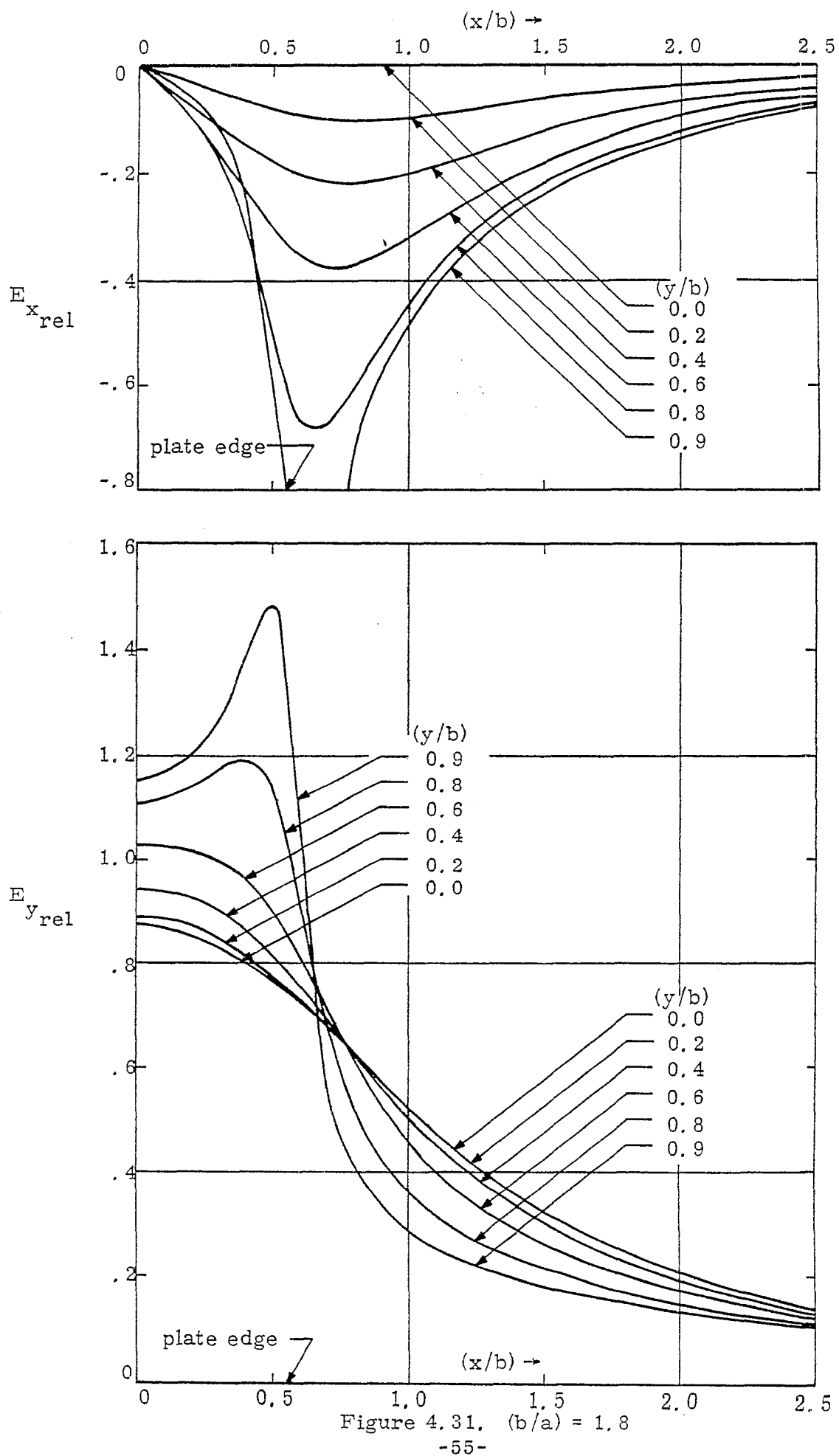


Figure 4.31.  $(b/a) = 1.8$

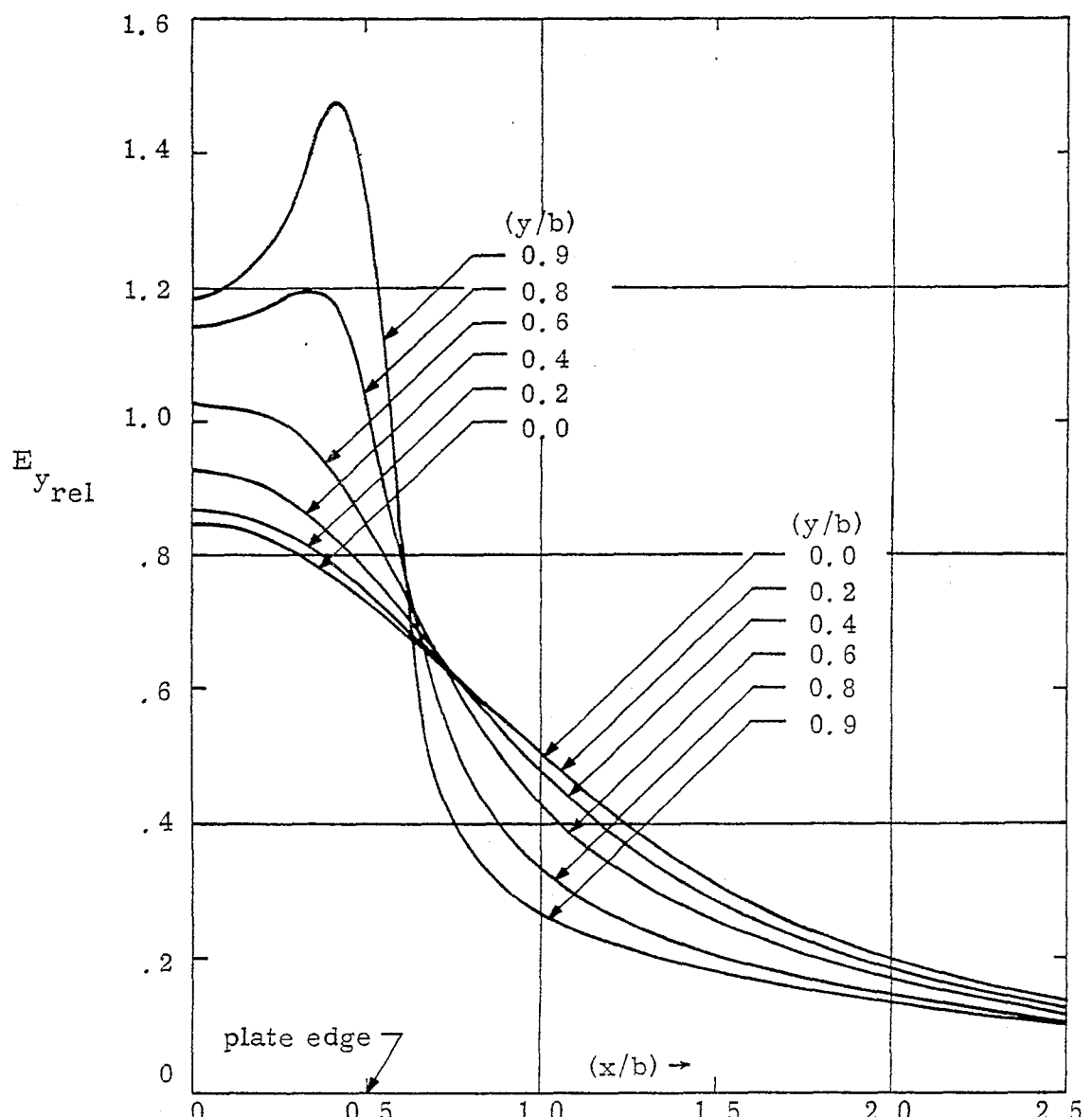
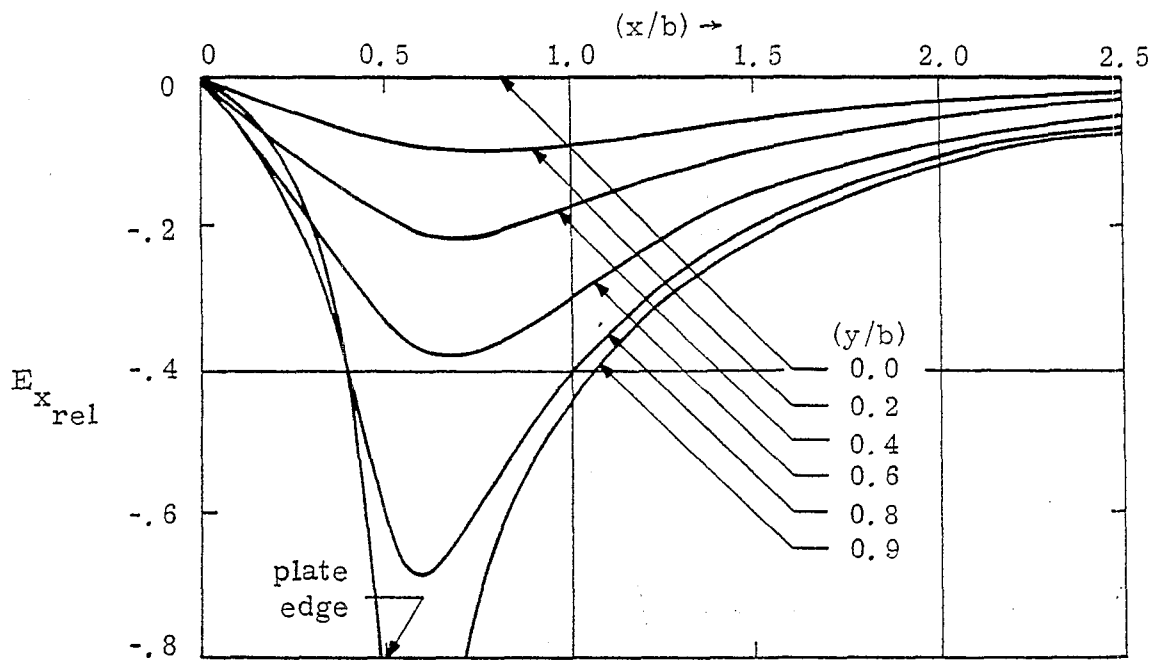


Figure 4.32.  $(b/a) = 2.0$

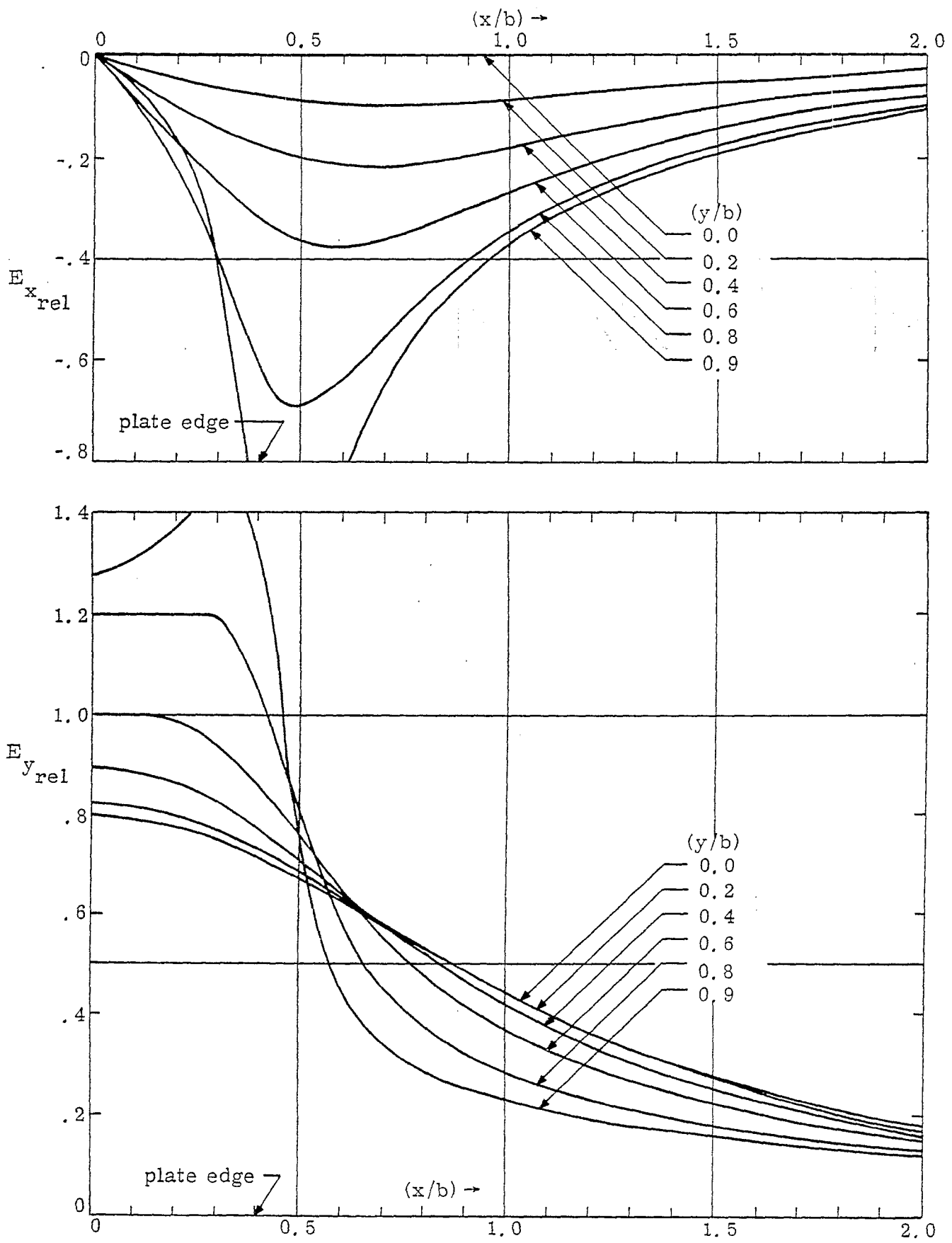


Figure 4.33.  $(b/a) = 2.5$

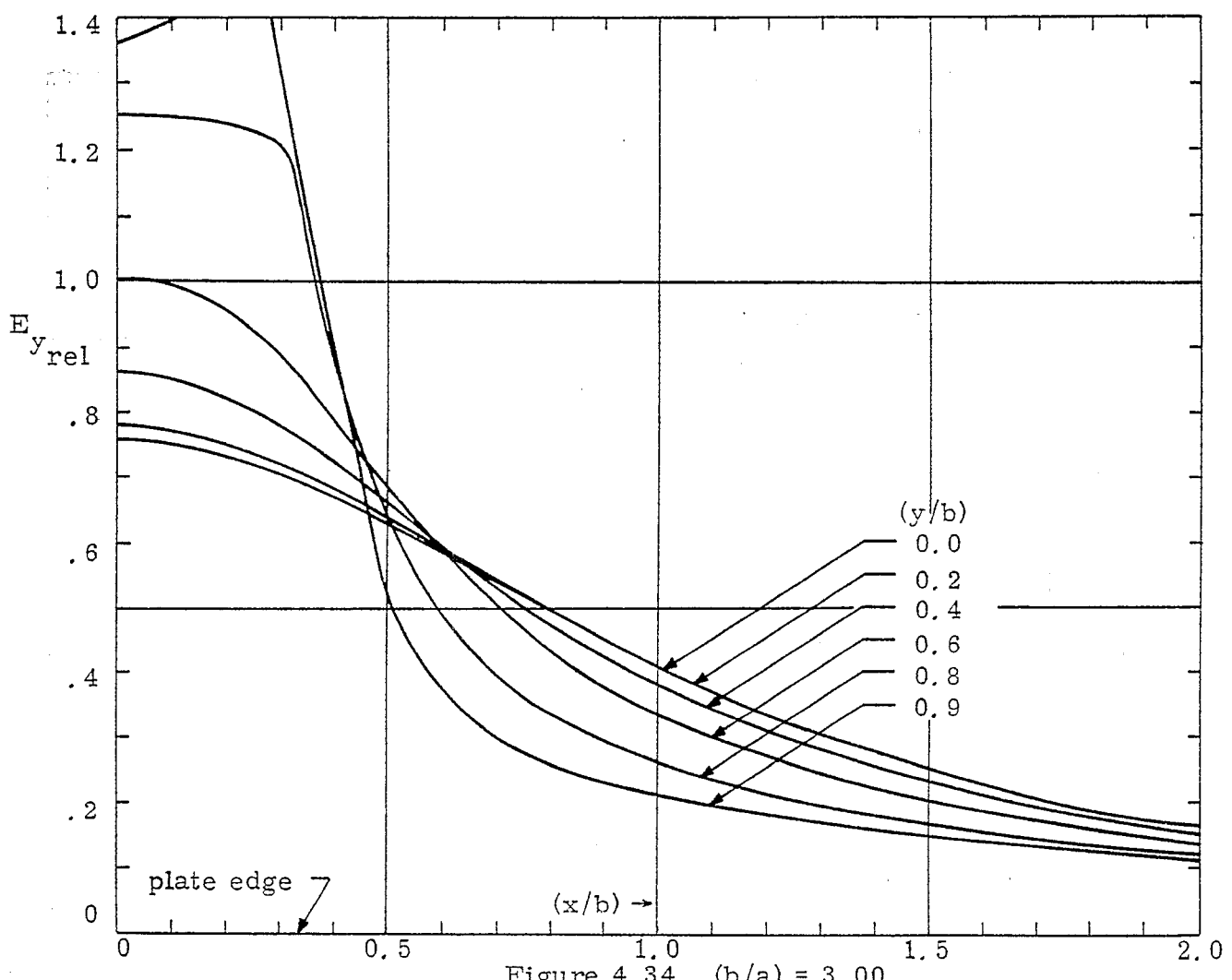
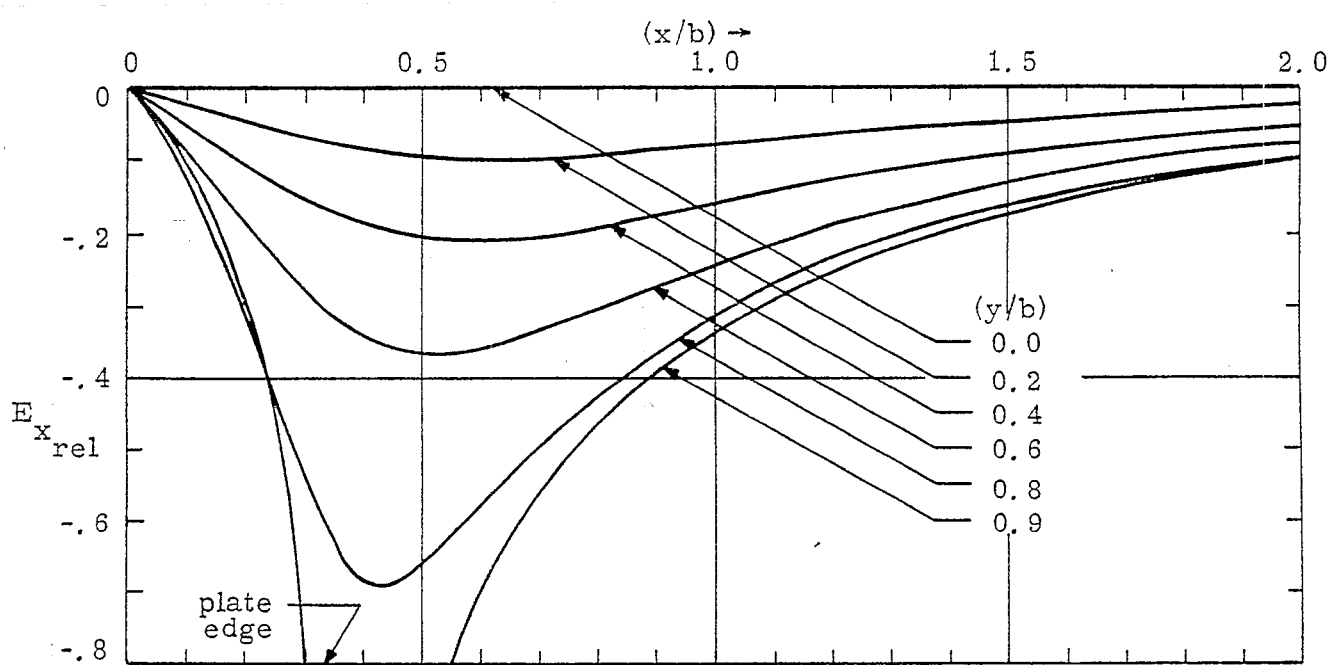


Figure 4.34.  $(b/a) = 3,00$

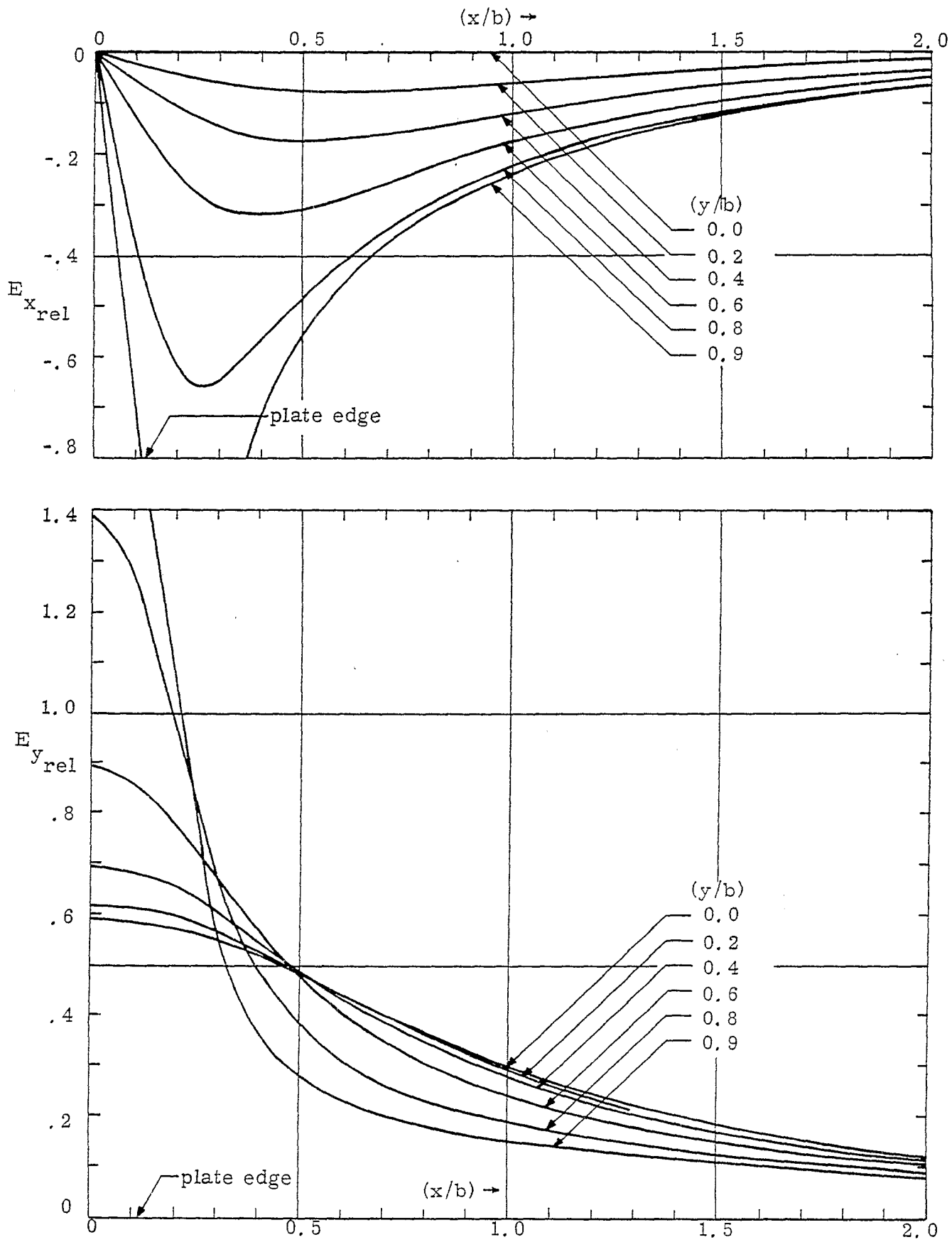


Figure 4.35.  $(b/a) = 6.99$

the two symmetry axes, i.e.,  $(y/b) = 0$  and  $(x/b) = 0$ . When  $(x/b) = 0$ ,  $(y/b)$  ranges from 0 to 1, whereas along the axis  $(y/b) = 0$ ,  $(x/b)$  ranges from 0 to nearly  $(a/b) + 2$ . Once again, the tabulation is done only for  $\xi$  in the first quadrant because of the inherent symmetry in the problem.

Table 4.2 is for the 17 values of  $b/a$  along the line  $(y/b) = 0$  and has  $v_{rel}(x, 0)$  and  $E_{y, rel}(x, 0)$ . The 17 cases considered in this table correspond to the 17 values of  $(b/a)$  described in table 4.1. Table 4.3 contains  $u_{rel}(0, y)$  and  $E_{y, rel}(0, y)$  as a function of  $y/b$  ranging from 0 to 1. By virtue of our normalization scheme described by equation 4.7,  $u_{rel}(0, y)$  attains its maximum value of unity for  $y/b = 1$ .

Table 4.2

Normalized magnetic potential ( $v_{rel}$ ) and normalized y-component of field ( $E_{yrel}$ ) along the symmetry axis  $y/b = 0$  with  $b/a$  as the parameter.

- Note 1. On the symmetry axis  $y/b = 0$ , the normalized electric potential ( $u_{rel}$ ) and the normalized x-component of field ( $E_{xrel}$ ) are both zero for all values of  $x/b$ .
2. See equations 4.7 through 4.11 for the normalization scheme and for the equivalence of electric and magnetic field components.

Case No.	1				
	$b/a = 0.1667, f_g = .13336, Z_c = 50.240\Omega$				
x/b	$v_{rel}$	$E_{Yrel}$	x/b	$v_{rel}$	$E_{Yrel}$
0.00	0.0000	1.0000			
.10	.0133	1.0000	4.10	.5467	.9989
.20	.0267	1.0000	4.20	.5600	.9985
.30	.0400	1.0000	4.30	.5733	.9980
.40	.0533	1.0000	4.40	.5867	.9972
.50	.0667	1.0000	4.50	.5999	.9962
.60	.0800	1.0000	4.60	.6132	.9948
.70	.0934	1.0000	4.70	.6265	.9929
.80	.1067	1.0000	4.80	.6397	.9904
.90	.1200	1.0000	4.90	.6529	.9869
1.00	.1334	1.0000	5.00	.6660	.9823
1.10	.1467	1.0000	5.10	.6791	.9760
1.20	.1600	1.0000	5.20	.6920	.9677
1.30	.1734	1.0000	5.30	.7049	.9568
1.40	.1867	1.0000	5.40	.7175	.9426
1.50	.2000	1.0000	5.50	.7300	.9245
1.60	.2134	1.0000	5.60	.7422	.9017
1.70	.2267	1.0000	5.70	.7540	.8739
1.80	.2400	1.0000	5.80	.7655	.8408
1.90	.2534	1.0000	5.90	.7764	.8028
2.00	.2667	1.0000	6.00	.7869	.7605
2.10	.2801	1.0000	6.10	.7967	.7150
2.20	.2934	1.0000	6.20	.8059	.6679
2.30	.3067	1.0000	6.30	.8145	.6205
2.40	.3201	1.0000	6.40	.8225	.5741
2.50	.3334	1.0000	6.50	.8298	.5298
2.60	.3467	1.0000	6.60	.8366	.4883
2.70	.3601	1.0000	6.70	.8429	.4499
2.80	.3734	1.0000	6.80	.8486	.4148
2.90	.3867	1.0000	6.90	.8540	.3829
3.00	.4001	1.0000	7.00	.8589	.3541
3.10	.4134	1.0000	7.10	.8634	.3282
3.20	.4267	.9999	7.20	.8676	.3048
3.30	.4401	.9999	7.30	.8715	.2837
3.40	.4534	.9999	7.40	.8752	.2648
3.50	.4667	.9998	7.50	.8786	.2477
3.60	.4801	.9998	7.60	.8818	.2322
3.70	.4934	.9997	7.70	.8848	.2182
3.80	.5067	.9996	7.80	.8876	.2054
3.90	.5201	.9994	7.90	.8903	.1938
4.00	.5334	.9992			

Table 4.2

Case No.	2		3		4	
b/a = f <sub>g</sub> = Z <sub>c</sub> = x/b	0.40679		0.5		0.6	
	0.26534		0.30642		0.34613	
	99.961Ω		115.439Ω		130.397Ω	
v <sub>rel</sub>	E <sub>yrel</sub>	v <sub>rel</sub>	E <sub>yrel</sub>	v <sub>rel</sub>	E <sub>yrel</sub>	
0.00	0.0000	.9997	0.0000	.9986	0.0000	.9959
.10	.0265	.9996	.0306	.9985	.0345	.9957
.20	.0530	.9996	.0612	.9983	.0689	.9950
.30	.0796	.9995	.0918	.9979	.1033	.9939
.40	.1061	.9994	.1223	.9973	.1377	.9922
.50	.1326	.9991	.1529	.9964	.1720	.9898
.60	.1591	.9989	.1834	.9952	.2062	.9864
.70	.1856	.9984	.2139	.9935	.2403	.9817
.80	.2121	.9979	.2443	.9912	.2742	.9754
.90	.2386	.9971	.2746	.9880	.3078	.9670
1.00	.2650	.9961	.3048	.9837	.3411	.9558
1.10	.2914	.9946	.3349	.9780	.3739	.9414
1.20	.3178	.9927	.3647	.9704	.4062	.9228
1.30	.3441	.9901	.3943	.9603	.4377	.8995
1.40	.3703	.9865	.4236	.9470	.4684	.8710
1.50	.3964	.9817	.4523	.9300	.4980	.8371
1.60	.4224	.9752	.4805	.9085	.5263	.7979
1.70	.4482	.9666	.5079	.8820	.5532	.7543
1.80	.4737	.9553	.5345	.8500	.5785	.7075
1.90	.4988	.9407	.5600	.8128	.6021	.6588
2.00	.5236	.9220	.5843	.7709	.6241	.6097
2.10	.5477	.8985	.6072	.7252	.6443	.5618
2.20	.5712	.8699	.6287	.6773	.6630	.5160
2.30	.5938	.8359	.6487	.6285	.6801	.4730
2.40	.6155	.7968	.6672	.5803	.6958	.4334
2.50	.6361	.7535	.6843	.5340	.7101	.3972
2.60	.6555	.7069	.7000	.4903	.7233	.3643
2.70	.6736	.6588	.7144	.4497	.7354	.3347
2.80	.6904	.6104	.7276	.4125	.7465	.3081
2.90	.7060	.5632	.7397	.3787	.7567	.2842
3.00	.7203	.5181	.7508	.3481	.7662	.2627
3.10	.7335	.4759	.7610	.3206	.7750	.2434
3.20	.7456	.4370	.7705	.2958	.7831	.2261
3.30	.7567	.4014	.7792	.2736	.7906	.2104
3.40	.7669	.3691	.7873	.2537	.7977	.1963
3.50	.7763	.3400	.7948	.2357	.8042	.1835
3.60	.7850	.3138	.8017	.2195	.8104	.1719
3.70	.7930	.2902	.8082	.2049		
3.80	.8004	.2691	.8143	.1916		
3.90	.8073	.2500	.8200	.1796		
4.00	.8137	.2328	.8253	.1687		
4.10	.8197	.2173				
4.20	.8253	.2033				

Table 4.2 (Cont'd.)

Case No.	5		6		7	
b/a = f <sub>g</sub> = Z <sub>c</sub> =	0.7 0.38204 143.927Ω		0.8 0.41479 156.266Ω		0.9 0.44487 167.595Ω	
x/b	v <sub>rel</sub>	E <sub>yrel</sub>	v <sub>rel</sub>	E <sub>yrel</sub>	v <sub>rel</sub>	E <sub>yrel</sub>
0.00	0.0000	.9912	0.0000	.9847	0.0000	.9763
.10	.0379	.9908	.0408	.9839	.0434	.9752
.20	.0757	.9895	.0816	.9817	.0867	.9718
.30	.1135	.9872	.1222	.9777	.1298	.9659
.40	.1511	.9837	.1627	.9718	.1726	.9571
.50	.1886	.9787	.2028	.9634	.2150	.9449
.60	.2259	.9718	.2426	.9520	.2566	.9286
.70	.2628	.9625	.2818	.9370	.2975	.9076
.80	.2994	.9502	.3202	.9177	.3373	.8813
.90	.3354	.9342	.3578	.8934	.3758	.8495
1.00	.3707	.9138	.3943	.8638	.4128	.8121
1.10	.4051	.8885	.4294	.8286	.4480	.7698
1.20	.4385	.8577	.4629	.7882	.4813	.7236
1.30	.4706	.8216	.4947	.7435	.5124	.6748
1.40	.5012	.7804	.5246	.6957	.5413	.6251
1.50	.5302	.7351	.5524	.6464	.5680	.5758
1.60	.5574	.6871	.5782	.5970	.5925	.5283
1.70	.5827	.6378	.6020	.5489	.6150	.4835
1.80	.6061	.5888	.6238	.5031	.6356	.4419
1.90	.6277	.5413	.6437	.4603	.6544	.4038
2.00	.6475	.4963	.6620	.4209	.6716	.3692
2.10	.6656	.4544	.6787	.3850	.6873	.3379
2.20	.6823	.4159	.6940	.3526	.7017	.3099
2.30	.6975	.3809	.7080	.3234	.7149	.2847
2.40	.7114	.3492	.7209	.2971	.7271	.2621
2.50	.7242	.3207	.7327	.2736	.7383	.2419
2.60	.7359	.2951	.7436	.2525	.7486	.2237
2.70	.7468	.2721	.7537	.2335	.7582	.2074
2.80	.7568	.2515	.7630	.2165	.7671	.1928
2.90	.7660	.2330	.7717	.2012	.7754	.1795
3.00	.7746	.2163	.7797	.1874	.7831	.1675
3.10	.7826	.2013	.7872	.1749	.7903	.1567
3.20	.7900	.1877	.7942	.1636		
3.30	.7969	.1755				
3.40	.8034	.1644				

Table 4.2 (Cont'd.)

Case No.	8		9		10	
b/a =	1.0		1.20		1.23526	
fg =	0.47264		0.52245		0.53061	
Z <sub>c</sub> =	178.058Ω		196.824Ω		199.896Ω	
x/b	v <sub>rel</sub>	E <sub>yrel</sub>	v <sub>rel</sub>	E <sub>yrel</sub>	v <sub>rel</sub>	E <sub>yrel</sub>
0.00	0.0000	.9666	0.0000	.9442	0.0000	.9399
.10	.0457	.9650	.0493	.9418	.0498	.9374
.20	.0912	.9604	.0983	.9346	.0994	.9298
.30	.1364	.9524	.1469	.9223	.1484	.9168
.40	.1811	.9406	.1946	.9046	.1966	.8981
.50	.2252	.9243	.2413	.8810	.2436	.8733
.60	.2684	.9031	.2866	.8513	.2892	.8424
.70	.3105	.8765	.3301	.8156	.3329	.8055
.80	.3512	.8441	.3717	.7745	.3745	.7632
.90	.3902	.8062	.4110	.7289	.4138	.7168
1.00	.4273	.7633	.4478	.6804	.4506	.6678
1.10	.4623	.7166	.4820	.6304	.4847	.6177
1.20	.4950	.6675	.5137	.5805	.5161	.5681
1.30	.5254	.6176	.5427	.5322	.5450	.5203
1.40	.5534	.5683	.5693	.4864	.5714	.4751
1.50	.5792	.5209	.5936	.4438	.5955	.4333
1.60	.6027	.4763	.6158	.4047	.6174	.3950
1.70	.6242	.4350	.6360	.3691	.6374	.3603
1.80	.6439	.3972	.6544	.3370	.6557	.3290
1.90	.6618	.3629	.6712	.3082	.6724	.3009
2.00	.6782	.3320	.6866	.2824	.6877	.2758
2.10	.6933	.3042	.7008	.2593	.7017	.2533
2.20	.7070	.2793	.7138	.2386	.7146	.2332
2.30	.7197	.2570	.7258	.2201	.7265	.2152
2.40	.7314	.2371	.7368	.2035	.7375	.1990
2.50	.7421	.2191	.7470	.1886	.7477	.1845
2.60	.7521	.2031	.7565	.1752	.7571	.1714
2.70	.7614	.1886	.7654	.1631	.7659	.1596
2.80	.7700	.1755	.7736	.1521	.7741	.1490
2.90	.7780	.1637				
3.00	.7855	.1531				

Table 4.2 (Cont'd.)

Case No.	11		12		13	
	b/a =	1.4	E <sub>y</sub> rel	1.6	E <sub>y</sub> rel	1.8
	f <sub>g</sub> =	0.56609	v <sub>rel</sub>	0.60483	v <sub>rel</sub>	0.63962
Z <sub>c</sub> =	213.262Ω			227.859Ω		240.966Ω
x/b	v <sub>rel</sub>	E <sub>y</sub> rel	v <sub>rel</sub>	E <sub>y</sub> rel	v <sub>rel</sub>	E <sub>y</sub> rel
0.00	0.0000	.9200	0.0000	.8956	0.0000	.8720
.10	.0520	.9168	.0541	.8918	.0557	.8676
.20	.1037	.9073	.1077	.8803	.1108	.8546
.30	.1546	.8912	.1604	.8611	.1648	.8331
.40	.2045	.8685	.2117	.8345	.2172	.8036
.50	.2528	.8390	.2612	.8008	.2675	.7670
.60	.2993	.8032	.3085	.7609	.3152	.7245
.70	.3436	.7617	.3532	.7160	.3601	.6778
.80	.3855	.7157	.3950	.6678	.4019	.6288
.90	.4246	.6669	.4339	.6180	.4405	.5792
1.00	.4610	.6168	.4698	.5683	.4760	.5306
1.10	.4945	.5672	.5027	.5202	.5084	.4842
1.20	.5252	.5192	.5328	.4745	.5380	.4408
1.30	.5533	.4738	.5602	.4321	.5649	.4009
1.40	.5789	.4318	.5851	.3932	.5893	.3646
1.50	.6022	.3933	.6078	.3579	.6116	.3318
1.60	.6235	.3584	.6285	.3261	.6319	.3024
1.70	.6429	.3269	.6473	.2976	.6503	.2760
1.80	.6606	.2987	.6645	.2721	.6672	.2525
1.90	.6768	.2734	.6803	.2493	.6827	.2315
2.00	.6916	.2509	.6947	.2290	.6969	.2128
2.10	.7052	.2307	.7080	.2108	.7100	.1960
2.20	.7177	.2126	.7203	.1945	.7220	.1810
2.30	.7293	.1965	.7316	.1799	.7331	.1676
2.40	.7400	.1819	.7421	.1668	.7435	.1555
2.50	.7499	.1689	.7518	.1550	.7531	.1446
2.60	.7592	.1571	.7608	.1443		
2.70	.7677	.1464				

Table 4.2 (Cont'd.)

Case No.	14		15		16		17	
b/a = f/g = Z <sub>c</sub> = x/b	2.0 0.67116 252.848Ω		2.5 0.73901 278.407Ω		3.0 0.79525 299.593Ω		6.99 1.06103 399.722Ω	
	v <sub>rel</sub>	E <sub>y rel</sub>	v <sub>rel</sub>	E <sub>y rel</sub>	v <sub>rel</sub>	E <sub>y rel</sub>	v <sub>rel</sub>	E <sub>y rel</sub>
0.00	0.0000	.8497	0.0000	.8004	0.0000	.7597	0.0000	.5940
.10	.0569	.8449	.0590	.7949	.0603	.7539	.0628	.5884
.20	.1132	.8307	.1172	.7788	.1196	.7370	.1245	.5722
.30	.1682	.8074	.1739	.7529	.1772	.7100	.1839	.5470
.40	.2214	.7758	.2283	.7186	.2323	.6747	.2403	.5152
.50	.2722	.7372	.2799	.6777	.2844	.6335	.2931	.4792
.60	.3202	.6933	.3284	.6325	.3330	.5886	.3419	.4413
.70	.3652	.6458	.3733	.5850	.3779	.5422	.3868	.4035
.80	.4069	.5967	.4148	.5372	.4192	.4963	.4276	.3671
.90	.4453	.5478	.4528	.4908	.4569	.4522	.4647	.3330
1.00	.4804	.5005	.4874	.4467	.4912	.4108	.4984	.3015
1.10	.5125	.4559	.5189	.4058	.5224	.3727	.5288	.2730
1.20	.5417	.4145	.5475	.3683	.5506	.3380	.5564	.2473
1.30	.5682	.3767	.5734	.3344	.5762	.3068	.5814	.2243
1.40	.5924	.3424	.5970	.3039	.5995	.2788	.6041	.2039
1.50	.6143	.3116	.6184	.2766	.6206	.2538	.6247	.1856
1.60	.6343	.2840	.6379	.2522	.6399	.2315	.6436	.1694
1.70	.6525	.2594	.6557	.2305	.6575	.2116	.6608	.1550
1.80	.6691	.2374	.6720	.2111	.6736	.1939	.6765	.1422
1.90	.6844	.2178	.6870	.1938	.6884	.1781	.6910	.1308
2.00	.6984	.2003	.7007	.1784	.7020	.1640	.7043	.1205
2.10	.7113	.1846	.7134	.1646	.7145	.1514	.7166	.1114
2.20	.7232	.1706	.7251	.1522	.7261	.1401		
2.30	.7342	.1580	.7359	.1411	.7368	.1299		
2.40	.7445	.1466	.7460	.1311				
2.50	.7540	.1364						

Table 4.2 (Cont'd.)

Table 4.3

Normalized electric potential ( $u_{\text{rel}}$ ) and normalized y-component of field ( $E_{y\text{rel}}$ ) along the symmetry axis  $x/b = 0$  with  $b/a$  as the parameter.

- Note 1. On the symmetry axis  $x/b = 0$ , the normalized magnetic potential ( $v_{\text{rel}}$ ) and the normalized x-component of field ( $E_{x\text{rel}}$ ) are both zero for  $(0 \leq y/b < 1)$ .
2. See equations 4.7 to 4.11 for the normalization scheme and for the equivalence of electric and magnetic field components.

Case No.	1		2		3	
b/a = f/g = $Z_c =$	0.1667		0.40679		0.5	
y/b	$u_{rel}$	$E_{yrel}$	$u_{rel}$	$E_{yrel}$	$u_{rel}$	$E_{yrel}$
0.00	0.0000	1.0000	0.0000	.9997	0.0000	.9986
.05	.0500	1.0000	.0500	.9997	.0499	.9986
.10	.1000	1.0000	.1000	.9997	.0999	.9986
.15	.1500	1.0000	.1500	.9997	.1498	.9987
.20	.2000	1.0000	.1999	.9997	.1997	.9988
.25	.2500	1.0000	.2499	.9998	.2497	.9990
.30	.3000	1.0000	.2999	.9998	.2996	.9991
.35	.3500	1.0000	.3499	.9998	.3496	.9993
.40	.4000	1.0000	.3999	.9999	.3996	.9996
.45	.4500	1.0000	.4499	.9999	.4495	.9998
.50	.5000	1.0000	.4999	1.0000	.4995	1.0000
.55	.5500	1.0000	.5499	1.0001	.5495	1.0002
.60	.6000	1.0000	.5999	1.0001	.5996	1.0004
.65	.6500	1.0000	.6499	1.0002	.6496	1.0007
.70	.7000	1.0000	.6999	1.0002	.6996	1.0008
.75	.7500	1.0000	.7499	1.0002	.7497	1.0010
.80	.8000	1.0000	.7999	1.0003	.7997	1.0012
.85	.8500	1.0000	.8500	1.0003	.8498	1.0013
.90	.9000	1.0000	.9000	1.0003	.8999	1.0014
.95	.9500	1.0000	.9500	1.0003	.9499	1.0014
1.00	1.0000	1.0000	1.0000	1.0003	1.0000	1.0014

Case No.	4		5		6	
b/a = f/g = $Z_c =$	0.6		0.7		0.8	
y/b	$u_{rel}$	$E_{yrel}$	$u_{rel}$	$E_{yrel}$	$u_{rel}$	$E_{yrel}$
0.00	0.0000	.9959	0.0000	.9912	0.0000	.9847
.05	.0498	.9959	.0496	.9914	.0492	.9848
.10	.0996	.9961	.0991	.9917	.0985	.9854
.15	.1494	.9963	.1487	.9922	.1478	.9863
.20	.1992	.9966	.1984	.9929	.1971	.9875
.25	.2491	.9971	.2480	.9938	.2465	.9890
.30	.2989	.9976	.2977	.9948	.2960	.9908
.35	.3488	.9981	.3475	.9960	.3456	.9928
.40	.3987	.9987	.3973	.9972	.3953	.9950
.45	.4487	.9993	.4472	.9985	.4451	.9974
.50	.4987	1.0000	.4972	.9999	.4950	.9998
.55	.5487	1.0006	.5472	1.0013	.5451	1.0022
.60	.5987	1.0013	.5973	1.0027	.5953	1.0046
.65	.6488	1.0019	.6475	1.0040	.6456	1.0069
.70	.6989	1.0024	.6977	1.0052	.6960	1.0091
.75	.7491	1.0029	.7480	1.0062	.7465	1.0110
.80	.7992	1.0034	.7983	1.0072	.7971	1.0127
.85	.8494	1.0037	.8487	1.0079	.8477	1.0140
.90	.8996	1.0040	.8991	1.0085	.8984	1.0150
.95	.9498	1.0041	.9496	1.0088	.9492	1.0156
1.00	1.0000	1.0042	1.0000	1.0089	1.0000	1.0158

Table 4.3

Case No.	7		8		9	
$b/a =$	0.9		1.0		1.2	
$f_g =$	0.44487		0.47264		0.52245	
$Z_c =$	167.595Ω		178.058Ω		196.824Ω	
$y/b$	$u_{rel}$	$E_{yrel}$	$u_{rel}$	$E_{yrel}$	$u_{rel}$	$E_{yrel}$
0.00	0.0000	.9763	0.0000	.9666	0.0000	.9442
.05	.0488	.9766	.0483	.9669	.0472	.9448
.10	.0977	.9774	.0967	.9680	.0945	.9465
.15	.1466	.9787	.1452	.9699	.1419	.9494
.20	.1956	.9806	.1937	.9724	.1895	.9534
.25	.2446	.9829	.2424	.9756	.2373	.9585
.30	.2938	.9856	.2913	.9794	.2853	.9646
.35	.3432	.9887	.3404	.9837	.3337	.9716
.40	.3927	.9921	.3897	.9885	.3825	.9794
.45	.4424	.9957	.4392	.9936	.4317	.9879
.50	.4923	.9995	.4890	.9989	.4813	.9968
.55	.5424	1.0033	.5391	1.0043	.5314	1.0061
.60	.5926	1.0070	.5895	1.0097	.5819	1.0155
.65	.6431	1.0107	.6401	1.0150	.6329	1.0246
.70	.6937	1.0140	.6909	1.0199	.6844	1.0334
.75	.7445	1.0171	.7421	1.0244	.7362	1.0414
.80	.7954	1.0198	.7934	1.0282	.7885	1.0485
.85	.8464	1.0219	.8449	1.0314	.8411	1.0543
.90	.8976	1.0235	.8965	1.0337	.8939	1.0586
.95	.9488	1.0244	.9482	1.0352	.9469	1.0613
1.00	1.0000	1.0248	1.0000	1.0356	1.0000	1.0622

Case No.	10		11		12	
$b/a =$	1.23526		1.4		1.6	
$f_g =$	0.53061		0.56609		0.60483	
$Z_c =$	199.896Ω		213.262Ω		227.859Ω	
$y/b$	$u_{rel}$	$E_{yrel}$	$u_{rel}$	$E_{yrel}$	$u_{rel}$	$E_{yrel}$
0.00	0.0000	.9399	0.0000	.9200	0.0000	.8956
.05	.0470	.9406	.0460	.9207	.0448	.8965
.10	.0941	.9424	.0921	.9231	.0897	.8994
.15	.1413	.9455	.1383	.9270	.1348	.9042
.20	.1887	.9498	.1848	.9324	.1801	.9109
.25	.2363	.9552	.2316	.9394	.2259	.9194
.30	.2842	.9617	.2788	.9477	.2721	.9298
.35	.3325	.9692	.3264	.9574	.3189	.9420
.40	.3811	.9776	.3746	.9684	.3663	.9559
.45	.4302	.9867	.4233	.9804	.4145	.9714
.50	.4798	.9963	.4726	.9933	.4635	.9882
.55	.5299	1.0063	.5226	1.0068	.5134	1.0061
.60	.5804	1.0165	.5733	1.0207	.5641	1.0248
.65	.6315	1.0264	.6247	1.0346	.6158	1.0438
.70	.6831	1.0360	.6767	1.0480	.6685	1.0625
.75	.7351	1.0447	.7295	1.0605	.7221	1.0802
.80	.7875	1.0524	.7828	1.0716	.7765	1.0963
.85	.8403	1.0588	.8366	1.0809	.8317	1.1098
.90	.8934	1.0635	.8908	1.0879	.8874	1.1201
.95	.9466	1.0665	.9453	1.0922	.9436	1.1265
1.00	1.0000	1.0675	1.0000	1.0937	1.0000	1.1287

Table 4.3 (Cont'd.)

Case No.	13		14		15	
b/a =	1.8		2.0		2.5	
f <sub>g</sub> =	0.63962		0.67116		0.73901	
Z <sub>c</sub> =	240.966Ω		252.848Ω		278.407Ω	
y/b	u <sub>rel</sub>	E <sub>yrel</sub>	u <sub>rel</sub>	E <sub>yrel</sub>	u <sub>rel</sub>	E <sub>yrel</sub>
0.00	0.0000	.8720	0.0000	.8497	0.0000	.8004
.05	.0436	.8731	.0425	.8509	.0400	.8018
.10	.0873	.8764	.0851	.8545	.0802	.8059
.15	.1313	.8819	.1280	.8606	.1207	.8129
.20	.1756	.8896	.1712	.8691	.1616	.8227
.25	.2203	.8995	.2150	.8801	.2030	.8357
.30	.2656	.9116	.2593	.8937	.2452	.8518
.35	.3115	.9260	.3044	.9099	.2882	.8712
.40	.3582	.9425	.3503	.9287	.3324	.8943
.45	.4058	.9612	.3973	.9502	.3777	.9210
.50	.4543	.9817	.4454	.9741	.4245	.9518
.55	.5040	1.0040	.4947	1.0003	.4730	.9865
.60	.5548	1.0275	.5455	1.0286	.5232	1.0251
.65	.6067	1.0518	.5976	1.0582	.5755	1.0673
.70	.6599	1.0762	.6513	1.0885	.6300	1.1121
.75	.7143	1.0997	.7065	1.1182	.6868	1.1584
.80	.7699	1.1213	.7631	1.1460	.7458	1.2036
.85	.8264	1.1398	.8210	1.1702	.8071	1.2449
.90	.8838	1.1541	.8800	1.1892	.8702	1.2784
.95	.9417	1.1631	.9398	1.2013	.9347	1.3005
1.00	1.0000	1.1662	1.0000	1.2054	1.0000	1.3082

Case No.	16		17	
b/a =	3.0		6.99	
f <sub>g</sub> =	0.79525		1.06103	
Z <sub>c</sub> =	299.593Ω		399.722Ω	
y/b	u <sub>rel</sub>	E <sub>yrel</sub>	u <sub>rel</sub>	E <sub>yrel</sub>
0.00	0.0000	.7597	0.0000	.5940
.05	.0380	.7612	.0297	.5954
.10	.0762	.7656	.0596	.5997
.15	.1146	.7730	.0897	.6069
.20	.1535	.7836	.1203	.6174
.25	.1930	.7975	.1515	.6314
.30	.2333	.8149	.1835	.6493
.35	.2746	.8363	.2165	.6718
.40	.3170	.8619	.2508	.6996
.45	.3608	.8921	.2866	.7338
.50	.4063	.9274	.3243	.7760
.55	.4537	.9683	.3644	.8281
.60	.5032	1.0150	.4073	.8930
.65	.5553	1.0677	.4539	.9746
.70	.6101	1.1260	.5052	1.0786
.75	.6680	1.1885	.5623	1.2126
.80	.7290	1.2527	.6271	1.3865
.85	.7932	1.3140	.7018	1.6096
.90	.8602	1.3661	.7888	1.8774
.95	.9295	1.4015	.8894	2.1356
1.00	1.0000	1.4141	1.0000	2.2520

Table 4.3 (Cont'd.)

## V. Summary

This note has documented a set of parametric curves and tables for the TEM fields of a symmetrical two-parallel-plate transmission line. This data can be used for design and analysis of this class of EMP simulators.

The two-dimensional complex field approach applies to various cross section shapes of cylindrical TEM transmission-line waveguides. The present example illustrates how it is used to give formulas for the complex field. Similar formulas are possible for other transmission lines which have conformal transformations for the complex potential in terms of special functions.

## VI. Acknowledgment

The authors wish to express their thanks to Mr. Joe Martinez of The Dikewood Corporation for providing the computer programs that evaluate the Jacobian functions. The subroutine BRUT<sup>11</sup> which was used in generating the contour plots and subroutine TEK which evaluates complete elliptic integrals were kindly provided by Mr. Terry L. Brown also of The Dikewood Corporation. For this and for many helpful discussions on the numerical aspects of this note, we are grateful to Mr. Brown.

## VII. References

1. C. E. Baum, Impedances and Field Distributions for Parallel Plate Transmission Line Simulators, Sensor and Simulation Note 21, June 1966.
2. T. L. Brown and K. D. Granzow, A Parameter Study of Two Parallel Plate Transmission Line Simulators of EMP Sensor and Simulation Note 21, Sensor and Simulation Note 52, April 1968.
3. C. E. Baum, General Principles for the Design of ATLAS I and II, Part V: Some Approximate Figures of Merit for Comparing the Waveforms Launched by Imperfect Pulser Arrays onto TEM Transmission Lines, Sensor and Simulation Note 148, May 1972.
4. L. Marin, Modes on a Finite Width, Parallel-Plate Simulator, I. Narrow Plates, Sensor and Simulation Note 201, September 1974.
5. A.E.H. Love, Some Electrostatic Distributions in Two Dimensions, Proc. London Math. Soc., Vol. 22, pp. 337-369, 1923.
6. R. E. Collin, Field Theory of Guided Waves, McGraw Hill, 1960.
7. Moon and Spencer, Field Theory Handbook, Springer, 1961.
8. Abramowitz and Stegun, ed., Handbook of Mathematical Functions, National Bureau of Standards, 1964.
9. B. K. Singaraju, D. V. Giri and C. E. Baum, Further Developments in the Application of Contour Integration to the Evaluation of the Zeros of Analytic Functions and Relevant Computer Programs, Mathematics Note 42, March 1976.
10. P. F. Byrd and M. D. Friedman, Handbook of Elliptical Integrals for Engineers and Scientists, Eqs. 115.01, 02 and 03 on pp. 12-18, Springer-Verlag, 1971.
11. Terry L. Brown, BRUT--A System of Subroutines for the Generation of Contours, Mathematics Note 26, July 1972.
12. E. H. Neville, Jacobian Elliptic Functions, Oxford at the Clarendon Press, 1951.

## Appendix A. Illustration of the Periodicity in the Conformal Transformation

Let us shift the Jacobi zeta function using the relation for the incomplete elliptic integral of the second kind as<sup>8</sup>

$$\begin{aligned} E(p|m) &= E(p + 2NK(m) + i2MK(m_1)|m) \\ &\quad - 2NE(m) - i2M[K(m_1) - E(m_1)] \end{aligned} \quad (A.1)$$

Then the Jacobi zeta function is

$$\begin{aligned} Z(p|m) &= E(p|m) - p \frac{E(m)}{K(m)} \\ &= E(p + 2NK(m) + i2MK(m_1)|m) \\ &\quad - \left[ p + 2NK(m) + i2MK(m_1) \right] \frac{E(m)}{K(m)} \\ &\quad + i2M \left\{ \left[ \frac{E(m)}{K(m)} - 1 \right] K(m_1) + E(m_1) \right\} \\ &= Z(p + 2NK(m) + 2MiK(m_1)|m) \\ &\quad + \frac{2Mi}{K(m)} \left\{ K(m)E(m_1) + E(m)K(m_1) - K(m)K(m_1) \right\} \\ &= Z(p + 2NK(m) + i2MK(m_1)|m) + \frac{iM\pi}{K(m)} \end{aligned} \quad (A.2)$$

using a formula called Legendre's relation.<sup>8</sup> This gives a somewhat general periodicity relationship.

The conformal transformation (equation 2.9) can now be rewritten as

$$\begin{aligned}
\xi &= -\frac{2K(m)}{\pi} Z(p + 2NK(m) + i2MK(m_1)|m) - i(2M+1) \\
&= -\frac{2K(m)}{\pi} Z(iw + (2N+1)K(m) + i(2M+1)K(m_1)|m) - i(2M+1)
\end{aligned} \tag{A.3}$$

where N and M are any integers (positive, negative, or zero). For use with this expression equation 3.8 can be generalized to

$$\begin{aligned}
b \frac{dw}{dz} &= \frac{i\pi}{2K(m)} \left\{ \operatorname{dn}^2(p + 2NK(m) + i2MK(m_1)) - \frac{E(m)}{K(m)} \right\}^{-1} \\
&= \frac{i\pi}{2} \left\{ K(m) \operatorname{dn}^2(iw + (2N+1)K(m) + i(2M+1)K(m_1)) - E(m) \right\}^{-1}
\end{aligned} \tag{A.4}$$

for use in determining the normalized complex field.

Noting that the Jacobi zeta function is an odd function of the argument as

$$Z(p|m) = -Z(-p|m) \tag{A.5}$$

one also has (using N + 1 and M + 1 in place of N and M)

$$Z(p|m) = -Z(-p + 2NK(m) + i2MK(m_1)|m) - \frac{iM\pi}{K(m)} \tag{A.6}$$

Using this relation the conformal transformation can be written as

$$\begin{aligned}
\xi &= \frac{2K(m)}{\pi} Z(-p + 2NK(m) + i2MK(m_1)|m) + i(2M-1) \\
&= \frac{2K(m)}{\pi} Z(-iw + (2N-1)K(m) + i(2M-1)K(m_1)|m) + i(2M-1)
\end{aligned} \tag{A.7}$$

For this we have the corresponding result

$$\begin{aligned}
 b \frac{dw}{dz} &= \frac{i\pi}{2K(m)} \left\{ \operatorname{dn}^2(-p + 2NK(m) + i2MK(m_1)) - \frac{E(m)}{K(m)} \right\}^{-1} \\
 &= \frac{i\pi}{2} \left\{ K(m) \operatorname{dn}^2(-iw + (2N - 1)K(m) + i(2M - 1)K(m_1)) - E(m) \right\}^{-1}
 \end{aligned}
 \tag{A.8}$$

For convenience one can summarize the results for the Jacobi zeta function from equations A.2 and A.6 as

$$Z(p|m) = \pm Z(\pm p + 2NK(m) + i2MK(m_1)|m) \pm \frac{iM\pi}{K(m)} \tag{A.9}$$

## Appendix B. Reduction of the Conformal Transformation for Special Points and Lines in the Complex Coordinate Plane

In this appendix, we shall simplify the conformal transformation given by equation 2.15 for certain special points and lines in the first quadrant of the normalized complex coordinate ( $\xi$ ) plane. From considerations of symmetry, the results of computations in the first quadrant are easily extended to other quadrants.

The conformal transformation is given by

$$\xi \equiv \frac{z}{b} = \left( \frac{x}{b} + i \frac{y}{b} \right) = \frac{2i}{\pi} \left[ K(m) E(w|m_1) + w(E(m) - K(m)) \right] \quad (B.1)$$

The special lines (s.l.) and points (s.p.) considered in this appendix are as follows:

s.l. 1.	x = 0	}
s.l. 2.	y = 0	
s.l. 3.	$\left[ \begin{array}{l} (y/b) = 1.0 \text{ for } x < a/b \text{ (right half of} \\ \text{the top plate excluding the edge)} \end{array} \right]$	
s.p. 1.	$\xi = 0$	
s.p. 2.	$\xi = 0 + i1.0+$	}
s.p. 3.	$\xi = 0 + i1.0-$	

(B.2)

After finding the conformal transformation for the above described special cases, we shall find the complex field using the following set of equations

$$\begin{aligned}
 E_{\text{rel}}(z) &= E_{x_{\text{rel}}} (z) - i E_{y_{\text{rel}}} (z) = H_{y_{\text{rel}}} (z) + i H_{x_{\text{rel}}} (z) \\
 &= \frac{b}{K(m_1)} \left[ \frac{dw(z)}{dz} \right] \\
 &= \frac{b}{K(m_1)} \left[ \frac{1}{2} \left( \frac{\partial}{\partial x} - i \frac{\partial}{\partial y} \right) w(x, y) \right]; \text{ with } w(x, y) = u(x, y) + iv(x, y) \\
 &= \frac{b}{K(m_1)} \frac{1}{2} \left[ \left( \frac{\partial u}{\partial x} + \frac{\partial v}{\partial y} \right) - i \left( \frac{\partial u}{\partial y} - \frac{\partial v}{\partial x} \right) \right]
 \end{aligned} \quad (B.3)$$

or

$$\begin{aligned} E_{x_{\text{rel}}} &= H_{y_{\text{rel}}} = \frac{b}{K(m_1)} \frac{1}{2} \left( \frac{\partial u}{\partial x} + \frac{\partial v}{\partial y} \right) \\ E_{y_{\text{rel}}} &= -H_{x_{\text{rel}}} = \frac{b}{K(m_1)} \frac{1}{2} \left( \frac{\partial u}{\partial y} - \frac{\partial v}{\partial x} \right) \end{aligned} \quad (\text{B.4})$$

If we exclude the points of nonanalyticity in the conformal transformation (see figure 4.1), the Cauchy-Rieman conditions

$$(\partial u / \partial x) = (\partial v / \partial y) \text{ and } (\partial u / \partial y) = -(\partial v / \partial x) \quad (\text{B.5})$$

are satisfied so that the field components are now given by

$$\begin{aligned} E_{x_{\text{rel}}} &= H_{y_{\text{rel}}} = \left[ \frac{b}{K(m_1)} \frac{\partial u}{\partial x} \right] = \left[ \frac{b}{K(m_1)} \frac{\partial v}{\partial y} \right] \\ E_{y_{\text{rel}}} &= -H_{x_{\text{rel}}} = \left[ \frac{b}{K(m_1)} \frac{\partial u}{\partial y} \right] = \left[ \frac{-b}{K(m_1)} \frac{\partial v}{\partial x} \right] \end{aligned} \quad (\text{B.6})$$

We now proceed to consider all of above mentioned special cases individually.

#### s.1.1.

This line corresponds to the  $y$  ( $y/b$ ) axis of the  $z$  ( $\xi$ ) plane. The transformation of equation B.1 becomes

$$\frac{y}{b} = \frac{2}{\pi} \left[ K(m) E(u + iv|m_1) + (u + iv)(E(m) - K(m)) \right] \quad (\text{B.7})$$

We know from figure 4.1 that along the  $y$  axis the magnetic potential  $v$  is given by

$$\begin{aligned} v(0, y) &= 0 \quad ; \text{ for } 0 \leq y < b \\ v(0, y) &= -K(m) \quad ; \text{ for } b < y \leq \infty \end{aligned} \quad (\text{B.8})$$

Using equation B.8, for  $x/b = 0$ , equation B.7 becomes

$$\frac{y}{b} = \frac{2}{\pi} \left[ K(m) E(u|m_1) + u(E(m) - K(m)) \right]; \quad \text{for all } y \quad (\text{B.9})$$

or

$$\frac{y}{b} = \frac{2}{\pi} \left[ K(m) Z(u|m_1) + \frac{u\pi}{2K(m_1)} \right]; \quad \text{for all } y \quad (\text{B.10})$$

also

$$\frac{1}{b} \frac{dy}{du} = \frac{2}{\pi} \left[ K(m) dn^2(u|m_1) + (E(m) - K(m)) \right]$$

The field components are given by using equation B.6 to be

$$E_{x_{\text{rel}}} (0, y) = H_{y_{\text{rel}}} (0, y) = 0; \quad \text{for } 0 \leq y \leq \infty \quad (\text{B.11})$$

$$\begin{aligned} E_{y_{\text{rel}}} (0, y) &= -H_{x_{\text{rel}}} (0, y) = \frac{1}{K(m_1)} \left( \frac{1}{b} \frac{dy}{du} \right)^{-1} \\ &= \frac{1}{K(m_1)} \frac{\pi}{2} \left[ K(m) dn^2(u|m_1) + E(m) - K(m) \right]^{-1} \end{aligned}$$

or by using equation 16.9.1 of ref. 8,

$$= \frac{\pi}{2K(m_1)} \left[ E(m) - m_1 K(m) sn^2(u|m_1) \right]^{-1} \quad \text{for } 0 \leq y < b \quad (\text{B.12})$$

### s.1.2.

This line corresponds to the x ( $x/b$ ) axis in the z ( $\zeta$ ) plane. The transformation now becomes

$$\frac{x}{b} = \frac{2i}{\pi} \left[ K(m) E(u + iv|m_1) + (u + iv)(E(m) - K(m)) \right] \quad (\text{B.13})$$

From figure 4.1, we know that the electric potential

$$u(x, 0) = 0 \quad , \quad \text{for } 0 \leq x \leq \infty \quad (\text{B.14})$$

so that

$$\frac{x}{b} = \frac{2}{\pi} \left[ K(m) E(iv|m_1) + iv(E(m) - K(m)) \right]$$

Using Jacobi's imaginary transformation (equation 17.4.10 of ref. 8),

$$\frac{x}{b} = \frac{2}{\pi} \left[ K(m) E(v|m) - v E(m) - K(m) dn(v|m) sc(v|m) \right] \\ \text{for } 0 \leq x \leq \infty \quad (\text{B.15})$$

or, in terms of Jacobi zeta function

$$\frac{x}{b} = \frac{2}{\pi} K(m) \left[ Z(v|m) - dn(v|m) sc(v|m) \right] , \text{ for } 0 \leq x \leq \infty \quad (\text{B.16})$$

from which, we also have using the derivative formulas (equation 16.16 of ref. 8)

$$\frac{1}{b} \frac{dx}{dv} = \frac{2}{\pi} K(m) \left[ dn^2(v|m) - \frac{E(m)}{K(m)} - \frac{dn^2(v|m)}{cn^2(v|m)} + m sn^2(v|m) \right]$$

Using the relations between the squares of Jacobian functions given by equations 16.9 of ref. 8,

$$\frac{1}{b} \frac{dx}{dv} = - \frac{2}{\pi} K(m) \left[ m_1 sc^2(v|m) + \frac{E(m)}{K(m)} \right] \quad (\text{B.17})$$

Consequently, the field components are given by,

$$E_{x_{\text{rel}}} (x, 0) = H_{y_{\text{rel}}} (x, 0) = 0, \quad ; \quad \text{for } 0 \leq x \leq \infty$$

and

$$\begin{aligned} E_{y_{\text{rel}}}^x(x, 0) &= -H_{x_{\text{rel}}}^x(x, 0) = \frac{b}{K(m_1)} \left( -\frac{dv}{dx} \right) \\ &= \frac{(-1)}{K(m_1)} \left( \frac{1}{b} \frac{dx}{dv} \right)^{-1} \\ &= \frac{\pi}{2 K(m_1)} \left[ E(m) + m_1 K(m) \operatorname{sc}^2(v|m) \right]^{-1} \\ &\quad \text{for } 0 \leq x \leq \infty \end{aligned} \tag{B.18}$$

### s.1.3

This is a special line right along the plate. For  $(x/b) < a$ , equation B.1 becomes

$$\frac{x}{b} + i = \frac{2i}{\pi} \left[ K(m) E(u + iv|m_1) + (u + iv)(E(m) - K(m)) \right] \tag{B.19a}$$

From figure 4.1, we know that  $u = K(m_1)$  so that

$$\frac{x}{b} + i = \frac{2i}{\pi} \left[ K(m) E(K(m_1) + iv|m_1) + (K(m_1) + iv)(E(m) - K(m)) \right] \tag{B.19b}$$

Using the addition theorem for  $E(p + q|m)$ ,<sup>12</sup> we have

$$\begin{aligned} \frac{x}{b} + i_1 &= \frac{2i}{\pi} \left[ K(m) \left\{ E(m_1) + E(iv|m_1) - m_1 \operatorname{sn}(K(m_1)|m_1) \operatorname{sn}(iv|m_1) \right. \right. \\ &\quad \left. \left. \operatorname{sn}(K(m_1) + iv|m_1) \right\} + E(m)K(m_1) - K(m)K(m_1) + iv(E(m) - K(m)) \right] \end{aligned} \tag{B.19c}$$

Now, using the Legendre relation,<sup>8</sup> equation B.19 becomes

$$\frac{x}{b} = \frac{2i}{\pi} \left[ K(m) \left\{ E(iv|m_1) - m_1 \operatorname{sn}(K(m_1)|m_1) \operatorname{sn}(iv|m_1) \right. \right. \\ \left. \left. \operatorname{sn}(K(m_1) + iv|m_1) \right\} + iv(E(m) - K(m)) \right] \quad (B.20)$$

We make use of the following<sup>8</sup> to further simplify equation B.20

$$\operatorname{sn}(K(m_1)|m_1) = 1; \text{ using equation 16.5.3 of ref. 8}$$

$$\operatorname{sn}(iv|m_1) = i \operatorname{sc}(v|m); \text{ using equation 16.20.1 of ref. 8}$$

$$E(iv|m_1) = i[v + dn(v|m) \operatorname{sc}(v|m) - E(v|m)]; \text{ using equation 17.4.10} \quad (B.21)$$

which leads to

$$\frac{x}{b} = \frac{2}{\pi} \left[ K(m) E(v|m) - vE(m) - K(m)dn(v|m)\operatorname{sc}(v|m) \right. \\ \left. + m_1 K(m)\operatorname{sc}(v|m) \operatorname{sn}(K(m_1) + iv|m_1) \right] \quad (B.22a)$$

Let us consider  $\operatorname{sn}(K(m_1) + iv|m_1)$  appearing in the r.h.s. of equation B.22a

$$\begin{aligned} & \operatorname{sn}(K(m_1) + iv|m_1) \\ &= \operatorname{sn}[-i(-v + iK(m_1)|m_1)] \\ &= -\operatorname{sn}[i(-v + iK(m_1)|m_1)]; \text{ because sn is an odd function} \\ &= -i \operatorname{sc}[-v + iK(m_1)|m]; \text{ using equation 16.20.1 of ref. 8} \\ &= nd(-v|m) = nd(v|m); \text{ using equation 16.8.9 of ref. 8} \\ & \quad \text{and evenness} \end{aligned} \quad (B.22b)$$

Using the above in equation B.22a, we finally have

$$\frac{x}{b} = \frac{2}{\pi} \left[ K(m) E(v|m) - v E(m) - K(m) \operatorname{dn}(v|m) \operatorname{sc}(v|m) + m_1 K(m) \operatorname{nd}(v|m) \operatorname{sc}(v|m) \right] \quad (\text{B.23a})$$

or, in terms of Jacobi zeta functions,

$$\frac{x}{b} = \frac{2}{\pi} \left[ K(m) Z(v|m) - K(m) \operatorname{dn}(v|m) \operatorname{sc}(v|m) + m_1 K(m) \operatorname{nd}(v|m) \operatorname{sc}(v|m) \right] \quad (\text{B.23b})$$

Using the relation between squares of Jacobian functions, equation 16.9.5 of ref. 8,

$$\frac{x}{b} = \frac{2}{\pi} K(m) \left[ Z(v|m) - m \operatorname{sn}(v|m) \operatorname{cd}(v|m) \right] \quad (\text{B.24})$$

Varying  $v$  from 0 to  $-K(m)$  corresponds to moving from  $x = 0$  to  $x = a/b$  on the inside of the top plate and then from  $x = a/b$  to  $x = 0$  on the outside of the top plate. This is evident from figure 4.1.

Once again using equations 16.16 and 16.9.1 of ref. 8,

$$\frac{1}{b} \frac{dx}{dv} = \frac{2}{\pi} \left[ m_1 K(m) \operatorname{nd}^2(v|m) - E(m) \right] \quad (\text{B.25})$$

Consequently, the field components for this special line along the top plate are given by using equation B.6 as

$$\left. \begin{array}{l} E_{x_{\text{rel}}}^{(x,b+)} = H_{y_{\text{rel}}}^{(x,b-)} = 0 \\ E_{x_{\text{rel}}}^{(x,b-)} = H_{y_{\text{rel}}}^{(x,b-)} = 0 \end{array} \right\} \quad \text{for } (0 \leq x < a/b) \quad (\text{B.26})$$

$$\begin{aligned}
 E_y_{\text{rel}}(x, b\pm) &= -H_x_{\text{rel}}(x, b\pm) = \frac{1}{K(m_1)} \left[ -\frac{1}{b} \frac{dx}{dv} \right]^{-1} \\
 &= \pm \left\{ \frac{\pi}{2K(m_1)} \left[ m_1 K(m) \operatorname{nd}^2(v|m) - E(m) \right]^{-1} \right\} \\
 &\quad \text{for } (0 \leq x < a/b) \tag{B.27}
 \end{aligned}$$

It is emphasized that the special cases worked out here are consistent with previous work of Baum,<sup>1</sup> i.e., equations B.16, B.18, B.24, and B.27 are consistent with equations 77, 79, 72 and 74 of ref. 1, respectively, if we recognize that

$$w \text{ (in this note)} \equiv v + i(K(m) - u) \text{ (of ref. 1)}$$

or by replacing

$$u \text{ (in ref. 1) by } v + K(m) \tag{B.28}$$

and

$$v \text{ (in ref. 1) by } u$$

The sets of equations have been verified to be identical.

In conclusion, it is observed that for all the three special lines considered here, the conformal transformation becomes a transcendental equation in real variables and hence the field components are more easily derived.

#### s.p. 1

This corresponds to the origin of the complex coordinate system, leading to

$$0 = \frac{2i}{\pi} \left[ K(m) E(u + iv|m_1) + (u + iv)(E(m) - K(m)) \right] \tag{B.29}$$

Equation B.29 has a trivial solution for  $w$  given by

$$w = u + iv = 0 \quad (B.30)$$

Put differently, the origin is transformed into itself (the point B in figure 4.1). Consequently using equations B.6 and B.18 the field components at the origin of the coordinate system are given by

$$\begin{aligned} E_{x_{\text{rel}}}^{(0,0)} &= H_{y_{\text{rel}}}^{(0,0)} = 0 \\ E_{y_{\text{rel}}}^{(0,0)} &= -H_{x_{\text{rel}}}^{(0,0)} = \left[ \frac{\pi}{2K(m_1)E(m)} \right] \end{aligned} \quad (B.31)$$

so that the total electric field at the origin is given by

$$\begin{aligned} E_{\text{rel}}^{(0,0)} &= E_{x_{\text{rel}}}^{(0,0)} - iE_{y_{\text{rel}}}^{(0,0)} \\ &= \left[ 0 - i \frac{\pi}{2K(m_1)E(m)} \right] \end{aligned} \quad (B.32)$$

Equation B.32 is used in section IV.A where contour plots are generated for the quantity  $|[E_{\text{rel}}(x,y) - E_{\text{rel}}^{(0,0)}]/E_{\text{rel}}^{(0,0)}|$  which is a measure of nonuniformity in the absolute value of the complex field with respect to the field at the origin of the coordinate system.

### s.p.2 and 3

These two special points ( $\zeta = 0 + i1\pm$ ) correspond to points just above and below the top plate at its middle. It is evident from figure 4.1 that the potentials at these special points (E and C in figure 4.1) are given by

$$\left. \begin{aligned} u(0,b+) &= K(m_1) \quad \text{and} \quad v(0,b+) = -K(m) \\ u(0,b-) &= K(m_1) \quad \text{and} \quad v(0,b-) = 0 \end{aligned} \right\} \quad (B.33)$$

Consequently, using equations B.26 and B.27 at  $x = 0$ , we have

$$E_{x_{\text{rel}}}^{(0, b\pm)} = H_{y_{\text{rel}}}^{(0, b\pm)} = 0 \quad (\text{B. 34})$$

$$E_{y_{\text{rel}}}^{(0, b+)} = -H_{x_{\text{rel}}}^{(0, b+)} = \frac{\pi}{2 K(m_1) [K(m) - E(m)]} \quad (\text{B. 35})$$

and

$$E_{y_{\text{rel}}}^{(0, b-)} = -H_{x_{\text{rel}}}^{(0, b-)} = \frac{\pi}{2 K(m_1) [E(m) - m_1 K(m)]} \quad (\text{B. 36})$$

Once again, it is observed that equations B.31, B.35, and B.36 are consistent with equations 80, 76, and 75 of earlier work by Baum.<sup>1</sup>